INVESTIGATING THE GASTRIC DISINTEGRATION AND EMPTYING KINETICS OF SOLID FOODS AND THE EFFICACY OF DIGESTIVE ENZYMES; AN *IN VITRO* STUDY USING DYNAMIC STOMACH MODEL

by

DUC HUY TRAN DO

(Under the Direction of FANBIN KONG)

ABSTRACT

The objectives of this project were to use *in vitro* gastric simulation models to (1) evaluate the influence of particle size and food texture on digestion rate, (2) determine the effect of viscosity on altering the rate of gastric digestion, (3) examine the structural breakdown and protein hydrolysis of cheeses in the gastric environment, and (4) compare the efficacy of certain digestive enzyme supplements under simulated gastric conditions.

A simplified dynamic gastric model that incorporates the simulation of gastric secretions, gastric peristaltic forces, and gastric emptying was created and used to investigate the effects of the gastric environment on the digestion of food with various particle sizes, textures, and rheological properties. The results indicated that regulating the particle size and food texture has the potential to alter the rate of gastric digestion. Changing the rheological properties of gastric fluid modulated the rate of gastric digestion by influencing the disintegration rate and the emptying of solids. The acidic gastric environment has been commonly thought to weaken the structure of food and encourage protein hydrolysis; while this study indicated that the gastric environment strengthened the structure of cheeses and reduced the hydrolysis of protein in certain cheeses.

Various digestive enzymes supplements were also evaluated based on their efficacy to degrade casein and food mixture, and the results demonstrated significant improvements in the digestion of food with commercial enzymes by releasing greater amounts of bioaccessible nutrients. The study proves that dynamic gastric model is an effective tool to study the behavior of food and enzyme under gastric conditions providing more comprehensive and accurate information as compared to static models.

INDEX WORDS: Dynamic Gastric Model, Gastric Disintegration, Gastric Emptying, Structural Breakdown, Bioaccessibility, Supplemental Digestive Enzymes.

INVESTIGATING THE GASTRIC DISINTEGRATION AND EMPTYING KINETICS OF SOLID FOODS AND THE EFFICACY OF DIGESTIVE ENZYMES; AN *IN VITRO* STUDY USING DYNAMIC STOMACH MODEL

by

DUC HUY TRAN DO

B.S., The University of Georgia, 2008

A Dissertation Submitted to the Graduate Faculty of The University of Georgia in Partial Fulfillment of the Requirements for the Degree

DOCTOR OF PHILOSOPHY

ATHENS, GEORGIA

2017

© 2017

Duc Huy Tran Do

All Rights Reserved

INVESTIGATING THE GASTRIC DISINTEGRATION AND EMPTYING KINETICS OF SOLID FOODS AND THE EFFICACY OF DIGESTIVE ENZYMES; AN IN VITRO STUDY USING DYNAMIC STOMACH MODEL

by

DUC HUY TRAN DO

Major Professor:	Fanbin Kong
Committee:	George A. Cavender
	Ronald B. Pegg
	William L. Kerr

Electronic Version Approved:

Suzanne Barbour
Dean of the Graduate School
The University of Georgia
December 2017

DEDICATION

To my parents, Thom Thi Tran and Do Sy Duy Anh for their supports through the many years of struggle and hard work. To my brothers Binh Duy Do, Anh-Vu Do, and Phiet Do for keeping me going every day. To my girlfriend, Jeewon Koh, for supporting me when I felt discouraged. To God for giving the strength through the troubled times.

ACKNOWLEDGEMENTS

I wish to thank the following people for helping me along my journey:

Dr. Fanbin Kong, for guiding me through my doctorate program.

Chris Penet, Deborah Winetzky, and Kelly Gregory for their amazing financial supports and research inputs during my doctorate program.

Dr. George Cavender for his insightful input to improve my study.

Dr. William Kerr for teaching me what it means to be a great professor.

Dr. Ronald Pegg for enhancing my knowledge of food science both inside and outside of the classroom.

Dr. Harrison for effectively advising me through my graduate program.

Dr. Shewfelt for inspiring me to enter this program.

To the past and present members of Dr. Kong's Lab: Erik, Nathan, Dr. Wei, Lingling, Breeanna, Vijendra, Samet, Luna, Yiwen, Jin, Nakia, Vivian, and Jiannan for your friendship and input on my project.

To the past and present friends: Ali, Anuj, Christina, George, Roy, Tracy, Sue-jee, Jeewon, Brittnee, Daoyuan, Xuan, Quynh, Lauren, Moon, Jason, Maria, Nats, Sonya, Sharon (my Grandma), Andy, Dien, Duy, Sang, and Tuyen for your friendship and advises.

To the staff working in the department for having to put up with my foolery behavior: Karen, Lisa P. Lisa C., Dorris, Pam, Ken, Danny, and Vickie.

Forgive me if I left out your name, but I would also like to thank you.

TABLE OF CONTENTS

Page

LIST OF TABLES

Page

LIST OF FIGURES

CHAPTER 1

INTRODUCTION

The objectives of this study focus on the inherent physical properties of food that affect the rate of gastric digestion. Many researchers have used *in vivo* digestion trials with live animals and humans to investigate the behavior of food during the gastric phase (Dikeman et al., 2006; Fuente et al., 1998; Holm et al., 1988). High cost and ethical issues have limited the *in vivo* trials and compelled researchers to develop *in vitro* models. Simplified *in vitro* static models are defined by an unchanging environment with constant pH, substrate concentrations, and enzymes concentrations (Kong & Singh, 2010). The introduction of more complex *in vitro* dynamic models improves the simulation of digestion by incorporating dynamic parameters that mimic the physiological changes occurring in the digestive tract. Examples include TNO (gastro-) Intestinal Models (TIM), Dynamic Gastric Model (DGM), and the Human Gastric Simulator (HGS) developed by The Netherlands Organization for Applied Science Research, The Institute of Food Research, and researchers at The University of California Davis, respectively (Chessa et al., 2014; Minekus et al., 1995; Kong & Singh, 2010). The high cost of acquiring these dynamic models led to the development of a simplified dynamic gastric model in this study, Dynamic Gastric Simulation Model (DGSM). The model simulates the physiological changes in the stomach by incorporating the simulation of gastric secretions, gastric contractions, and gastric emptying. Through the simulation of gastric secretion, the model mimics the continuous acidification process that is responsible for activating both acid and enzymatic hydrolysis of food (Wey et al., 2014). In addition, the simulation of peristaltic contractions generates the necessary forces to physically

disintegrate the food through mixing and grinding (Qing et al., 2017). Furthermore, the simulation of the gastric emptying alters the environment of the gastric digesta by removing smaller particles while retaining particles with larger sizes (Collins et al., 1996). Beyond the physiological changes in the stomach, the physical properties of food may also affect the rate of gastric digestion. Ingested food moves through the gastric conditions with varying particle size, texture, and rheological properties. The changes in these parameters are speculated to influence the release of bioaccessible components (Bornhorst et al., 2015). For example, the changes in the viscosity of the digesta has been shown to impact digestion by increasing or decreasing the rate of gastric emptying (Marciani et al., 2001; Paulson, et al., 2001). Understanding the influence of the physical properties of food on gastric digestion may provide future researchers with knowledge that will enable them to design better foods with physical properties that are able to control the rate of food digestion. The behavior of meats, vegetables, and nuts in the gastric environment has been previously studied (Kong & Singh, 2008; Lentle & Janssen, 2011). However, only a few studies have focused on the behavior of cheese in the gastric environment. The variations in cheese structure are governed by the composition of the cheese, the arrangement of the macronutrients, and the processing techniques (Mistry & Anderson, 1993). These variations in structure make cheese an excellent substrate for the study of structural breakdown kinetics under human digestive conditions. Results from these studies may further clarify the behavior of food during gastric digestion.

In addition to study of the fundamental aspects that affect gastric digestion, the DGSM model was applied to study the efficacy of supplemental digestive enzymes in improving the release of bioaccessible components. Due to sickness and aging, decreasing amounts of digestive enzymes are secreted by the body (Roxas, 2008). The reduction in the secretion of digestive enzymes diminishes the rate and extent of food digestion and limits the body from absorbing

nutrients. One potential solution for improving the breakdown of food is to consume digestive enzymes supplements containing enzymes isolated from animals, plants, and fungi (Roxas, 2008). Extensive research has been conducted to determine the effects of digestive enzymes supplements under static *in vitro* digestion conditions. However, the dynamic conditions that exist in the human stomach may impact the efficiency of supplemental digestive enzymes, which has not been fully studied (Dodge & Turck, 2006; Schneider et al.,1985). This study utilizes the DGSM to investigate the efficacy of supplemental digestive enzymes in aiding digestion. It is our hypothesis that *in vitro* dynamic simulation model is a better tool for assessing the overall efficacy of digestive enzyme supplements. The capability of the dynamic gastric models to simulate the continuous acidification process allows the assessment of the digestive enzyme supplements over a wide range of gastric pH's. In addition, the simulation of continuous gastric juice secretion with acids and proteolytic enzymes may further deactivate the digestive enzyme supplements with similar trend occurring in the human stomach. Although the dynamic gastric model may not replace *in vivo* trials, the dynamic GI model provides an improved method of assessing the overall efficacy of digestive enzyme supplements when compared the static *in vitro* method.

References

Bornhorst, G. M., Ferrua, M. J., & Paul Singh, R. (2015). A proposed food breakdown classification system to predict food behavior during gastric digestion. *Journal of Food Science, 80*(5), R924-R934.

Chessa, S., Huatan, H., Levina, M., Mehta, R. Y., Ferrizzi, D., & Rajabi-Siahboomi, A. R. (2014). Pharmaceutical Nanotechnology: Application of the Dynamic Gastric Model to evaluate the effect of food on the drug release characteristics of a hydrophilic matrix formulation. *International Journal of Pharmaceutics, 466*, 359-367.

Collins, P. J., Horowitz, M., Maddox, A., Myers, J. C., & Chatterton, B. E. (1996). Effects of increasing solid component size of a mixed solid/liquid meal on solid and liquid gastric emptying. *American Journal of Physiology, 271*(4), G549-G554.

Dikeman, C. L., Murphy, M. R., & Fahey, G. C., Jr. (2006). Dietary fibers affect viscosity of solutions and simulated human gastric and small intestinal digesta. *Journal of Nutrition, 136*(4), 913-919.

Dodge, J. A., & Turck, D. (2006). Cystic fibrosis: Nutritional consequences and management. *Best Practice & Research Clinical Gastroenterology, 20*, 531-546.

Fuente, J. M., Ayala, P. P., Flores, A., & Villamide, M. J. (1998). Effect of storage time and dietary enzyme on the metabolizable energy and digesta viscosity of barley-based diets for poultry. *Poultry Science, 77*(1), 90-97.

Holm, J., Lundquist, I., Björck, I., Eliasson, A.C., & Asp, N.G. (1988). Degree of starch gelatinization, digestion rate of starch in vitro, and metabolic response in rats. *American Journal of Clinical Nutrition, 47*(6), 1010-1016.

Kong, F., & Singh, R. P. (2008). Disintegration of Solid Foods in Human Stomach. *Journal of Food Science, 73*(5), R67-R80.

Kong, F., & Singh, R. P. (2010). A human gastric simulator (HGS) to study food digestion in human stomach. *Journal of Food Science, 75*(9), E627-E635.

Lentle, R. G., & Janssen, P. W. (2011). The physical processes of digestion: New York : Springer, 2011.

Marciani, L., Gowland, P. A., Spiller, R. C., Manoj, P., Moore, R. J., Young, P., & Fillery-Travis, A. J. (2001). Effect of meal viscosity and nutrients on satiety, intragastric dilution, and emptying assessed by MRI. *American Journal of Physiology. Gastrointestinal Liver Physiology, 280*(6), G1227-1233.

Minekus, M., Huis in 't Veld, J., Havenaar, R., & Marteau, P. (1995). A multicompartmental dynamic computer-controlled model simulating the stomach and small intestine. *Alternatives to Laboratory Animals, 23*(2), 197-209.

Mistry, V. V., & Anderson, D. L. (1993). Composition and microstructure of commercial full-fat and low-fat cheeses. *Food Structure, 12*(2), 259-266.

Paulson, S. K., Vaughn, M. B., Jessen, S. M., Lawal, Y., Gresk, C. J., Yan, B., Maziasz, T. J., Cook, C. S., & Karim, A. (2001). Pharmacokinetics of celecoxib after oral administration in dogs and humans: effect of food and site of absorption. *Journal of Pharmacology Experimental Therapeutics,, 297*(2), 638-645.

Qing, G., Bellissimo, N., & Rousseau, D. (2017). Role of gel structure in controlling in vitro intestinal lipid digestion in whey protein emulsion gels. *Food Hydrocolloids, 69*, 264-272.

Roxas, M. (2008). The Role of Enzyme Supplementation in Digestive Disorders. *Alternative Medicine Review, 13*(4), 307-314.

Schneider, M. U., Knoll-Ruzicka, M. L., Domschke, S., Heptner, G., & Domschke, W. (1985). Pancreatic enzyme replacement therapy: comparative effects of conventional and enteric-coated microspheric pancreatin and acid-stable fungal enzyme preparations on steatorrhoea in chronic pancreatitis. *Hepato-Gastroenterology, 32*(2), 97-102.

Wey, A. S., Cookson, A. L., Roy, N. C., McNabb, W. C., Soboleva, T. K., Wieliczko, R. J., & Shorten, P. R. (2014). A mathematical model of the effect of pH and food matrix composition on fluid transport into foods: an application in gastric digestion and cheese brining. *Food Research International, 57*, 34-43.

CHAPTER 2

REVIEW OF LITERATURE

2.1. The human digestive system and gastric digestion

The human digestive system is depicted in Figure 2.1. The gastrointestinal tract consists of several organs that digest food, release and absorb nutrients, and excrete undigested food. During the oral phase, food is reduced to smaller particle sizes through mastication, and the enzyme alpha-amylase initiates the degradation of carbohydrates. Lingual lipases are also secreted in the oral phase, but only limited lipolysis occurs in the mouth when compared to other digestive organs (Pendersen et al., 2002). Through the first phase of disintegration, most foods are reduced to an average size of 5.0 mm. The size of the food being ingested depends on the types of food and the amount of time they spend in the oral phase (Jalabert-Malbos et al., 2007). Masticated food forms into a bolus before the deglutition process moves the food down the esophagus and into the stomach (Barrett, 2014). Once the food is deposited in the stomach, the gastric digestion phase breaks down food through chemical and physical degradation (Kong & Singh, 2009). The human gastric digestion phase may last between 15 minutes to 3 hours with an acidic pH ranging from 1 to 5. Once mixed with gastric juice, the food is further chemically degraded, and the contents is called chyme (Kozu et al., 2014). The chyme is then emptied into the small intestine to be further broken down through enzymatic hydrolysis (Meyer et al., 1981). Known as the duodenum, the first part of the small intestine secretes hydrolytic enzymes to decompose carbohydrates, fats, and proteins. Secreted enzymes include amyloglucosidase, trypsin, and intestinal lipases that degrade

macronutrients. The secretion of bile salts emulsified and fats into small droplets and further facilitate the breakdown of fats (Carrière et al., 2001). The small intestine absorbs the digested nutrients while moving undigested contents into the large intestine. In the large intestinal phase, the majority of water is absorbed, and fermentation by the microbiome further breaks down macronutrients (Bornhorst, 2017). The remaining undigested food is excreted through the anus.

One of the major organs that helps to breakdown food through chemical and physical degradation is the human stomach. An image depicting the regions of the stomach is shown in Figure 2.2. The shape of the stomach resembles that of a letter "J" due to the shorter region created by the Lesser Curvature and a longer stomach region created by the Greater Curvature (Mahadevan, 2014). Three main parts of the stomach includes the body, antrum, and pylorus. The body of the stomach functions as a reservoir to hold the contents, and distention allows it to accommodate up to 2 L of food (Sernka and Jacobson, 1979). Although it is not fully understood, the changes in gastric environment has been associated with altering the digestion rate. The gastric environment may impact important parameters including the release of bioaccessible components and efficiency of supplemental digestive enzymes. Further understanding about the impact of the gastric environment on food digestion will allow researchers to optimize food systems that regulate both nutrients being released and absorbed. Most of the gastric digestion occurs within the antrum of the stomach with the pylorus functioning as the site for filtering and emptying of the gastric contents (Schwizer et al., 2006). Furthermore, physiological changes in the human stomach modifies the gastric environment through secretion of acids and enzymes, peristaltic contractions, and emptying. These processes generate a dynamic gastric environment that digests food both chemically and physically. A fundamental understanding of these processes are needed to predict the behavior of food degradation in the gastric environment.

2.2. Methods of studying gastric digestion

Historically, researchers have use *in vivo* models to study the gastric digestion. Reports of animal testing from as early as 1679 were performed through the dissection of wolfs, dogs, and cats to monitor the rate of gastric digestion (Hertz, 1910). Currently, common *in vivo* methods utilize dogs, chickens, rats, and pigs to monitor the rate of gastric digestion (Holm et al., 1988; Fuente et al., 1998; Dikeman et al., 2006; Bornhorst et al. 2013). To monitor the various phases of digestion, a cannula is surgically inserted at various points along the digestive tract of an animal to collect digesta for analysis (Decuypere et al., 1977). Another technique is the slaughtering of the animal before dissecting the digestive organs to analyze the digesta (Bornhorst et al., 2013). Common *in vivo* method used to study human digestion includes the placement of a fistula in the digestive tract and collect digesta samples (Bornhorst, 2017). For example, patients suffering from Crohn's disease often have a portion of their small intestine removed, and the cut ends attached to a pouch positioned outside the body. The aspirated waste materials are used to study the product of the upper gastro- intestinal tract (McLeod et al., 1985). Other noninvasive studies to monitor gastric digestion have been performed using X-rays, scintigraphy, stable isotope breath tests, ultrasonography, wireless capsules, and Magnetic Resonance Imaging (Vantrappen, 1994; Cannon, 1898). Though *in vivo* trials are considered the gold standard when it comes to investigating the factors affecting the human digestive system, cost and ethical issues limit their use. Instead, researchers use *in vitro* methods to investigate different factors influencing the rate of gastric digestion.

In vitro methods are used to examine the factors influencing digestion due to their better control of factors as such is not always possible with i*n vivo* digestion studies (Bornhorst, 2017). The *in vitro* methods can be divided into either *in vitro* static (IVS) or *in vitro* dynamic gastric

simulation (IVD). The simplest IVS model involves the incubation of substrates and enzymes in a water bath. The incubation of the mixture at 37°C for 2-3 hours allows the enzymes and acid to simulate the hydrolysis that occurs within the stomach (Hur et al., 2011). Another model involves the agitation of the mixture at 37°C to simulate the hydrodynamic forces occurring in the stomach (Bornhorst & Singh, 2013). The simplicity of the static *in vitro* methods makes the model highly preferable. However, the application of this model to simulate complex gastric digestion is lacking due to the absence of adequate physical and hydrodynamic forces that are found in the human stomach (Bornhorst, 2014). Researchers showed that agitation alone does not sufficiently simulate the physical forces present in the stomach (Kamba et al., 2003). An alternative *in vitro* method includes the simulation of the dynamic gastric environment. This method requires the production of a model that incorporates gastric secretions, gastric peristaltic forces, and gastric emptying. Three examples of dynamic simulation digestion models are shown in Figure 2.3. The first example includes the Dynamic Gastric Model created by The Institute of Food Research. This device incorporates gastric secretion by injecting in acid and enzyme into the model, while facilitating gastric emptying by withdrawing content from the emptying point. In addition, the DGM incorporate pistons and barrel that simulate gastric mixing and disintegration occurring at the antrum part of the model (Chessa et al., 2014). More complex model includes the TNO (gastro) Intestinal Models (TIM) developed by The Netherlands Organization for Applied Science Research. This model simulates both the stomach and the small intestine portion with sections of gastric juice and intestinal juices incorporated to resemble the conditions found in the human digestive tract. Furthermore, water pressure applied to the inner flexible wall of the TIM provides the forces to facilitate both mixing and disintegration Minekus et al., 1995). Another important dynamic gastric model includes the Human Gastric Simulator (HGS) developed at The University

of California, Davis (Kong & Singh, 2010). In addition to simulating gastric secretion and gastric emptying, the HGS contains rollers that squeeze to facilitate the mixing and compressing of the food similarly found in the human stomach. The three important parameters that are commonly found in these models include the incorporation of secretion, emptying, and peristaltic forces. These models are more complex to construct, and they often require more time and knowledge to maintain. However, these dynamic models enable the investigation of both the chemical and physical breakdown of food under realistic physiological conditions in the digestive tract.

2.3. Gastric secretions and effect of dynamic changes in pH on food digestion

The secretion of gastric juice helps to chemically digest food entering the stomach. The rate varies greatly from 1-50 mL/min (Arnold & Dubois, 1983). The initial high rate of gastric juice secretion is triggered by the ingestion of a large meal to further digest the food in the full-state (Castro-Combs et al., 2014). To protect the lining of the stomach from degradation, gastric glands secrete mucus and bicarbonate ions to neutralize the acid (Bornhorst, 2017). The hydrochloric acid found in gastric juice is responsible for the chemical degradation of food through acid hydrolysis. The acid is secreted by Parietal cells through the H+/K+ ATPase transport mechanism by the (Van Den Abeele et al., 2017). The rate of acid secretion is controlled by the endocrine hormones gastrin and somatostatin. The secretion of gastrin by G-cells stimulates and increases the secretion of gastric acid. The secretion of somatostatin by D-cells inhibits the acid secretion (Schubert and Peura, 2008). In addition to acid secreted by the Parietal cells, the Chief cells secrete inactive pepsinogen and gastric lipase. In the presence of gastric acid, the cleavage of the pepsinogen activates the proteolytic activity of pepsin and initiates enzymatic protein hydrolysis. The secretion of these enzymes is further upregulated by the neurotransmitter of acetylcholine while downregulating the endocrine hormone of somatostatin (Gritti et al., 2000).

It is estimated, in the fasted state, there are roughly 30-50 mL of gastric juice remains in the stomach in an average adult (Mudie et al., 2014). With a set amount of gastric juice in the stomach, the resting pH has a mean range of 2.5 to 2.9 with median range closer to 1.5-1.8 (Lindahl et al., 1997). Upon consumption of a meal, the pH of the digesta increases up to 7.5 depending on the buffering capacity and the absorption of acids by the meal (Lindahl et al., 1997). This initial high pH encourages the continuation of alpha- amylase activity while initiating lipid digestion by activating gastric lipases when the pH of the digesta falls to 5.5 (Van Den Abeele et al., 2017). Further acidification of the digesta deactivates amylase and lipase while activating the proteolytic activity of pepsin (Johnston et al., 2007). On average, the pH of the digesta falls below 2 around 120 minutes after the consumption of a meal (Dressman et al., 1990). This wide range of pH helps to regulate the chemical digestion of macronutrients by controlling both the rates of acid and enzymatic hydrolysis occurring in the human stomach. With static digestive models only simulating one set of pH condition, they show limited utility to simulate the range of pH that exist in the stomach to regulate the overall macronutrient breakdown.

2.4. Food breakdown kinetics in human stomach

The stomach is surrounded by branches of celiac arteries that supply blood while venous blood drains through the portal system (Ellis, 2011). Stomach contractions are regulated by stimuli triggered the Enteric Nervous System (Farré & Tack, 2013). The stimulus further regulates the vagal nerve that controls the rate of gastric contraction (Lakkireddy et al., 2015). The proximal and the distal regions, with different muscularis layers, behave differently during the contractions of the human stomach (Soybel, 2005). The expansion and contraction of the proximal region allows the distension in the stomach to accommodate a large meal. In contrast, the contractions in the distal region controls the rate of grinding, mixing, and emptying of the digesta (Hasler, 2009).

The human stomach contracts on average three times per minute (Marciani et al., 2001). These contractions are further broken down into three phases that make up the Migrating Motor Complex (Vantrappen et al., 1979). Phase I is a resting position with no gastric contraction. More mechanical pressure is exerted in Phase II, which involves an antral contraction with a pressure closely to 40 mm Hg. Phase III delivers the highest mechanical pressure, up to 200 mm Hg, with strong bursts of contractions for 2-6 minutes (Cassilly et al., 2008). The high pressure exerted by these stomach contractions is responsible for the grinding process that disintegrates food through fragmentation. Furthermore, the contractions facilitate the mixing process through retropropulsive phenomena (Bouldby et al., 1999). The constriction of the pylorus during the contractions allows the expulsion of particles with smaller in size into the intestine while reverting particles with larger size back into the stomach. This process facilitates the mixing of particles to encourage the disintegration of food through erosion (Qing et al., 2014).

Food moves into the stomach with varying physical properties in terms of particle size and texture. These two factors may alter gastric digestion by affecting the disintegration kinetics of solids. The sizes ingested food depends on the duration of mastication within the oral cavity (Bornhorst & Singh, 2012). For example, the median particle size of peanuts was found to be 0.82 mm after 10 participants chewed until swallowing was initiated (Malbos et al., 2007). In contrast, the median particle size of carrots being swallowed after five chews with particles remaining relatively large having average size of 8.70 mm before they enter the stomach (Jalabert- Lucas and Luke, 1986). The differences in surface areas resulting from various particle sizes may alter the disintegration kinetics and emptying rate by affecting the rate of grinding, mixing, and retention time (Bornhorst & Singh, 2014). Furthermore, ingested food may have both soft and hard textures in the stomach, as shown in boiled almonds and roasted peanuts, respectively (Kong & Singh,

2009). The initial hardness and the rate of softening have been proposed in a recent publication as indicators of food disintegration and food emptying (Bornhorst et al., 2015). Investigating the behavior of these various textures under gastric conditions may provide an insightful information that will be useful in developing food systems that can control the rates of disintegration and gastric emptying.

Food viscosity can be altered with the incorporation of dietary fibers. The inclusion of dietary fibers may increase the digesta viscosity up to value of 29.5 Pa·s, as was observed in *in vivo* digestion trials (Marciani et al., 2001). Furthermore, the acidification of certain dietary fibers has been reported to increase the viscosity of the digesta. An example includes increasing viscosity of rats digesta upon fed with a meal containing xanthan gum and milk proteins (Cameron-Smith et al. 1994). However, it was reported that the secretion of gastric juice diminishes the viscosity with reason attributed to the gastric juice ability to dilute and hydrolyze the dietary fibers in the digesta (Versantvoort et al., 2004). For example, the highly viscous meal contained a dietary fiber with 1.5% locust bean gum decreased in viscosity from the initial 11 Pa·s to 2 Pa·s immediately after the secretion of gastric juice. As greater amount of gastric juice was secreted the viscosity of the digesta in the same experiment dropped to 0.3 Pa·s after the digesta spent 30 minutes inside the stomach (Marciani et al., 2000). Various viscosities have been reported to exist in the stomach with a low viscosity of 1.7 mPa·s to the maximum value of 29.5 Pa·s as observed in *in vivo* digestion trials (Marciani et al., 2001). Researchers suggested that viscosity may influence digestion by impacting the rates of disintegration and emptying in the human stomach (Sirios et al., 1990). In one study, an increase in digesta viscosity increases the retention time of food to be further broken down by the stomach (Marciani et al., 2001). In another study, an increase in digesta viscosity was shown to decrease the disintegration through the early removal of solids with particle

sizes greater than 4.0 mm (Paulson et al., 2001). Additional investigation may clarify the effects of viscosity on the disintegration kinetics.

Researchers have investigated several different factors in the gastric environment that impact the structural breakdown of various foods including vegetables, legumes, and nuts (Kong and Singh, 2008). However, limited research has been conducted on the structural behavior of cheese in the human digestive tract (Lentle & Janssen, 2011). Cheeses are predominantly composed of casein, fat, water, and minerals. However, great variations in cheese structure are created by the differences in the cheese composition, the arrangement of macronutrients, and the processing techniques. Most of the structure is attributed to the casein matrix that provides the hardness of the cheese while water and fat globules give cheese its smoothness (Mistry & Abdersibe, 1993). The arrangement of macronutrients in the cheese matrix also contributes to the structure of cheese. For example, the hardness of Mozzarella cheese is influenced by the fibrous protein matrix and a low amount of fat globules (Gunasekaran & Ak, 2003). The hardness of Cheddar cheese is mainly governed by the protein aggregates that have a combination of globular and sub-micellar shapes, and large coalesced fat globules reduce its hardness. High amount of fat globules also weakens the Parmesan cheese structure (Michalski et al., 2007). Further processing of cheeses also influences cheese structures. The typical stretching during the production of Mozzarella gives it a fibrous and compact structure (Gunasekaran & Ak, 2003). The stacking of cheese curd through the Cheddaring process creates larger coalesced fat globules that gives Cheddar cheese its distinct hardness (Guinee et al., 2000). In addition, aging of Parmesan cheese impacts structure through protein degradation and reduction of moisture content (Fox et al., 1993). These variations in the structure make cheese an excellent substrate for the study of structural

breakdown kinetics and protein hydrolysis under human gastric conditions with recent studies showing resistance of cheese proteins to gastric environment (Rolet-Repecaud et al., 2017).

2.5. Gastric emptying and influencing factors

Stomach contractions facilitate the emptying of digested contents. The rate varies for solids, semisolids, and liquids. Within the Migrating Motor Complex, the rate of liquid gastric emptying was reported to be correlated to the contraction phases. A study reported that the fluid flow rate is lowest in Phase I while the highest fluid flow rate occurs during Phase III contractions (Savoye et al., 2003). The rate of gastric emptying of non-digestible solids is correlated to peristaltic contractions. The rate of emptying non-digestible solids has been reported to follow first order kinetics with initially rapid emptying that slowing down at the later stages (Gonzalez et al., 2000). Emptying rates become more complex when the digesta contains nutrients. A feedback mechanism slows down gastric emptying in response to nutrients including carbohydrates, proteins, and fats (Di Lorenzo et al., 1988). Various nutrients elicit signals that decrease gastric emptying by applying the "Ileal Brake" (Spiller et al., 1984). Other factors including pH, nutrient load, and osmolality further regulate the emptying rate (Chaw et al., 2001). Gastric emptying during the digestion of caloric solids has been described as following a biphasic pattern with a lag phase (Collin et al., 1996). During the lag phase, a very limited amount of gastric contents is emptied. This lag phase provides the needed processing time to reduce the digesta to particles small enough for emptying (Gonzalez et al., 2000). The absence of a lag phase during digestion of a liquid is a further evidence that the lag phase provides the needed processing time to reduce the digesta to particles small enough to be emptied (Collin et al.,1996). Very limited studies have been performed to evaluate the influence of stomach morphology on the lag phase of gastric emptying (Liding et al., 2016). The "J" shape of the stomach situates the pylorus roughly 3.0 cm above the

base of the stomach (Savoye et al., 2003). This height difference may limit the initial removal of large and dense particles due to their settling at the base of the stomach. Further gastric digestion reduces the size of larger particles. After sufficient mixing, the smaller particles rise to the site of the pylorus to be emptied. The gastric morphology may affect the gastric emptying rate by acting as a sieve that passes smaller particles into the intestines while providing an initial lag phase for larger particles to be reduced in size before emptying (Vardakou et al., 2011).

Beyond the shape of the stomach, the physical characteristics of food has been hypothesized to affect the pattern of gastric emptying. Particle size, density, and viscosity of food are the physical characteristics that have been proposed to influence the kinetic of gastric emptying (Sirois et al., 1990). On average, foods are digested to particle sizes less than 1 mm before emptying from the stomach (Meyer et al., 1981). The particle size of the ingested food is thought to be inversely proportional with the rate of solid emptying with larger particle emptying later (Itoh et al., 1962). However, researchers speculate that particle size and density interact and influence the overall residence time of a solid (Bechgaard et al., 1985). For example, when the density of the particles matches the density of the digesta, particles with greater size than 5 mm have been shown to continuously emptied during gastric digestion (Takashi et al., 1983). Further influencing the patterns of emptying is the viscosity of the digesta. It is speculated that the increase in viscosity reduces the flow characteristic and diminishes the rate of gastric emptying (Marciani et al., 2001). However, studies have also shown that increasing in viscosity improves the emptying of larger particles from the stomach (Meyer et al., 1981; Sirios et al., 1990). Further research will help to clarify the influence of particle size, density, and viscosity on gastric digestion as research speculated that these factors may interact with each other to impact the overall outcome of the solids emptying rate (Sirios et al., 1990).

2.6. Supplemental digestive enzymes impacting gastric digestion

Enzymes for use as digestive supplements are often isolated from animals, plants, and fungi. These enzymes may work synergistically when used in tandem with each other to help aid the digestion of food. Three main categories of digestive enzyme supplements include carbohydrases, proteases, and lipases. With few safety concerns for allergic reactions and gastrointestinal discomfort, digestive enzymes supplements are frequently used to help improve the digestion in the old and sick (Roxas, 2008). Cattles and pigs are the two most common animal sources of enzymes for dietary supplements, with common enzymes including trypsin and chymotrypsin extracted from the pancreas of cattle, and lipases extracted from the pancreas of pigs. Another example includes the mixture of lipase, amylase, and proteases known as Pancreatin, which is often isolated from both pigs and cattle (Griffin et al., 1989). The other major source enzyme for dietary supplements are plants, and the majority of enzymes isolated from plants are non-specific proteases that enhance proteolytic digestion of food. Examples include bromelain, papain, and ficin that are isolated from pineapple, papaya, and figs (Brocklehurst et al., 1987; Houck et al., 1983; Tyler et al., 1981). Finally, the majority of enzymes used to make dietary supplements are isolated from fungi. Examples include lipases isolated from *Aspergillus oryzae* and lactase isolated from *Kluyveromyces lactis*. The advantages of using fungal enzymes include their broader pH range of optimal activity and the lower dosages necessary to improve digestion (Roxas, 2008). The wide variety of fungal enzymes and multiple side activities enables them to be versatile source of enzymes for dietary supplements. For example, the use of fungal lipases improves the absorption of fats while preventing steatorrhea (Schneider et al., 1985; Nakamura et al., 1998).

Over the years, a variety of digestive enzyme supplements have been used to improve human digestion and absorption of nutrients. One population that enzyme supplements can benefit are those patients suffering from pancreatitis. It was estimated that 23.6 million children and adults are suffering from various forms of pancreatitis (Roxas, 2008). Pancreatitis occurs when the organ is unable to produce and secrete normal levels of digestive enzymes, and supplementation therapy allows the patients to have relatively normal digestion of foods. For example, porcine lipases are often prescribed to patients' dosages of 25,000-40,000 units daily to improve fat digestion and absorption (Dodge & Turck, 2006). Another example includes the incorporation of bromelain to improve the digestion of protein. One published study, using weight gain as a marker of efficacy, claimed that the combination of bromelain with other exogenous pancreatic enzymes greatly lowered the excreted fat, relieved digestive pain, reduced flatulence, and improved the absorption of nutrients (Balakrishma et. al, 1981). Another clinical study showed the improvement of fat retention in patients suffering from pancreatic diseases when placed on a regime of 75,000 porcine lipase units per day (Schneider et al., 1985). There are concerns about over dosing and allergic reactions from the supplemental digestive enzymes due to their high levels of activities. Overdosing may lead to fatigue and cause gastrointestinal pain with excess uric acid in the urine and blood (Cichoke, 2000). Risk of allergic reactions can be reduced by simply adjusting the dose to the need.

2.7. Evaluating the efficacy of digestive enzyme supplements

With the abundance of new digestive enzymes being isolated from various sources, testing the efficacy of all these enzymes under *in vivo* digestion may be costly and unethical (Hur et al. 2011). Alternatively, many researchers utilized *in vitro* static digestion to test the overall activities of the enzymes due to the simplicity (Boisen & Eggum, 1991). However, a static environment

overestimates the efficacy of enzymes with optimum pH similar to the test conditions. On the contrary, the static environment also undermines the efficacy of digestive enzymes with optimum pH's outside of the tested conditions. Long incubation periods without changes in the digesta volume also increases products formation due to the high retention time of substrates and enzymes. The increases in products by the static model reiterate the point that digestive enzyme supplements may work better in the laboratory setting than in the human body. An example is that commercial pancreatic extract showed high enzymatic activities under static conditions at the pH of 7.4 (Graham, 1977). When similar pancreatic enzyme extracts were tested with clinical trials, the gastric acid and pepsin inactivated one third of the trypsin and one half of the lipase (Heizer et al., 1965). Furthermore, the human gastric conditions have been shown to rapidly and irreversibly inactivate pancreatic enzymes (Veeger et al., 1962). The pancreatic enzymes supplements, shown to have high activities under static digestion, were deemed ineffective under *in vivo* digestion trials.

References

Arnold, J., & Dubois, A. (1983). In vitro studies of intragastric digestion. *Digestive Diseases Sciences, 28*(8), 737-741.

Barrett, K. (2014). Gastrointestinal Physiology (2nd ed.). New York: McGraw-Hill Medical.

Balakrishnan, V., Hareendran, A., & Nair, C. (1981). Double-blind cross-over trial of an enzyme preparation in pancreatic steatorrhoea. *The Journal Of The Association Of Physicians Of India, 29*(3), 207-209.

Bechgaard, H., Christensen, F., Davis, S., Hardy, J., Taylor, M., Whalley, D., & Wilson, C. (1985). Gastrointestinal transit of pellet systems in ileostomy subjects and the effect of density. *Journal of Pharmacy Pharmacology*, 37, 718-721.

Billigmann, P. (1995). Enzyme therapy-an alternative in treatment of herpes zoster. A controlled study of 192 patients. *Fortschritte Der Medizin, 113*(4), 43-48.

Boisen, S., & Eggum, B. O. (1991). Critical evaluation of in vitro methods for estimating digestibility in simple-stomach animals. *Nutrition Research Reviews, 4*(1), 141-162.

Blonstein, J. L. (1960). The use of 'buccal varidase' in boxing injuries. *The Practitioner, 185*, 78-79.

Bornhorst, G. M., Ferrua, M. J., & Paul Singh, R. (2015). A proposed food breakdown classification system to predict food behavior during gastric digestion. *Journal of Food Science, 80*(5), R924-R934.

Bornhorst, G. M., & Singh, R. P. (2012). Bolus formation and disintegration during digestion of food carbohydrates. *Comprehensive Reviews in Food Science and Food Safety*, 11(2), 101-118.

Bornhorst, G. M., Chang, L. Q., Rutherfurd, S. M., Moughan, P. J., & Singh, R. P. (2013). Gastric emptying rate and chyme characteristics for cooked brown and white rice

Bornhorst, G. M., & Singh, R. P. (2014). Gastric digestion in vivo and in vitro: how the structural aspects of food influence the digestion process. *Annual Review of Food Science and Technology, 5*, 111-132.

Bornhorst, G. M., Ferrua, M. J., & Singh, R. P. (2015). A proposed food breakdown classification system to predict food behavior during gastric digestion. *Journal of Food Science, 80*(5), R924-R934.

Bornhorst, G. M. (2017). Gastric mixing during food digestion: mechanisms and applications. *Annual Review of Food Science and Technology*, 8, 523-542.

Boulby, Moore, Gowland, Spiller, & Spiller, R. (1999). Fat delays emptying but increases forward and backward antral flow as assessed by flow-sensitive magnetic resonance imaging. *Neurogastroenterology & Motility, 11*(1), 27-36.

Brocklehurst, K., & Neuberger, A. (1987). Hydrolytic enzymes / editors, A. Neuberger and K. Brocklehurst. In *New comprehensive biochemistry ; v. 16*): Amsterdam ; New York : Elsevier ; New York : Sole distributors for the U.S. and Canada, Elsevier Science Pub. Co., Inc., 1987. 39–158.

Cannon, W. (1898). The movements of the stomach studied by means of Röntgen rays. *American Journal of Physiology,* 1, 359–382.

Cassilly, D., Kantor, S., Knight, L. C., Maurer, A. H., Fisher, R. S., Semler, J., & Parkman, H. P. (2008). - Gastric emptying of a non-digestible solid: assessment with simultaneous SmartPill pH and pressure capsule, antroduodenal manometry, gastric emptying scintigraphy. *Neurogastroenterology and Motility, 20*(4), 311-319.

Cameron-Smith, D., Collier, G., and O'dea, K., (1994). Effect of soluble dietary fibre on the viscosity of gastrointestinal contents and the acute glycaemic response in the rat. *British Journal of Nutrition*, 71(04), 563-571.

Castro-Combs, J., Garcia, C. J., Majewski, M., Wallner, G., & Sarosiek, J. (2014). Impaired viscosity of gastric secretion and its mucin content as potential contributing factors to the development of chronic constipation. *Digestive Diseases Sciences, 59*(11), 2730-2734.

Chaw, C. S., Yazaki, E., & Evans, D. F. (2001). The effect of pH change on the gastric emptying of liquids measured by electrical impedance tomography and pH-sensitive radiotelemetry capsule. *International Journal of Pharmaceutics, 227*(1-2), 167-175.

Chessa, S., Huatan, H., Levina, M., Mehta, R. Y., Ferrizzi, D., & Rajabi-Siahboomi, A. R. (2014). Pharmaceutical Nanotechnology: Application of the Dynamic Gastric Model to evaluate the effect of food on the drug release characteristics of a hydrophilic matrix formulation. *International Journal of Pharmaceutics, 466,* 359-367.

Cichoke A. Pancreatic enzymes. In: Pizzorno J., Murray, M. eds. Textbook of Natural Medicine, 3rd ed., Volume 1. St. Louis, MO: Churchill Livingstone; 2006; 1131-1146.

Collins, P. J., Horowitz, M., Maddox, A., Myers, J. C., & Chatterton, B. E. (1996). Effects of increasing solid component size of a mixed solid/liquid meal on solid and liquid gastric emptying. *The American Journal of Physiology*, 271(4), G549-G554.

Decuypere, J. A., Vervaeke, I. J., Henderickx, H. K., & Dierick, N. A. (1977). Gastro-intestinal cannulation in pigs: a simple technique allowing multiple replacements. *Journal of Animal Science*, 45(3), 463-468.

Di Lorenzo, C., Williams, C. M., Hajnal, F., & Valenzuela, J. E. (1988). Pectin delays gastric emptying and increases satiety in obese subjects. *Gastroenterology*, *95*(5), 1211-1215.

Dikeman, C. L., Murphy, M. R., & Fahey, G. C. (2006). Dietary fibers affect viscosity of solutions and simulated human gastric and small intestinal digesta. *Journal of Nutrition, 136*(4), 913-919.

Dodge, J. A., & Turck, D. (2006). 6: Cystic fibrosis: Nutritional consequences and management. *Best Practice & Research Clinical Gastroenterology, 20*, 531-546.

Dressman, J. B., Berardi, R. R., Dermentzoglou, L. C., Russell, T. L., Schmaltz, S. P., Barnett, J. L., & Jarvenpaa, K. M. (1990). Upper gastrointestinal (GI) pH in young, healthy men and women. *Pharmaceutical Research*, *7*(7), 756-761.

Ellis, H. (2011). Anatomy of the stomach. *Surgery - Oxford International Edition, 29*(11), 541-543.

Farré, R., & Tack, J. (2013). Food and symptom generation in functional gastrointestinal disorders: physiological aspects. *American Journal of Gastroenterology*, *108*(5), 698-706.

Fox, P. Paul, L. McSweeney, H. Timothy, M. Cogan and Timothy P. Guinee (1993). Cheese: Chemistry, Physics and Microbiology (2nd ed.). London, UK, Chapman & Hall. 35-69.

Fuente, J. M., Ayala, P. P. d., Flores, A., & Villamide, M. J. (1998). Effect of storage time and dietary enzyme on the metabolizable energy and digesta viscosity of barley-based diets for poultry. *Poultry Science, 77*(1), 90-97.

Go, V. L., Poley, J. R., Hofmann, A. F., & Summerskill, W. H. (1970). Disturbances in fat digestion induced by acidic jejunal pH due to gastric hypersecretion in man. *Gastroenterology, 58*(5), 638-646.

Gonzalez, A., Mugueta, C., Parra, D., Labayen, I., Martinez, A., Varo, N., Monreal, I., & Gil, M. J. (2000). Characterisation with stable isotopes of the presence of a lag phase in the gastric emptying of liquids. *European Journal of Nutrition, 39*(5), 224.

Graham, D. (1997) Enzyme replacement therapy of exocrine pancreatic insufficiency in man. Relation between in vitro enzyme activities and in vivo potency in commercial pancreatic extracts. *New England Journal of Medicine,* 296(23):1314-1317.

Griffin, S. M., Alderson, D., & Farndon, J. R. (1989). Acid resistant lipase as replacement therapy in chronic pancreatic exocrine insufficiency: a study in dogs. *Gut, 30*(7), 1012-1015.

Gritti, I., Banfi, G., & Roi, G. S. (2000). Pepsinogens: physiology, pharmacology pathophysiology and exercise. *Pharmacological Research, 41*(3), 265-281.

Guinee, T. P., Auty, M. A. E., & Fenelon, M. A. (2000). The effect of fat content on the rheology, microstructure and heat-induced functional characteristics of Cheddar cheese. *International Dairy Journal, 10*(4), 277-288.

Gunasekaran, S.& Ak, M (2003). Factors affecting functional properties of cheese.*Cheese rheology and texture* (pp. 409–439). Boca Raton, FL, USA: CRC press.

Guerra, A., Etienne-Mesmin, L., Livrelli, V., Denis, S., Blanquet-Diot S., Alric, M., (2012). Relevance and challenges in modeling human gastric and small intestinal digestion. *Trends Biotechnology*., 30, 591-600.

Hasler, W.L. (2009). The Physiology of Gastric Motility and Gastric Emptying, Textbook of Gastroenterology. Blackwell Publishing Ltd. 207–230.

Heizer, W., Cleveland, C., Iber, F. (1965).Gastric inactivation of pancreatic supplements. Bull Johns Hopkins Hospital, 116; 261-270.

Hertz, A. F. (1909). The Motor Functions of the Stomach. *Quarterly Journal of Medicine, 176*, 373-394.

Holm, J., Lundquist, I., Björck, I., Eliasson, A. C., & Asp, N. G. (1988). Degree of starch gelatinization, digestion rate of starch in vitro, and metabolic response in rats. *American Journal of Clinical Nutrition, 47*(6), 1010-1016.

Houck, J. C., Chang, C. M., & Klein, G. (1983). Isolation of an effective debriding agent from the stems of pineapple plants. *International Journal Of Tissue Reactions, 5*(2), 125-134.

Hur, S., Lim, B., Decker, E., McClements, D. (2011). In vitro human digestion models for food applications. *Food Chemistry*, 125, 1–12.

Itoh, T., Higuchi, T., Gardner, C., & Caldwell, L. (1986). Effect of particle size and food on gastric residence time of non-disintegrating solids in beagle dogs. J*ournal of Pharmacy Pharmocology*, 38, 801-806

Jalabert-Malbos, M. L., Mishellany-Dutour, A., Woda, A., & Peyron, M. A. (2007). Particle size distribution in the food bolus after mastication of natural foods. *Food Quality and Preference, 18*(5), 803-812.

Johnston, N., Dettmar, P. W., Bishwokarma, B., Lively, M. O., & Koufman, J. A. (2007). Activity/stability of human pepsin: Implications for reflux attributed laryngeal disease: *Laryngoscope*, 117, 1036–1039.

Kamba, M., Seta, Y., Takeda, N., Hamaura, T., Kusai, A., Nakane, H., & Nishimura, K. (2003). Measurement of agitation force in dissolution test and mechanical destructive force in disintegration test. *International Journal of Pharmaceutics, 250*, 99-109.

Kelly, K., O'Mahony, B., Lindsay, B., Jones, T., Grattan, T. J., Rostami-Hodjegan, A., ... & Wilson, C. G. (2003). Comparison of the rates of disintegration, gastric emptying, and drug absorption following administration of a new and a conventional paracetamol formulation, using gamma scintigraphy. *Pharmaceutical Research*, 20(10), 1668-1673.

Klaue, P., Dilhert, G., Hinke, G., et al. (1979). Animal experimental research on enzyme treatment locally subdermal burns with bromelain. *Therapiewoche*, 29,796-799.

Kong, F., & Singh, R. P. (2010). A human gastric simulator (HGS) to study food digestion in human stomach. *Journal of Food Science, 75*(9), E627-E635.

Kong, F., & Singh, R. P. (2009). Modes of disintegration of solid foods in simulated gastric environment. *Food Biophysics, 4*(3), 180-190.

Kong, F., & Singh, R. P. (2008). Disintegration of Solid Foods in Human Stomach. *Journal of Food Science, 73*(5), R67-R80.

Kozu, H. (2015). Development of Human Gastric Models for Characterization of Food Digestion Phenomena (Doctoral dissertation). Retrieved from https://hdl.handle.net/2241/00128887

Kozu, H., Nakata, Y., Nakajima, M., Neves, M. A., Uemura, K., Sato, S., Kobayashi, I., & Ichikawa, S. (2014). Development of a human gastric digestion simulator equipped with peristalsis function for the direct observation and analysis of the food digestion process. *Food Science and Technology Research, 20*(2), 225-233.

Lakkireddy, D., Reddy, Y. M., Atkins, D., Rajasingh, J., Kanmanthareddy, A., Olyaee, M., Dusing, R., Pimentel, R., Bommana, S., & Dawn, B. (2015). Effect of atrial fibrillation ablation on gastric motility: the atrial fibrillation gut study. *Circulation. Arrhythmia and Electrophysiology, 8*(3), 531-536.

Lentle, R. G., & Janssen, P. W. (2011). *The physical processes of digestion. [electronic resource]*: New York : Springer, 2011.

Liding, C., Yufen, X., Tingting, F., Zhenkai, L., Peng, W., Xuee, W., & Xiao D., C. (2016). Gastric emptying and morphology of a "near real" in vitro human stomach model (RD-IV-HSM). *Journal of Food Engineering, 183*, 1-8.

Lindahl, A., Ungell, A. L., Knutson, L., & Lennernäs, H. (1997). Characterization of fluids from the stomach and proximal jejunum in men and women. *Pharmaceutical Research, 14*(4), 497-502.

Lucas, P. W., & Luke, D. A. (1986). Is food particle size a criterion for the initiation of swallowing? *Journal of Oral Rehabilitation, 13*(2), 127.

Marciani, L., Gowland, P. A., Spiller, R. C., Manoj, P., Moore, R. J., Young, P., Al-Sahab, S., Bush, D., Wright, J., & Fillery-Travis, A. J. (2000). Gastric response to increased meal viscosity assessed by echo-planar magnetic resonance imaging in humans. *Journal of Nutrition, 130*(1), 122-127.

Marciani, L., Gowland, P. A., Spiller, R. C., Manoj, P., Moore, R. J., Young, P., & Fillery-Travis, A. J. (2001). Effect of meal viscosity and nutrients on satiety, intragastric dilution, and emptying assessed by MRI. *American Journal of Physiology Gastrointestinal Liver Physiology, 280*(6), G1227-1233.

Mayordomo, I., Randez-Gil, F., & Prieto, J. A. (2000). Isolation, purification, and characterization of a cold-active lipase from Aspergillusnidulans. *Journal of Agricultural and Food Chemistry, 48*(1), 105-109.

McLeod, R. S., Lavery, I. C., Leatherman, J. R., Maryland, P. A., Fazio, V. W., Jagelman, D. G., & Weakley, F. L. (1985). Patient evaluation of the conventional ileostomy. *Diseases of the Colon & Rectum, 28*(4), 152.

Meyer, J. H., Ohashi, H., Jehn, D., & Thomson, J. B. (1981). Size of liver particles emptied from the human stomach. *Gastroenterology, 80*(6), 1489-1496.

Michalski, M. C., Camier, B., Gassi, J. Y., Briard-Bion, V., Leconte, N., Famelart, M. H., & Lopez, C. (2007). Functionality of smaller vs control native milk fat globules in Emmental cheeses manufactured with adapted technologies. *Food Research International, 40*(1), 191-202.

Minekus, M., Huis in 't Veld, J. H., Havenaar, R., & Marteau, P. (1995). A multicompartmental dynamic computer-controlled model simulating the stomach and small intestine. *Alternatives to laboratory animals, 23*(2), 197-209.

Mistry, V. V., & Anderson, D. L. (1993). Composition and microstructure of commercial full-fat and low-fat cheeses. *Food Structure, 12*(2), 259-266.

Mudie, D. M., Murray, K., Hoad, C. L., Pritchard, S. E., Garnett, M. C., Amidon, G. L., Gowland, P. A., Spiller, R. C., Amidon, G. E., & Marciani, L. (2014). Quantification of gastrointestinal liquid volumes and distribution following a 240 mL dose of water in the fasted state. *Molecular Pharmaceutics*, 11(9), 3039-3047.

Naikwade, S. R., Meshram, R. N., & Bajaj, A. N. (2009). Preparation and *in vivo* efficacy study of pancreatin microparticles as an enzyme replacement *Therapy for Pancreatitis. Drug Development & Industrial Pharmacy*, 35(4), 417-432.

Nakamura, T., Takeuchi, T., & Tando, Y. Pancreatic dysfunction and treatment options. *Pancreas*, 16, 329-336.

Paulson, S. K., Vaughn, M. B., Jessen, S. M., Lawal, Y., Gresk, C. J., Yan, B., Maziasz, T. J., Cook, C. S., & Karim, A. (2001). Pharmacokinetics of celecoxib after oral administration in dogs and humans: effect of food and site of absorption. *Journal of Pharmacology Experimental Therapeutics, 297*(2), 638-645.

Pedersen, P. B., Bar-Shalom, D., Baldursdottir, S., Vilmann, P., & Mullertz, A. (2014). Feasibility of capsule endoscopy for direct imaging of drug delivery systems in the fasted upper-gastrointestinal tract. *Pharmaceutical Research, 31*(8), 2044-2053.

Qing, G., Aiqian, Y., Lad, M., Dalgleish, D., & Harjinder, S. (2014). Effect of gel structure on the gastric digestion of whey protein emulsion gels. *Soft Matter, 10*(8), 1214-1223.

Qing, G., Bellissimo, N., & Rousseau, D. (2017). Role of gel structure in controlling in vitro intestinal lipid digestion in whey protein emulsion gels. *Food Hydrocolloids, 69*, 264-272.

Rolet-Repecaud, O., Arnould, C., Dupont, D., Gavoye, S., Beuvier, E., & Achilleos, C. (2017). Quantification of pepsin in rennet using a monoclonal antibody-based inhibition ELISA. *LWT -- Food Science and Technology, 76*(Part A), 190-196.

Roxas, M. (2008). The Role of Enzyme Supplementation in Digestive Disorders. *Alternative Medicine Review, 13*(4), 307-314.

Savoye, G., Savoye-Collet, C., Oors, J., & Smout, A. J. (2003). Interdigestive transpyloric fluid transport assessed by intraluminal impedance recording. *American Journal of Physiology Gastrointestinal Liver Physiology, 284*(4), G663-669.

Schneider, M. U., Knoll-Ruzicka, M. L., Domschke, S., Heptner, G., & Domschke, W. (1985). Pancreatic enzyme replacement therapy: comparative effects of conventional and enteric-coated microspheric pancreatin and acid-stable fungal enzyme preparations on steatorrhoea in chronic pancreatitis. *Hepato-Gastroenterology, 32*(2), 97-102.

Schubert, M. L., & Peura, D. A. (2008). Reviews in Basic and Clinical Gastroenterology: Control of Gastric Acid Secretion in Health and Disease. *Gastroenterology, 134*, 1842-1860.

Sirois, P., Amidon, G., Meyer, J., Doty, J., & Dressman, J. (1990). Gastric emptying of nondigestible solids in dogs: a hydrodynamic correlation. *American Journal of Physiology*, 258, G65-G72.

Soybel, D. (2005). Anatomy and physiology of the stomach. *Surgery Clinical North America*, 85, 875–894.

Spiller, R. C., Trotman, I. F., Higgins, B. E., Ghatei, M. A., Grimble, G. K., Lee, Y. C., Bloom, S. R., Misiewicz, J. J., & Silk, D. B. (1984). The ileal brake-inhibition of jejunal motility after ileal fat perfusion in man. *Gut, 25*(4), 365.

Takashi, N., Wiley, J., Overholt, B., & Bass, P. (1969). A realtion between gastroduodenal muscle contractions and gastric emptying. *Gut*, 10, 543-548.

Tyler, V., Brady, L., & Robbers, J. (1981). Enzymes and other proteins. Pharmacology. 8th ed. Philadelphia, PA; Lea oí Febiger, 290-291.

Van Den Abeele, J., Rubbens, J., Brouwers, J., & Augustijns, P. (2017). The dynamic gastric environment and its impact on drug and formulation behaviour. *European Journal of Pharmaceutical Sciences, 96*, 207-231.

Vantrappen, G. R., Peeters, T. L., & Janssens, J. (1979). The secretory component of the interdigestive migrating motor complex in man. *Scandinavian Journal of Gastroenterology, 14*(6), 663-667.

Vantrappen, G. (1994). Methods to study gastric emptying. *Digestive Diseases And Sciences, 39*, 91S-94S.

Vardakou, M., Mercuri, A., Barker, S. A., Craig, D. Q., Faulks, R. M., & Wickham, M. S. (2011). Achieving antral grinding forces in biorelevant in vitro models: comparing the USP dissolution apparatus II and the dynamic gastric model with human in vivo data. *AAPS PharmSciTech, 12*(2), 620-626.

Veeger, W., Abels, J., Hellemans N., et al. (1962). Effect of sodium bicarbonate and pancreatin on the absorption of viatamin V12 and fat in pancreatic insufficiency. New England Journal of Medicine, 267, 1341-1344.

Versantvoort, C., Van de Kamp, E., & Rompelberg, C. (2004). Development and applicability of an in vitro digestion model in assessing the bioaccessibility of contaminants from food. *Bilthoven, Inspectorate of Health Inspection*, 1–87.

Wey, A. S. v., Cookson, A. L., Roy, N. C., McNabb, W. C., Soboleva, T. K., Wieliczko, R. J., & Shorten, P. R. (2014). A mathematical model of the effect of pH and food matrix composition on fluid transport into foods: an application in gastric digestion and cheese brining. *Food Research International*, *57*, 34-43.

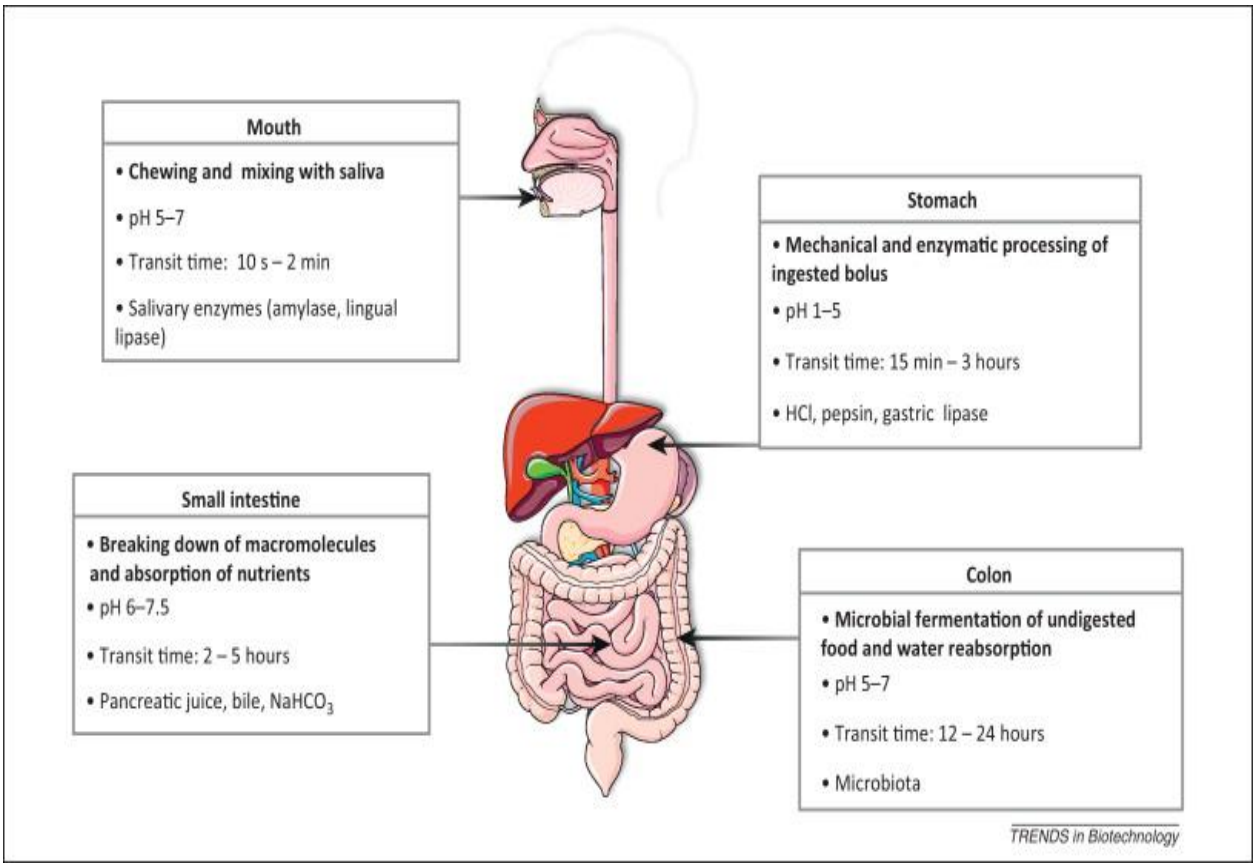

Figure 2.1. The major organs in the human digestive tract. (The image was gathered from Guerra et al. 2012 with the permission from Elsevier Science).

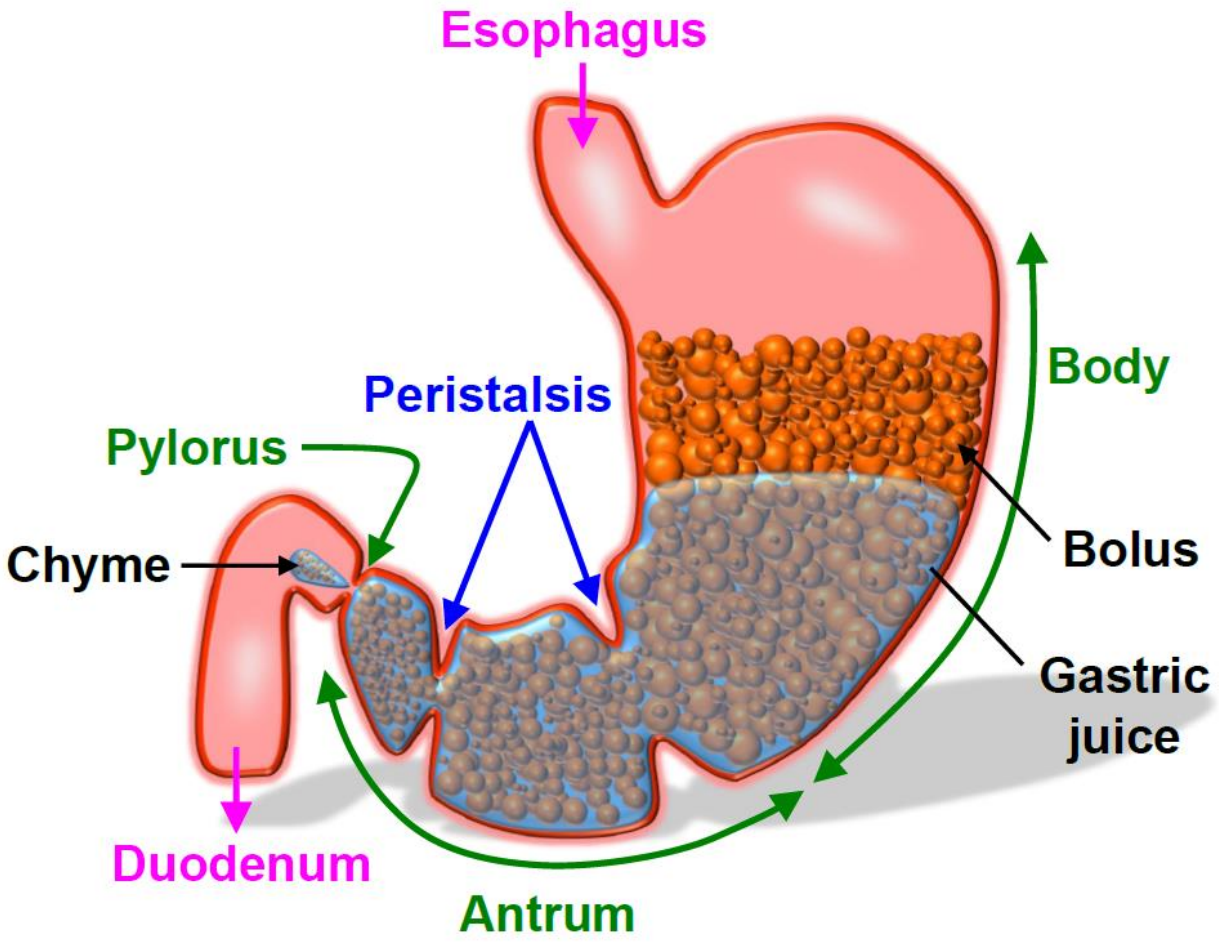

Figure 2.2. The regions of the human stomach (Figure is reproduced from Kozu, 2015)

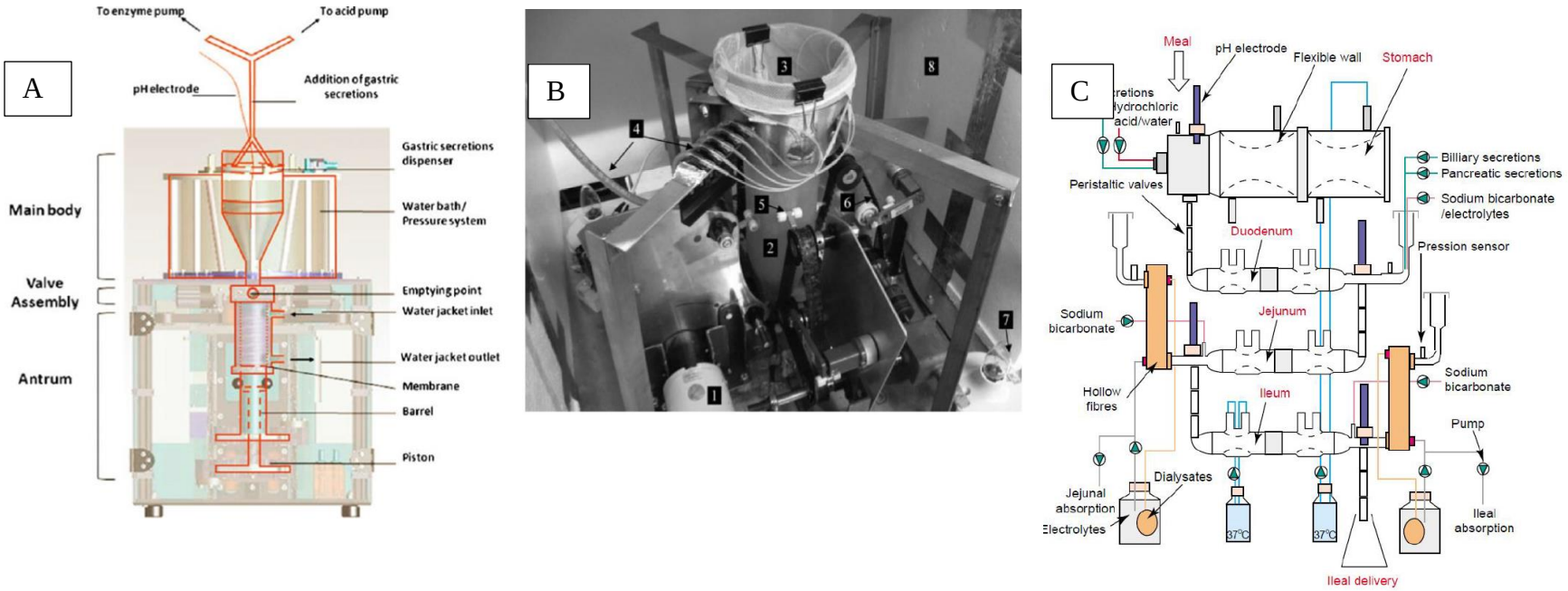

Figure 2.3. Images of *in vitro* dynamic digestion devices: a) Dynamic Gastric Model (DGM) (Figure is reproduced from Vardakou et al., 2011 with permission from Springer Verlag; b) Human Gastric Simulator (HGS) (Figure is reproduced from Kong and Singh, 2010 with permission from Wiley); c) TNO Gastrointestinal Model-1 (TIM-1) (Figures are reproduced from (Minekus et al., 1995 with permission from Elsevier Science)

CHAPTER 3

THE IMPACT OF PARTICLE SIZE AND FOOD TEXTURE RESISTANCE ON GASTRIC DISINTEGRATION AND EMPTYING

Do, D.H., AND F. KONG. To be submitted to: The Journal of Food Science.

3.0. Abstract

The objective of this study was to investigate the influence of initial food particle size and texture on gastric digestion by examining the changes in gastric disintegration and emptying rates. A water bath incubation method was used to perform *in vitro* static gastric digestion of carrot and ham. *In vitro* dynamic gastric digestion was conducted for various types of foods using a Dynamic Gastric Simulation Model (DGSM). The changes in the texture of gastric contents as indicated by bulk hardness resistance, the percent solids emptied, and the particle size distribution that encompassed 50% of digesta (D_{50}) were used as parameters to study disintegration kinetics and emptying patterns of different foods. Under static incubation, the tough structure of carrots showed slower rate of solids leaching than ham. In DGSM, medium size carrot particles (1.40- 2.00 mm) had the greatest disintegration with a faster bulk hardness reducing rate of 0.319N/min and a higher amount of solids emptied of 8.46% when compared to largest (2.00-3.34 mm) and smallest (1.14-1.40 mm) tested carrot particle ranges. Upon subjecting various foods to the DGSM, the behavior of the food texture influences the overall gastric digestion. Results from the simulated digestion trials indicate a high relationship between the initial bulk hardness predicting the final bulk hardness after 120 min digestion and the amount of solids emptied. Equations were derived to predict the level of food digestion as indicated by the final bulk hardness and the emptying rate by using the initial bulk hardness resistance.

Key Words: Gastric digestion, particle size, bulk hardness, gastric disintegration, gastric emptying.

3.1.Introduction

The stomach is one of the major organs responsible for digestion, and it relies on both physical and chemical degradation to achieve this task (Kong & Singh 2009). Chemical degradation of food is accomplished by gastric juice, which is composed of acid and enzymes. The secretion of hydrochloric acid by parietal cells in the stomach breaks down macronutrients through acid hydrolysis. In addition, the secretion of pepsinogen by chief cells in the stomach hydrolyzes protein through enzymatic reactions (Van Den Abeele et al., 2017). Acidification of the digesta enables hydrochloric acid and pepsin synergistically soften and increase nutrient leaching from ingested food (Kalantzi et al., 2006). In addition, the peristaltic contractions physically disintegrate food by grinding and mixing particles. Although the reported contraction forces are only 0.65 N, the sedimentation and stacking of particles enables the applied forces to grind and disintegrate the ingested food into smaller particles (Marciani et al., 2001). The contractions also increase the mixing of ingested food. The combination of the forceful waves and the constriction of the pylorus sphincter create a "retropropulsion" phenomenon (Ferrua & Singh 2010). During retropropulsion, smaller particles are emptied while larger particles are ejected back into the body of the stomach to be mixed (Abrahamsson et al., 2005). Increased mixing in the stomach further facilitates the disintegration of ingested food through erosion (Guo et al., 2014).

In addition to regulating the rate of disintegration, the peristaltic contractions also alter the gastric emptying patterns. As particles are initially required to be small enough in size to pass through the pylorus, the rate of gastric disintegration influences the rate of gastric emptying (Kong & Singh 2008). Beside the contractions, the physiological shape of the stomach influences the rate of solids being emptied. The shape of the stomach resembles the letter "J" with the site of gastric emptying (pylorus) roughly estimated to be 3 cm above the base of the stomach (Liding et al., 2016). Consumption of a large meal distends the stomach and increases the distance between the

emptying site and the base of the stomach (Hasler, 2009). The increased height difference may affect the rate of gastric digestion by retaining greater amount of solids. In addition to the physiological changes in the stomach during gastric digestion, physical properties of ingested food may influence the rate of digestion by altering both the disintegration kinetics and the emptying rate.

Food enters the stomach with different particle size ranges and various textures, and these two factors can influence gastric digestion by affecting disintegration kinetics and the emptying pattern of solids. Researchers have noted that foods pass into the gastric phase with varying particle sizes depending on the time of mastication within the oral phase (Bornhorst & Singh, 2012). Particle sizes may range from 0.82 mm for peanuts to 8.7 mm for carrots (Jalabert-Malbos et al., 2007, Lucas & Luke, 1986). The differences in surface areas resulting from the various particle sizes may alter the disintegration kinetics and emptying by affecting the rate of grinding, mixing, and retention time of ingested food (Bornhorst & Singh 2014). Foods may also enter the stomach with hard or soft texture. The initial hardness and the rates of softening have been proposed in recent publications to be used as indicators of food digestion (Bornhorst, Ferrua, and Singh, 2015). Investigation of the behavior of these various food textures in the gastric environment may provide useful information in developing foods with desired rates of disintegration and gastric emptying.

Cost, time, and ethical issues have forced scientists to develop alternative *in vitro* models to study the digestion of food (Bornhorst & Singh 2012). Simplified *in vitro* static gastric digestion trials are used to investigate the behavior of food under controlled conditions with constant pH and enzymes. More complex *in vitro* models incorporate important factors including gastric secretions, gastric forces, and gastric emptying to improve the simulation of the dynamic gastric environment (Hur, Decker, and McClements, 2009). One example is the Dynamic Gastric Simulation Model

(DGSM), which has been utilized to simulate dynamic gastric digestion (Do et al., 2016). The DGSM can simulate gastric contraction by using a probe to compress the food being digested, monitor the resistance the probe encounters when it moves into the gastric fluid, and indicate the textural change in digesta throughout the simulated gastric digestion. The emptying tube in the DGSM can be moved to different locations which allows for the study of gastric emptying rates at different stages of gastric distension. Ultimately, the objective of this study was to utilize DGSM to investigate the influence of initial particle size and food texture on disintegration kinetics and emptying rates.

3.2. Materials

Porcine mucin, porcine pepsin, and guar gum were obtained from Sigma–Aldrich Chemical Company (St. Louis, MO). Raw carrots, roasted peanuts, mozzarella cheese, parmesan cheese, ricotta cheese, ham, canned shrimp, tofu, croutons, and ground beef were purchased at a local supermarket (Athens, GA).

3.2.1. Methods

3.2.2. *In vitro* static gastric digestion of individual ham and carrots particles

Carrots and ham were subjected to static gastric digestion to investigate the influence of gastric juice on the chemical degradation of food as observed through textural changes and leaching of nutrients. The two foods were firstly cut into 3.0 mm cubes. Simulated gastric juice containing various salts, pepsin, and mucin were prepared following the method of Donhowe et al. (2014), and enzymes added on the day of the experiment. The simulated gastric juices were adjusted to an initial pH of 5.0, 3.0, and 1.5 with 1 N HCl to represent the environment from the initial, middle, and final stages of gastric digestion. Fifty (50) mL of simulated gastric juice at each pH were added to 6 Erlenmeyer's flasks. Carrots or ham (5.0 g) were placed in each set of six

Erlenmeyer's flasks and were incubated in a water bath at 37°C without any agitation. Over the 120-min experiment, a flask was removed every 20 min and the contents were filtered. Each cube was removed and subjected to a 50% compression test using a Food Technology Corporation TMS-Pro texture analyzer (Sterling, VA). The compression test utilized the probe from the DGSM, and the speed of compression was set to 30 mm/ min. A portion of the cubes were dried in a vacuum oven at 65.0°C at -20 in Hg for 24h. The weight differences before and after heating were determined, which represents the amount of leached nutrients from gastric juices at various pH.

3.2.3. Bulk hardness of gastric contents and its reduction during simulated digestion

During dynamic digestion trials, DGSM measured the resistance of the digesta containing both food and gastric juice, and recorded reduction of the resistance in real time throughout the experiments. This resistance is reported as "bulk hardness resistance" in this study, and is used as an indicator of overall changes of the texture of the gastric digesta. The peristaltic simulation was started with 3 contractions per minute. The minimum gap was set as 1 cm between the probe and the base of the stomach model where the maximum bulk force was recorded. Over 350 bulk hardness values were collected during the experiment. However, points were chosen at 0.1, 20, 40, 60, 80, 100, and 120 minutes to represent the overall trend for the bulk hardness reduction in the mixture containing simulated gastric juice and food.

3.2.4. Effect of particle size on gastric digestion

Carrots were reduced in size using a Ninja food processor, and wet sieved into three initial particle size ranges of 1.14-1.40 mm, 1.40- 2.00 mm, and 2.00-3.34 mm to represent small, medium, and large particles (Chino, CA). Carrots (20 g) were placed into simulated gastric juice (200 mL) at pH of 3.0 before transfer to the Dynamic Gastric Simulation Model. The model was started with the 1.0 mL/min continuous secretion of simulated gastric juice at pH 3.0. The

peristaltic simulation was started with 3 contractions per min with bulk hardness being measured continuously. Control trials were performed by placing the emptying tubes at 3 cm above the base of the model while collecting the digesta at the rate of 1.0 mL/min. Gastric distension was simulated in the DGSM by increasing the height differences between the base and the emptying site to 5 and 7 cm as depicted in Figure 3.2. Samples (20 mL) were collected every 20 min and analyzed for solids content by vacuum drying as described before. Particle size distribution was also measured with a Beckman Coulter LS- 12 320 particle size analyzer (Indianapolis, IN). The D_{50} value for each trial represents the theoretical particle size where 50% of the emptied digesta by volume can be filtered. The values reflect the level of erosion and fracturing of foods during simulated digestion.

3.2.5. Effect of food texture on gastric digestion

Raw carrots, mozzarella cheese, ham, canned shrimp, tofu, ricotta, and croutons were used as examples to test the effect of different food textures on the rate of disintegration and emptying. Additional trials were performed on ground beef that contained 70% beef/30% fat that was cooked on a skillet for 10 minutes. The moisture content of each food type was determined by grinding the samples to a particle size range of 1.14-1.40 mm and vacuum drying the samples as previously described. The foods were processed and sieved into a particle size range of 2.00-3.35 mm. Sample food (20 gram) were mixed with simulated gastric juice (200 mL) at pH 3.0. The resulting mixture was placed into the DGSM to digest for 120 min. During the digestion, the volume and pH were kept constant. Simulated gastric juice with a pH of 3.0 was pumped into the DGSM at a rate of 1.0 mL/min. The gastric emptying was simulated by removing the digesta at the rate of 1.0 mL/min with a peristaltic pump. Samples (20 mL) were continuously collected for 120 minutes at a location 3 cm above the base of the model (Fig. 1). Aliquots of the unfiltered samples was analyzed for

solids content by vacuum drying. The amount of solids removed were subtracted from the original solids content of 20 grams to obtain the solids remaining in the stomach chamber. The D_{50} values were determined by measuring the particle size distribution. The change in the bulk hardness of gastric content were measured in real time to indicate the softening and the disintegration of food due to continuously applied forces and chemical degradation.

3.2.6. Statistical analysis

Trials were conducted in triplicate. The means were compared between samples using Fisher's least significant difference test at $p < 0.05$ with SAS® software (version 9.3, SAS Institute Inc., Cary, NC). Regression equations and correlation coefficients (R^2) were derived using Microsoft™ Excel 2010.

3.3. Results and Discussion

3.3.1. *In vitro* static gastric digestion of ham and carrot

Static incubation experiments using carrots and ham were carried out to investigate the influence of gastric juice on the textural changes and solid leaching rates of the individual food particles. Due to the lack of mixing and mechanical forces, the digestion can be attributed solely to chemical degradation resulting from incubation with simulated gastric juice. Figures 3.3 A-B present the textural changes in carrots and ham upon incubating the food cubes at various pHs. Carrots had a firmer initial texture than ham with values of 14.87 N and 3.25 N, respectively. The textural changes of carrots followed power law decline in bulk hardness with faster rates occurring at lower pH.. At pH 5, rates of hardness reduction were small with a value of 0.037 N/min. Decreasing the pH to 3 and 1.5 showed increases in the hardness reduction rate to 0.071 N/min and 0.429 N/min, respectively. While changes in carrot texture showed an inverse relationship between declining hardness rates and simulated gastric pH, there were two patterns of hardness

reduction in ham. At the high pH of 5.0 and 3.0, the hardness reduction for ham followed linear trend with very limited rates of hardness reduction. Researchers have previously shown that ham resist hardness reduction during simulated gastric digestion (Kong & Singh, 2008). Much of the resistance in the hardness reduction of ham is attributed to the limited ability of gastric acid and enzyme to hydrolyze the native collagens (Weiss, 1976). Furthermore, power law reduction in the hardness of ham occurred at the highly acidic pH of 1.5. The power law reduction pattern resulted in an 86.1% reduction in the hardness of ham cube at pH 1.5 (Figure 3.3B). This is likely due to the synergistic effect of pepsin and hydrochloric acid on the protein structure in ham, as addition to facilitating acid hydrolysis, the highly acidic environment also encourages greater enzymatic hydrolysis of proteins as pepsin is more active at acidic conditions (Johnston et al., 2007).

The chemical degradation by gastric juice facilitated the leaching of nutrients. Figure 3.3C shows the leaching of nutrients resulting from the incubation of carrots and ham at pH of 1.5. The results showed that in both carrots and ham roughly 36% of solids leached out into the simulated gastric juice after 120 min. This agrees with previous reported similar mass losses in carrots and ham under static incubation conditions with simulated gastric juice (Kong & Singh, 2008). Figure 3.3C shows that the rates of solid loss for carrots followed a linear trend with the main reason attribute to the degradation of the cell walls through acid hydrolysis. In contrast, the leaching of solids from ham followed an exponential decay with 31.1% of solids loss within the first 40 min of gastric incubation. Previous researchers have attributed similar releases of solids to the combination of hydrochloric acid and pepsin working together to degrade the myofibrillar protein in ham while releasing fat (Lentle & Janssen, 2011). This chemical degradation further increases the rate of nutrients solubilizing with the gastric juice through the process known as dissolution. (Abrahamsson et al., 1998). Higher rates of food dissolution further promote greater emptying of

nutrients into the intestine as nutrients become soluble in the digesta (Kong & Singh, 2008, Amidon et al., 1995). Ultimately, the different structures and initial texture of carrots and ham influenced gastric digestion by regulating chemical degradation with great potential to alter the rate of nutrients leaving the stomach.

3.3.2. Effect of particle size on gastric digestion of carrots

During simulated digestion in DGSM, the progressive decline of bulk hardness was measured. The values were used as indicators of overall texture changes of the gastric content that are affected by both the rate of food softening and the rate of food disintegration. Bulk hardness is related to the overall disintegration with decreasing values indicating the production of particles with smaller size. As particles become smaller they give less resistance because the smaller particles take up less volume with lower void space. Figure 3.4 shows the initial bulk hardness and the bulk hardness changes of the carrot during digestion in DGSM with various particle size. The large carrot particles (2.00-3.35 mm) had a higher initial bulk hardness of 337 N and a power law declining trend during the digestion. When compared to the large carrot particles, reducing the particles to medium and small sizes led to lower initial bulk hardness values of 145 N and 39 N, respectively. Due to the large size, the carrot particles remained stagnant with poor mixing as shown in Figure 3.5A-C. The small particles are more influenced by the hydrodynamic mixing leaving less particles at the base of the model as shown in Figure 3.5D-E. Lower concentration of particles at the base created less resistance to the probe, and thus generating lower bulk hardness values.

Particle size affects gastric digestion by influencing the hydrodynamic mixing, which alters both the rates of disintegration and rates of gastric emptying. Adequate hydrodynamic mixing facilitates greater disintegration and emptying of food. Similar to the static incubation results, the

rates of hardness reduction follow a Power Law decline. The exponential value from the fitted power law decline was used to express the rates of bulk hardness reduction. Figure 3.4 shows that the medium size carrots (1.40-2.00mm) had the fastest rates of bulk hardness reduction of 0.319N/m. The results suggesting fast rates of softening and greater disintegration occurred in the medium size carrots. Data from Table 3.1 reaffirm the high disintegration of the medium carrot particles by showing a D_{50} (696 µm) value that was nearly half the size of the initial loaded particle range. The high level of disintegration combined with adequate mixing facilitated the greatest total percentage of emptied solids (8.46%) during the two hours digestion trial. Adequate mixing is thought to be the primary reason for the high disintegration and emptying of the medium size carrots. Within the medium size range, the smaller particles (close to 1.40 mm) were greatly mixed while the larger particles (close to 2.00 mm) were poorly mixed. The mixing of smaller particles permitted the carrots to disintegrate through erosion, and the poor mixing allowed the larger particles to settle near the base to be disintegrated through grinding. Moderate mixing further helped disperse particles near the opening of the emptying site to be removed. As shown in Table 3.1, the highest percentages of solids were emptied from the medium size carrots. This agrees with previously studies which reported that the suspension of medium size particles increased the solids to be emptied (Sirois et al., 1990).

The rates of disintegration and emptying of the small and large carrot particles are less than middle size carrots. The small carrot particles (1.14-1.40 mm) was observed to have the greatest mixing, but limited disintegration. Evidences of limited disintegration are shown through the lowest bulk hardness reducing rates of 0.213 N/min (Fig.3.3) and the retention of the initial particle size with a high D_{50} value of 998 µm (Table 3.1). This is because the hydrodynamic mixing mainly attributes to the disintegration of food through erosion (Guo et al. 2014). The high mixing

facilitates the greater dispersion of the small particles while showing moderate emptying rate with 4.33% of total solids emptied after 120 minutes. Moderate emptying was attributed to the smaller carrots size that were easily passed into the emptying tube. On the contrary, the large carrot particles are hard to disperse within the gastric fluid. As shown in Figure 3.5A-C, the particles reside at the base of the model with limited movement. The limited disintegration and dispersion prevented the particles from passing through the emptying tubes with a diameter of 2 mm. Although the rate of bulk hardness reduction was moderate with a value of 0.263 N/min, the retention of final bulk hardness of 86 N indicated limited disintegration. Disintegration occurred as shown through the small D_{50} value of 440 μm, but the rates of disintegration were low as reflected by the dismal 1.81% of total solids emptied after 120 minutes.

The different rates of gastric disintegration of various particles sizes also affect the amount and the size of the particles being emptied upon simulation of gastric distension. Table 3.1 indicates that the high amount of disintegration in the medium carrot particle sized carrots caused the height difference of emptying tube to have an inverse relationship to both the amount and the size of the particles being emptied. The greatest distension of the stomach was simulated with height difference of 7 cm. This height difference between the base of the model and the emptying site in the DGSM was selected to represent the initial stage of gastric digestion after consumption of a large meal. Both the amount and the size of the particles were small with values of 3.55% total solids emptied and a D_{50} value of 389μm even after 120 min of simulated gastric digestion. As gastric digestion proceeded, the height differences were lessening between the base of the stomach and the site of emptying to values of 5 and 3 cm. As the height differences decreased, both the amount and the particle size of solids emptied increased. Moving the emptying site to 5 cm increased the total percentage of solids emptied to 5.39% while significantly increasing the D_{50} to

486 μm. Furthermore, placing the emptying tube 3 cm above the base of the model significantly increased the total percentages of solids to 8.46% and increased the D_{50} to 696 μm. The data in Table 3.1 show that the gastric distension contributes to the reported gastric lag phase and gastric sieving effects through limiting both the percentages of solids emptied and allowing only smaller particles to be emptied at the initial stage of gastric digestion (Pera et al., 2002, Cassilly et al., 2008). Our results also indicate that gastric distension mainly influences the emptying rate of the medium carrot particles. Due to the limited disintegration of the small and large carrot particles, the gastric distension had only small influences in both the amount and size of particles being emptied. Ultimately, this study indicate that the particle size of foods could affect gastric digestion by influencing disintegration and emptying.

3.3.3 Effect of initial bulk hardness on gastric digestion

The initial bulk hardness of the gastric mixture containing food and gastric juice affects the overall disintegration kinetics and emptying patterns. Figure 3.6 and Table 3.2 indicate that in general, greater initial bulk hardness resisted softening and disintegration by retaining a high D_{50}. In addition, the higher initial bulk hardness also restricted the emptying rate by allowing low total percentages of solids emptied after 120 minutes of simulated gastric digestion. In contrast, food with lower initial bulk hardness generally showed faster rates of softening and quicker rates of disintegration with low D_{50} and high percentages of solids emptied. For example, carrots having the highest initial bulk hardness produced the largest D_{50} value of 440 μm and a dismal total solid emptying value of 1.81%. In contrast, tofu had a relatively low initial bulk hardness, and produced the lowest D_{50} of 18 μm and emptied the greatest number of solids (20.0%).

Variations in the initial bulk hardness has been attributed to the structural arrangements of elements in the microstructure (Aguilera and Lillford. 2008). The dense structure of raw carrots

generated a greater initial bulk hardness due to the intact cell walls, and when subjected to gastric juices showed resistance in bulk hardness reduction. The main reason is thought to be the high concentration of fiber in the carrot cell walls which impeded the chemical degradation from the simulated gastric juice (Kong and Singh, 2011). In contrast the weak structures of croutons, tofu, and ricotta cheese generated low initial bulk hardness resistance with quicker disintegration rates as depicted in Figure 3.7A. The weak structures of these foods are attributed to the processing methods that are often utilized to make the product. The stacking process of soy coagulants generate structure containing intermittent large cavities embed in the tofu (DeMan, DeMan, and Gupta 1986). Similarly, heating and acidification process further promote the formation of ricotta coagulant with weak structure (Lucey, Muno, and Singh 1999). The weak structures in these foods allowed greater gastric juice penetrations while permitting more chemical degradation through acids and enzyme hydrolysis upon entering the gastric environment. Simulation of the peristaltic contractions in DGSM enhanced fragmentation of particles as shown by the relatively low D_{50} values and the high total percentages of solids emptied after 120 minutes. The values are like the tofu disintegration results reported by researchers using another type of dynamic gastric model known as the Human Gastric Digestion Simulator (Kozu et al 2014). Similarly, high level of disintegration occurred in the ricotta cheese. This high level of disintegration allowed greater percentages of solids to be emptied. However, the ricotta cheese generated a higher D_{50} values with similar results in the literature showing the impact of acids and pepsin enzyme to generate larger coagulation of dairy proteins (Robinson et al., 1998).

Meats have different structures and showed different rates of gastric digestion, with cooked ground beef having the fastest rate of gastric digestion. This is likely due to the denaturation of the meat proteins which has been shown to generate macroscopic structural changes, enhancing the

permeability of acids and enzymes while facilitating chemical degradation in cooked ground beef (Lentle and Janseen, 2011). Ground beef had rapid disintegration shown through the low D_{50} value of 25.8 μm, and greater emptying with total 14.2% of the solids emptied after 120 minutes. In comparison, shrimp showed resistance to gastric digestion with relatively more intact solids, as shown in Figure 3.7B. Researchers have pointed out that the structural protein of shrimp resisted chemical degradation even after 16 h incubation with simulated gastric juice at pH 1.5 (Jackson, Duffy, and Jenkins 1987). In addition, certain proteins in shrimp have shown a high level of resistance to both pepsin and pancreatic digestion while remaining intact to elicit shellfish allergic responses (Toomer et al. 2015). Compared to the ground beef, shrimp showed moderate disintegration level as indicated by higher D_{50} value of 100 μm and lower amount of total solids emptied (8.9%). Even lower disintegration was observed in the digestion of muscle tissue. Researchers already found the high resistance of ham to the gastric environment and attributed the reason to the structure of ham. Ham is composed of myofibrillar proteins and collagen with intramuscular fat content. Roughly 10% of protein in ham is made up of collagen, the connective tissue which increases its tensile strength (Tornberg 2005). Researchers have found that the acids and pepsin in the gastric juice were unable to hydrolyze the peptide bonds in the helical region of the collagens (Weiss 1976). As a result, ham showed limited gastric digestion with low rates of bulk hardness reduction of 0.44 N/min and the least solids emptied (6.0%). Table 3.2 also shows that the D_{50} of ham was the smallest (18.01 μm). Figure 3.7C further demonstrate that most of the ham particle remained intact even after 120 min digestion in the DGSM suggesting low disintegration resulting from erosion and solid leaching.

3.3.4. Development of relationship between initial bulk hardness and food digestion

The initial bulk hardness affected the size of the emptied particle and the total percentage of solids emptied, and influenced the final bulk hardness of the gastric content containing food and gastric juices. An exponential relationship existed between the initial and final bulk hardness with an R^2 value of 0.89 as shown in Figure 3.8A. This correlation is developed based on eight out of the ten selected foods. Roasted peanuts and parmesan are not included as they had faster rates of bulk hardness reduction than other foods. The reason for this difference may be due to the low moisture and the relatively high fat content (>30%) in peanut and parmesan cheese. It has been reported that roasting of nuts and legumes liberates the water from the peanuts while disrupting the cell wall and the intercellular spaces of the food (Krokida and Philippopoulos. 2009). The relatively dried peanuts coupled with the disruption in cells walls is thought to allow diffusion of acids and enzymes into the voided space, which allows greater structural breakdown of roasted peanuts during digestion (Kong et al., 2013). In addition, the aging process removes the water and breakdown the structure of proteins in Parmesan cheese (Fox et al., 1993). When mixed with gastric juice, the acids and enzymes penetrate the spaces that were previously occupied by water, hydrolyze the matrix, and weaken the structure of Parmesan cheese. The high amount of fats in these two foods may also contribute to the faster rates of bulk hardness reduction. It was recognized that the fats in food provide the smoothness, but disrupt and weakens the food structural matrix (Michalski et al., 2007). In both cases, the hydrolysis of the protein liberates the fats from the structure leaving cavities within the food. Continuous contractions further facilitate the fast-structural breakdown leading to a low final bulk harness even with a high initial bulk hardness.

Excluding Parmesan cheese and peanut, an exponential relationship was used to predict the final bulk hardness with the given initial hardness. The graph on Figure 3.5 and the data on Table

3.2 show that the bulk hardness reduction rate follows a Power Law equation. Figure 3.8B-C showed that the final hardness also has a relatively high-power law relationship to the total percentage of solids emptied with an R^2 value of 0.88. Equations were derived using the data in Table 3.2 to predict the final hardness, the rates of hardness reduction, and the total solids emptied using the initial bulk hardness of the gastric mixture. Following equation can be used to calculate the final hardness:

$$y = 0.4237e^{0.0176x} \qquad [1]$$

where x= the initial bulk hardness, and y= the final bulk hardness. Figure 3.6 shows the bulk hardness of various foods follow a Power Law declining rate. Knowing the ratio differences between the final hardness and initial hardness allowed for the prediction of the hardness reducing rate at a given time set of 120 minutes. Equation 2 was used to calculate the rates of hardness reduction in the gastric mixture,

$$R= \ln (y/x)/ \ln (120) \qquad [2]$$

where R is the rate of bulk hardness reduction (unit: Newton/minute), x= the initial bulk hardness, and y= the final bulk hardness.

Equation 3, derived from the Power Law relationship, can be used to calculate the total percentage of solids emptied (ES%),

$$ES\%= 14.214(FH)^{-0.385} \qquad [3]$$

where ES is the total percentage of solids emptied, and FH= the final hardness. Two examples of calculation using these equations are shown on Table 3.3 which indicate a good agreement between the experimental values and the calculated values. To predict food digestion properties, the food can be mixed with gastric juice, and placed in a texture analyzer to measure initial bulk hardness. Then equation 1-3 can be used to estimate the final hardness and the emptying rate. However, as

all the trials were conducted using *in vitro* gastric model, further testing using *in vivo* trials are needed to validate these empirical equations.

3.3.5. Conclusion

In simulated gastric environment, food texture is degraded allowing nutrients to leak out with greater acidity promoting higher nutrient released. The greater breakdown occurred for the medium size carrot particles (1.40- 2.00 mm) with faster rate of disintegration and a higher emptying rate than small and large carrot particles. As food have various texture, the initial bulk hardness of food has been shown in this research to alter the rate of gastric digestion. With a tough structure containing large amount of indigestible cellulose, food like carrots showed the greatest resistance to gastric digestion with low disintegration rates, high D_{50} values, and low percentages of solids emptied. The weak tofu and ricotta cheese structure showed fast rates of gastric digestion by generating low bulk hardness with greater gastric disintegration. From the study, the initial bulk hardness resistance of the gastric mixture greatly impacts the digestion process allowing for the prediction of gastric disintegration and emptying. Ultimately, this study provides useful information in design of food structure that help regulate the rate of gastric digestion.

References

Abrahamsson, B., Alpsten, M., Bake, B., Larsson, A., & Sjogren, J. (1998). In vitro and in vivo erosion of two different hydrophilic gel matrix tablets. *European Journal of Pharmaceutics Biopharmarmaceutics*, *46*(1), 69-75.

Abrahamsson, B., Pal, A., Sjoberg, M., Carlsson, M., Laurell, E., & Brasseur, J. G. (2005). A novel in vitro and numerical analysis of shear-induced drug release from extended-release tablets in the fed stomach. *Pharmaceutical Research, 22*(8), 1215-1226.

Aguilera, J. M., & Lillford, P .J. (2008). Structure–Property Relationships in Foods.Food Materials Science. Springer, New York, NY

Amidon, G. L., Lennernas, H., Shah, V. P., & Crison, J. R. (1995). A theoretical basis for a biopharmaceutic drug classification: the correlation of in vitro drug product dissolution and in vivo bioavailability. *Pharmaceutical Research, 12*(3), 413-420.

Benini, L., Castellani, G., Brighenti, F., Heaton, K. W., Brentegani, M. T., Casiraghi, M. C., & ... et., a. (1995). Gastric emptying of a solid meal is accelerated by the removal of dietary fibre naturally present in food. *Gut*, 36(6), 825-830.

Bornhorst, G. M., & Singh, R. P. (2012). Bolus formation and disintegration during digestion of food carbohydrates. *Comprehensive Reviews in Food Science and Food Safety*, 11(2), 101-118.

Bornhorst, G. M., & Paul Singh, R. (2014). Gastric digestion in vivo and in vitro: how the structural aspects of food influence the digestion process. *Annual Review Food Science and Technology, 5*, 111-132.

Bornhorst, G. M., Ferrua, M. J., & Singh, R. P. (2015). A proposed food breakdown classification system to predict food behavior during gastric digestion. *Journal of Food Science, 80*(5), R924-934.

Cassilly, D., Kantor, S., Knight, L. C., Maurer, A. H., Fisher, R. S., Semler, J., & Parkman, H. P. (2008). Gastric emptying of a non-digestible solid: assessment with simultaneous SmartPill pH and pressure capsule, antroduodenal manometry, gastric emptying scintigraphy. *Neurogastroenterology Motility*, *20*(4), 311-319.

DeMan, J. M., deMan, L., & Gupta, S. (1986). Texture and microstructure of soybean curd (tofu) as affected by different coagulants. *Food Microstructure, 5*(1), 83-89.

Do, D. H., Fanbin, K., Penet, C., Winetzky, D., & Gregory, K. (2016). Using a dynamic stomach model to study efficacy of supplemental enzymes during simulated digestion. *LWT -- Food Science and Technology*, *65*, 580-588.

Donhowe, E. G., Flores, F. P., Kerr, W. L., Wicker, L., & Fanbin, K. (2014). Characterization and in vitro bioavailability of β-carotene: effects of microencapsulation method and food matrix. *LWT - Food Science and Technology, 57*(1), 42-48.

Ferrua, M. J., & Singh, R. P. (2010). Modeling the fluid dynamics in a human stomach to gain insight of food digestion. *Journal of Food Science*, 75(7), R151-R162.

Fox, P., Paul, L.. McSweeney, H.. Timothy, M., Cogan & Timothy P. G. (1993). Cheese: Chemistry, Physics and Microbiology (2nd ed.). London, UK, Chapman & Hall.

Grimes, D. S., & Goddard, J. (1977). Gastric emptying of wholemeal and white bread. *Gut,* 18(9), 725-729.

Guo, Q., Ye, A., Lad, M., Dalgleish, D., & Singh, H. (2014). Effect of gel structure on the gastric digestion of whey protein emulsion gels. *Soft Matter, 10*(8), 1214-1223.

Hasler, W.L., (2009). The Physiology of Gastric Motility and Gastric Emptying, Textbook of Gastroenterology. Blackwell Publishing Ltd. 207–230.

Hur, S. J., Decker, E. A., & McClements, D. J. (2009). Influence of initial emulsifier type on microstructural changes occurring in emulsified lipids during in vitro digestion. *Food Chemistry, 114*(1), 253-262.

Jackson, S., Duffy, D. C., & Jenkins, J. F. (1987). Gastric Digestion in Marine Vertebrate Predators: In vitro Standards. *Functional Ecology,*(3), 287.

Johnston, N., Dettmar, P. W., Bishwokarma, B., Lively, M. O., & Koufman, J. A. (2007). Activity/stability of human pepsin: implications for reflux attributed laryngeal disease. *Laryngoscope, 117*(6), 1036-1039.

Kalantzi, L., Goumas, K., Kalioras, V., Abrahamsson, B., Dressman, J. B., & Reppas, C. (2006). Characterization of the human upper gastrointestinal contents under conditions simulating bioavailability/bioequivalence studies. *Pharmaceutical Research Research, 23*(1), 165-176.

Kong, F., Singh, R. P. (2008). Disintegration of solid foods in human stomach. *Journal of Food Science, 73*(5), R67-80.

Kong, F., Singh, R. P. (2009). Digestion of raw and roasted almonds in simulated gastric environment. *Food Biophysics, 4*(4), 365-377.

Kong, F., & Singh, R. P. (2011). Solid loss of carrots during simulated gastric digestion. *Food Biophysics, 6*(1), 84-93.

Kong, F. B., Oztop, M. H., Singh, R. P., & McCarthy, M. J. (2013). Effect of boiling, roasting and frying on disintegration of peanuts in simulated gastric environment. *LWT - Food Science and Technology*, 50(1), 32-38

Krokida, M. K., & Philippopoulos, C. (2005). Rehydration of dehydrated foods. *Drying Technology*, 23(4), 799-830.

Jalabert-Malbos, M. L., Mishellany-Dutour, A., Woda, A., & Peyron, M. A. (2007). Particle size distribution in the food bolus after mastication of natural foods. *Food Quality and Preference, 18*(5), 803-812.

Lentle R. Janssen P. (2011). The physical processes of digestion, Springer, New York, NY, USA, 47–61

Liding, C., Yufen, X., Tingting, F., Zhenkai, L., Peng, W., Xuee, W., & Xiao Dong, C. (2016). Gastric emptying and morphology of a "near real" in vitro human stomach model (RD-IV-HSM). *Journal of Food Engineering, 183*, 1-8.

Lucas, P. W., & Luke, D. A. (1986). Is food particle size a criterion for the initiation of swallowing? *Journal of Oral Rehabilitation, 13*(2), 127.

Lucey, J. A., Munro, P. A., & Singh, H. (1999). Effects of heat treatment and whey protein addition on the rheological properties and structure of acid skim milk gels. *International Dairy Journal*, 9, 275-279

Marciani, L., Young, P., Wright, J., Moore, R., Coleman, N., Gowland, P. A., & Spiller, R. C. (2001). Antral motility measurements by magnetic resonance imaging. *Neurogastroenterology Motility, 13*(5), 511-518.

Michalski, M. C., Camier, B., Gassi, J. Y., Briard-Bion, V., Leconte, N., Famelart, M. H., & Lopez, C. (2007). Functionality of smaller vs control native milk fat globules in Emmental cheeses manufactured with adapted technologies. *Food Research International, 40*(1), 191-202.

Pera, P., Bucca, C., Borro, P., Bernocco, C., De, L. A., & Carossa, S. (2002). Influence of mastication on gastric emptying. *Journal of Dental Research*, 81(3), 179-181.

Robinson, R. K., R. Scott, & Wilbey, R. A. (1998). Cheesemaking Practice. Gaithersburg, Md: Aspen. 161-163.

Toomer, O. T., Do, A. B., Fu, T. J., & Williams, K. M. (2015). Digestibility and immunoreactivity of shrimp extracts using an in vitro digestibility model with pepsin and pancreatin. *Journal of Food Science, 80*(7), T1633-T1639.

Tornberg, E. (2005) Effects of heat on meat proteins - implications on structure and quality of meat products. *Meat Science*, 70, 493-508

Van Den Abeele, J., Brouwers, J., Tack, J., & Augustijns, P. (2017). Research paper: Exploring the link between gastric motility and intragastric drug distribution in man. *European Journal of Pharmaceutics and Biopharmaceutics, 112*, 75-84.

Weiss, J. B. (1976). Enzymatic degradation of collagen. *International Review of Connective Tissue Research*, 7, 101-157.

Results:

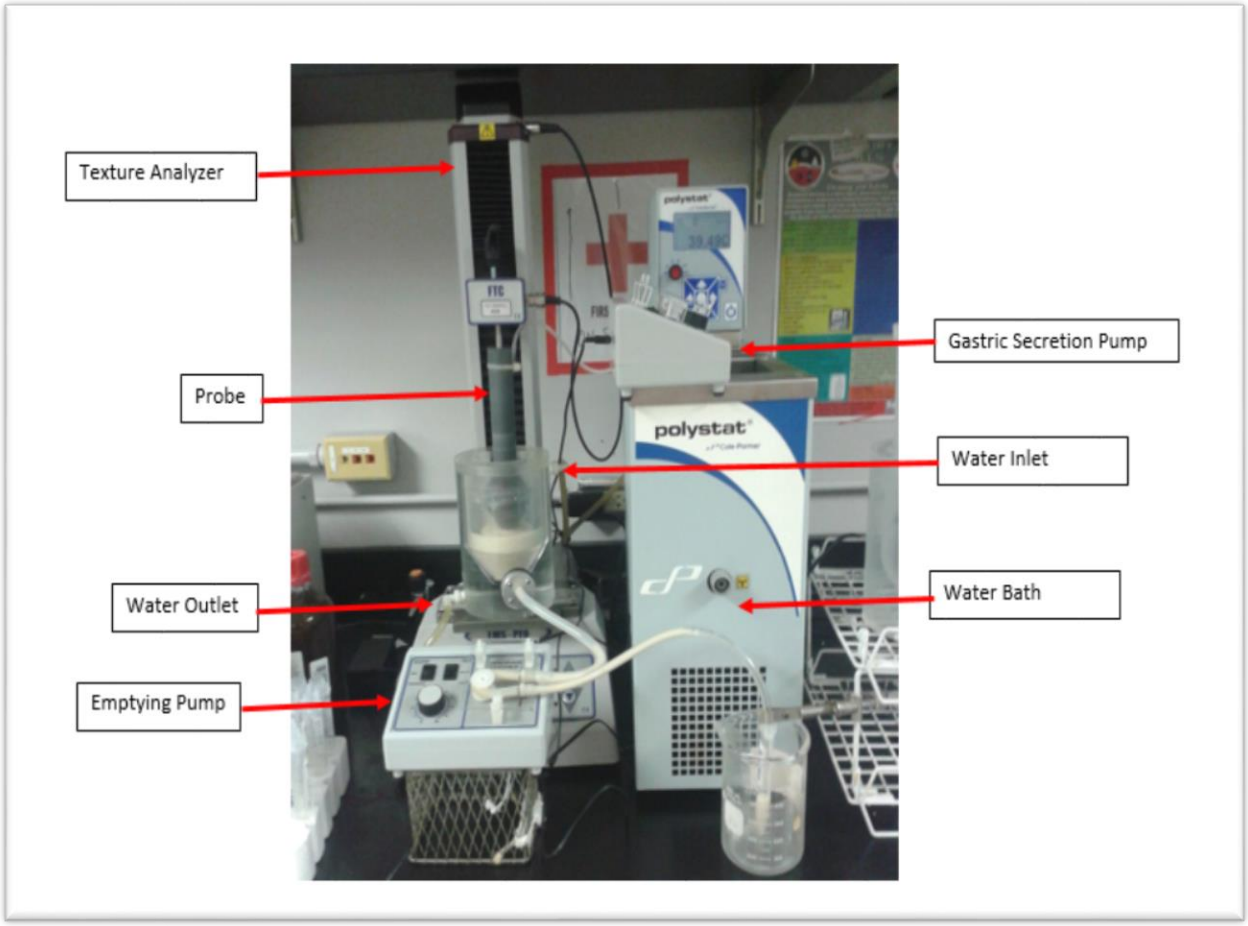

Figure 3.1. Schematic of the DGSM with pumps to simulate gastric secretion and gastric digestion. The probe is attached to the texture analyzer, and the gastric chamber is attached to a circulating water bath to ensure internal temperature of 37˚C.

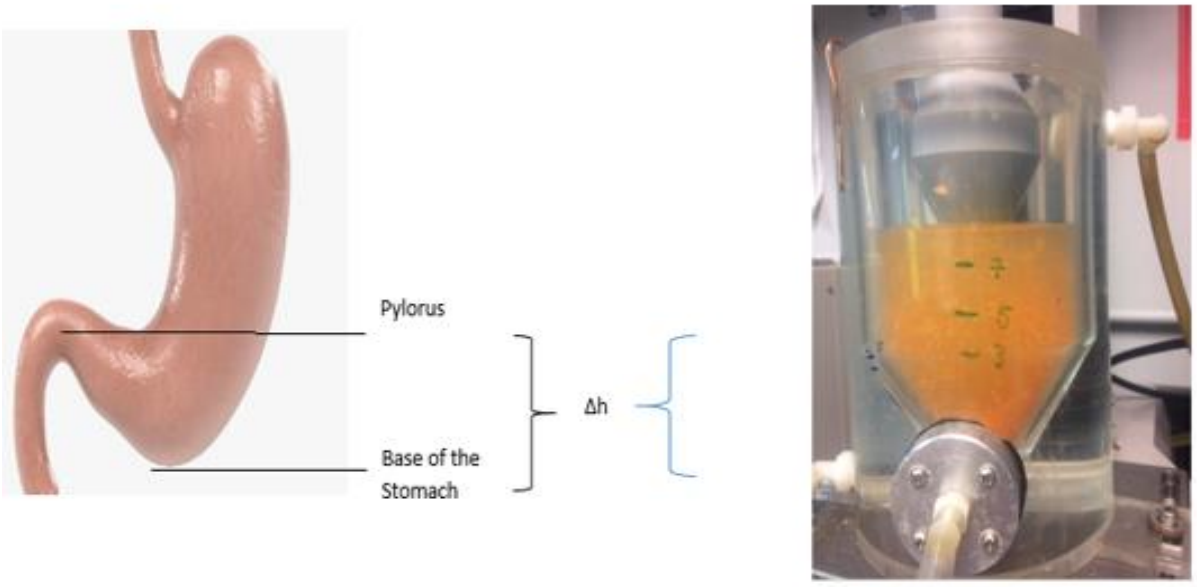

Figure 3.2. Simulation of gastric distension altering the emptying site. The emptying tube was placed 3, 5, and 7 cm above the base of the DGSM to simulate the height difference (Δh) resulting from gastric distension.

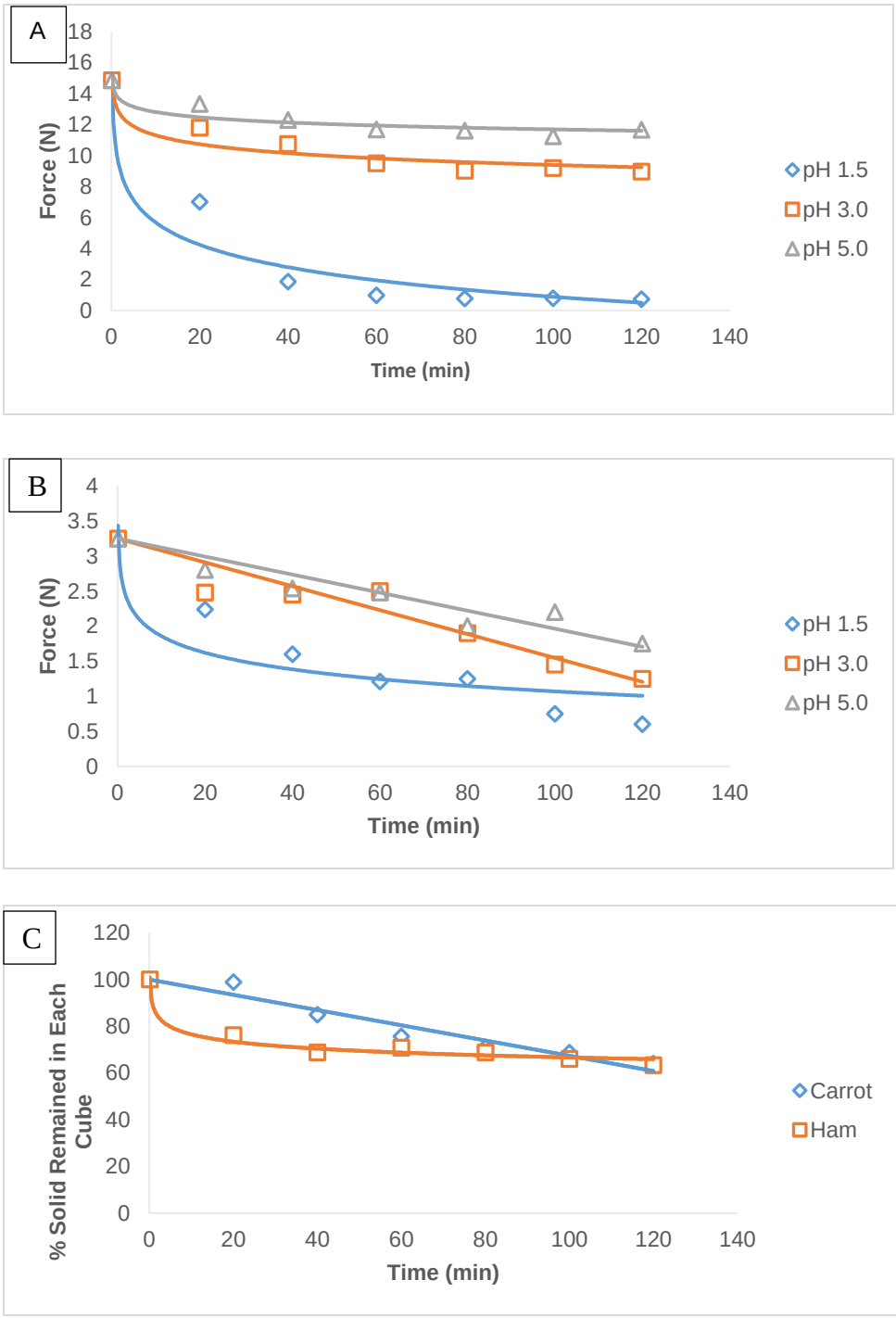

Figure 3.3. The hardness reduction for (A) Ham and (B) Carrots after incubation with simulated gastric juice at pH 1.5, 3.0, and 5.0. (C) Amount of solids leached for (◊) Carrots and (□) Ham during incubation at pH 1.5.

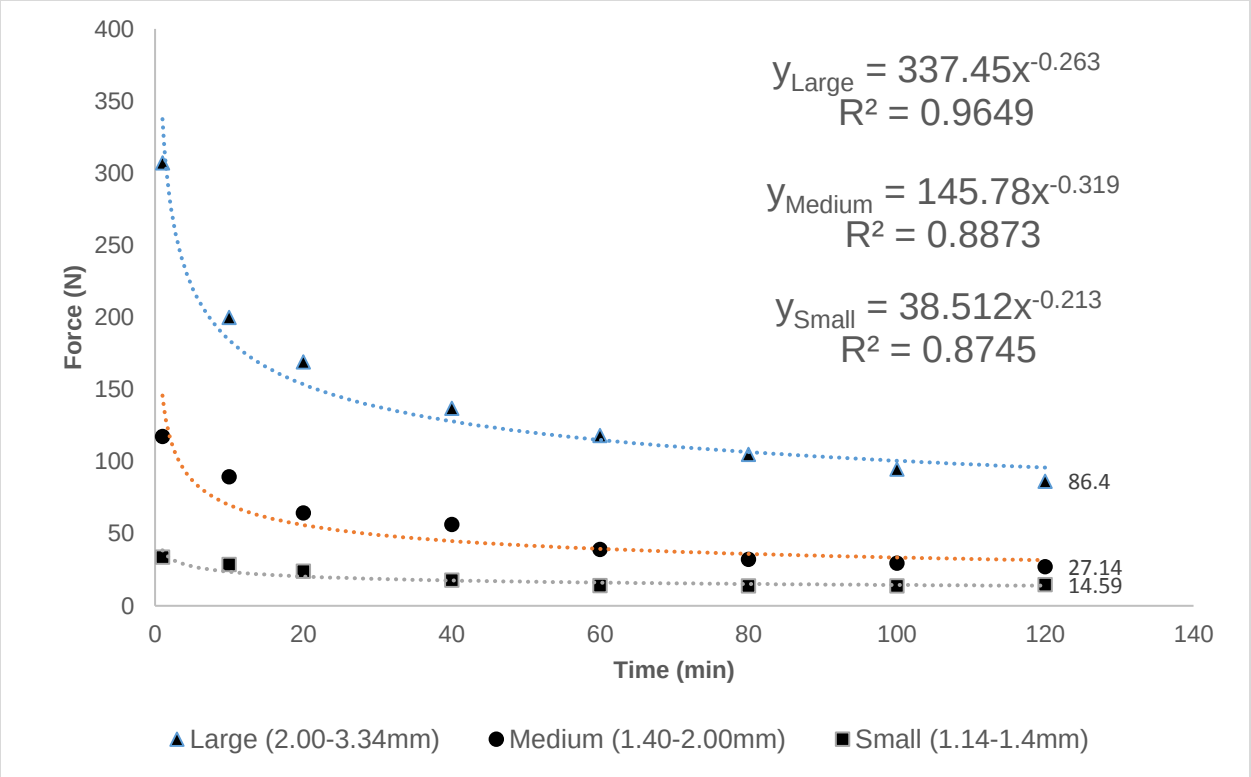

Figure 3.4. The initial hardness, the rate of hardness reduction, and the final hardness of carrots during dynamic digestion with initial particle size of [□] 1.14-1.40mm, [o] 1.40-2.00mm, [Δ] 2.00-3.35 mm. The softening profile of carrots followed Power Law decline in hardness.

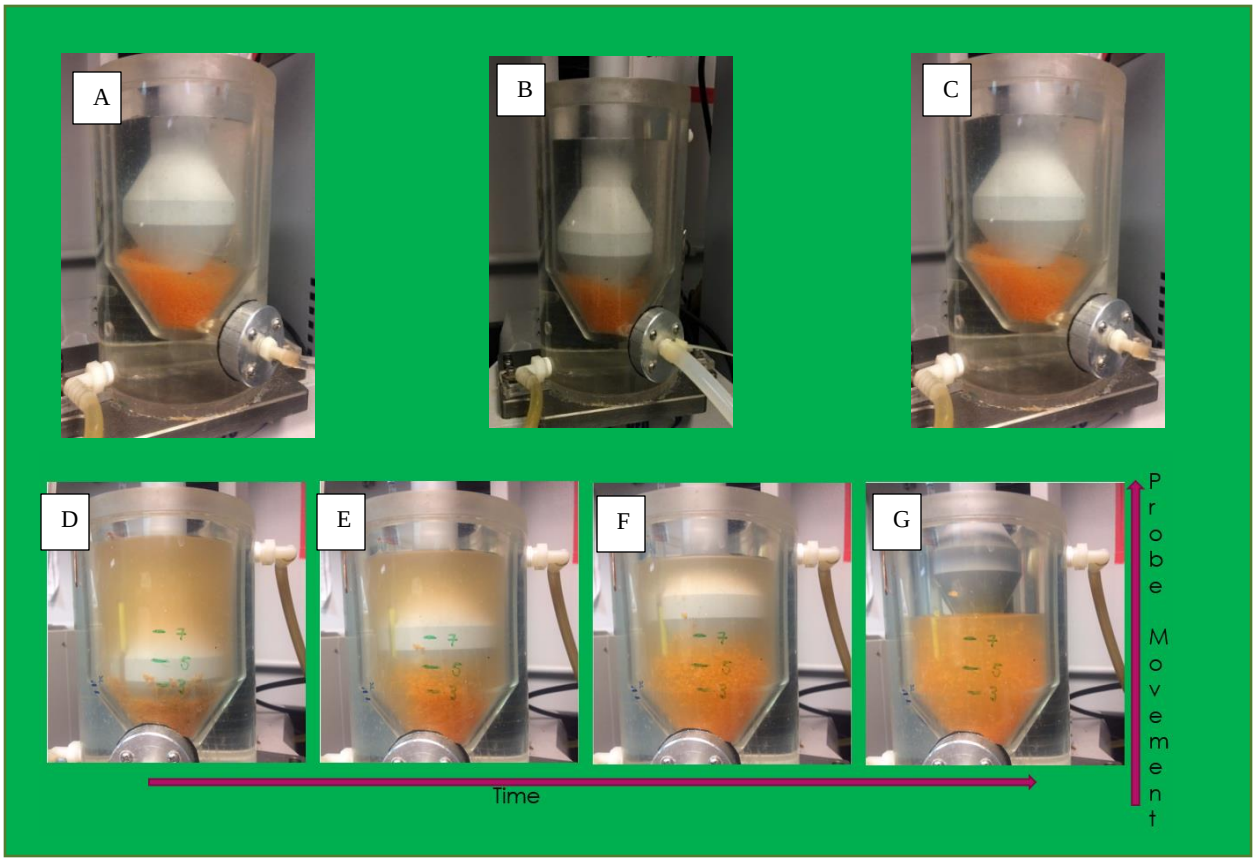

Figure 3.5. Mixing pattern of large 2.00-3.35 mm carrot particles in the DGSM shown on the top row from A through C. The mixing pattern of small (1.14-1.40mm) carrot particles is shown in the bottom row from D through G with limited movement of the carrot particles in the DGSM.

Table 3.1. The D_{50} and the total emptied content at various emptying locations

		Δ 3 cm	Δ 5 cm	Δ 7 cm
Small (1.14-1.40 mm)	Total Percentage Solids Emptied (%)	4.33^{b}_{x} ±0.4	2.81^{b}_{y} ±0.2	2.52^{b}_{y} ±0.2
	D_{50} (μm)	998^{a}_{x} ±24	950^{a}_{x} ±28	802^{a}_{y} ±25
Medium (1.40-2.00 mm)	Total Percentage Solids Emptied (%)	8.46^{a}_{x} ±0.6	5.39^{a}_{y} ±0.4	3.55^{a}_{z} ±0.3
	D_{50} (μm)	696^{b}_{x} ±33	486^{b}_{y} ±15	389^{b}_{z} ±36
Large (2.00-3.35 mm)	Total Percentage Solids Emptied (%)	1.81^{c}_{x} ±0.2	1.32^{c}_{x} ±0.2	1.82^{c}_{x} ±0.3
	D_{50} (μm)	439^{c}_{x}±41	375^{c}_{x} ±33	399^{c}_{x} ±35

The average values of total percentage of solids emptied and D_{50} are shown with the standard deviation. Different letter in the superscript indicates a significant difference at $p<0.05$ between the rows symbolizing the influence of particle size. Different letter in the subscript indicates a significant difference at $p<0.05$ between the column symbolizing the influence of heights.

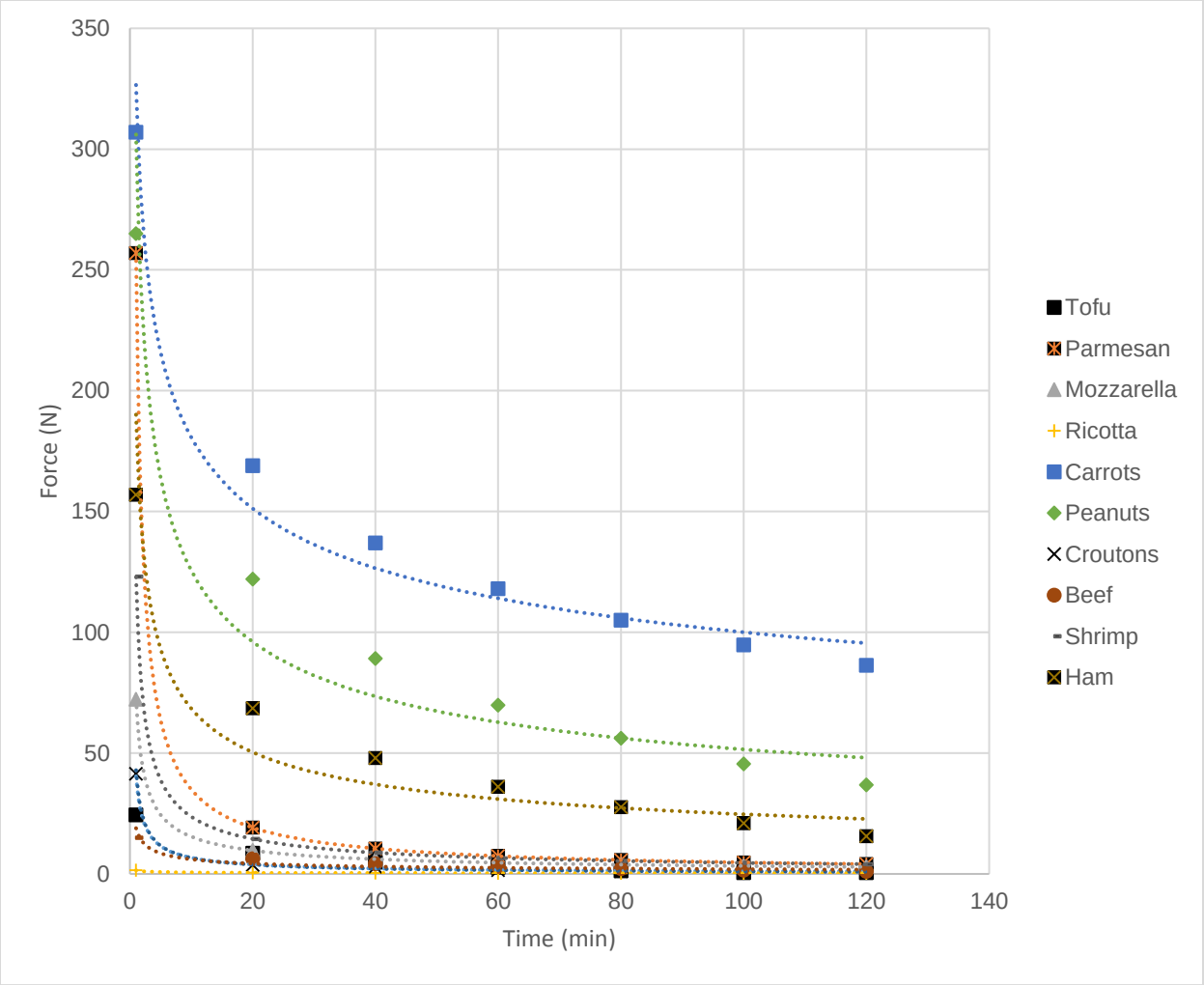

Figure 3.6. Hardness reduction of various food mixture during simulated gastric digestion

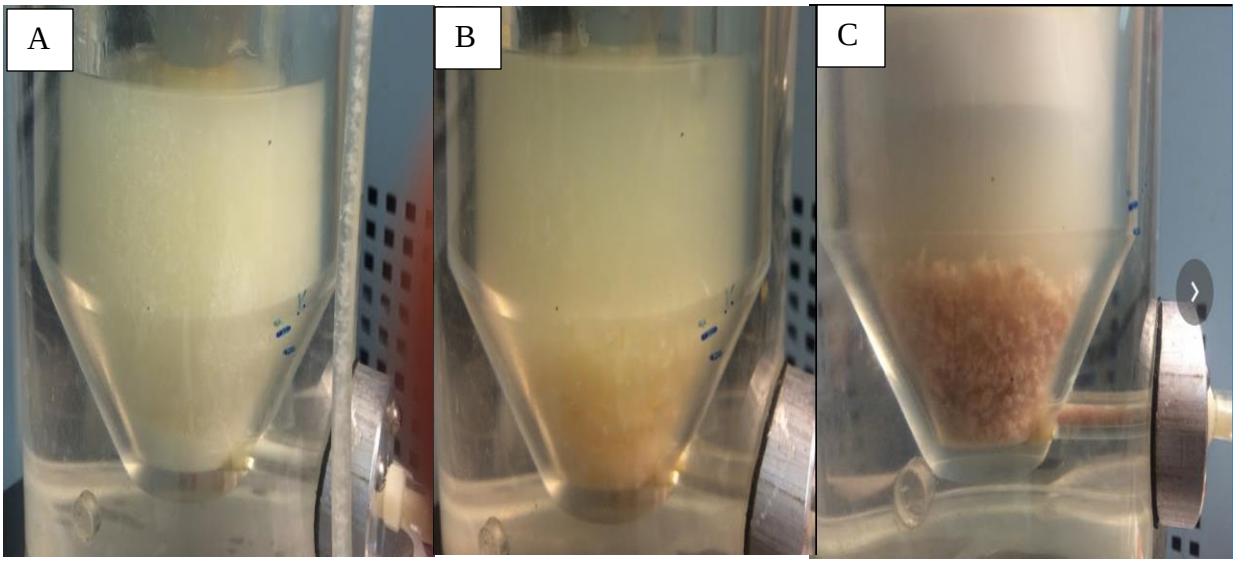

Figure 3.7. The food gastric disintegration shown through: A) high disintegration in tofu, B) moderate disintegration of shrimp, and C) low disintegration of ham after 120 minutes of gastric digestion inside the DGSM.

Table 3.2. The Disintegration and Emptying of Various Digested food

Food	**Moisture (%)**	**Initial Hardness (N)**	**Final Hardness (Newton)**	**Rates Newton /minute**	**D_{50} (µm)**	**Total solid removed (%)**
Carrots	91 ±2	326±9	86.0±3	0.26±0.03	440 ± 40	1.8±0.2
***Peanut (Roasted)**	1±0	306±4	37±1	0.39±0.02	24±2	6.51±0.5
***Parmesan**	21±0	257±7	4.0±1	0.87±0.03	39±2	9.1±0.1
Ham	65±0	190±4	16.0±2	0.44±0.06	18 ± 4	6.0±0.6
Shrimp	72 ±1	122±11	4.0±0	0.71±0.01	100 ±15	8.9±0.3
Mozzarella	46±0	72±3	3.0±0	0.67±0.04	27 ± 1	8.3±0.3
Tofu	84±1	42 ±5	1.0±0	0.88±0.02	18± 1	20.0±0.4
Croutons	5±1	40±2	1.0±0	0.78±0.04	48 ± 4	19.3±0.1
Cooked Ground Beef	23±0	19±2	1.0±0	0.49±0.02	26 ± 1	14.2±0.6

* The two selected foods that were not used as part of the correlation

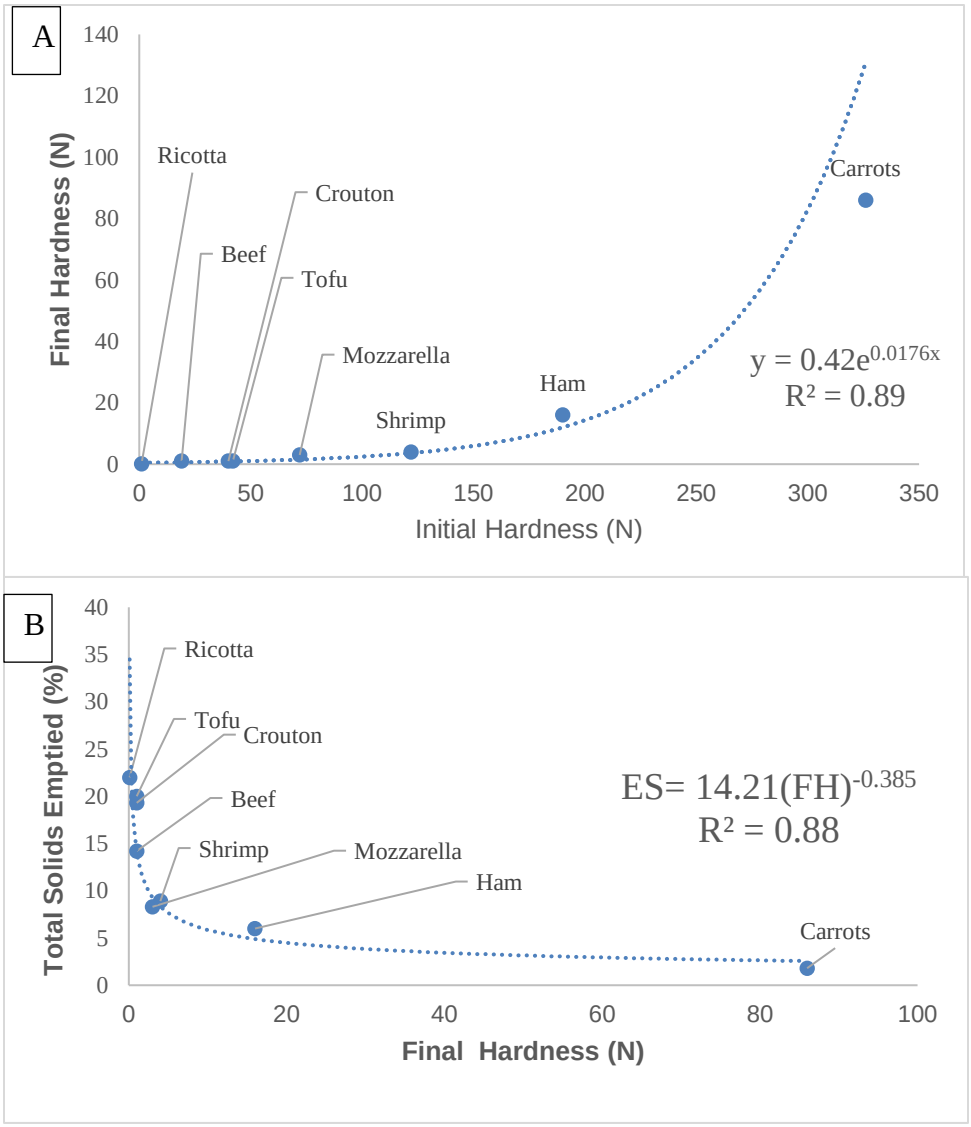

Figure 3.8. Correlation of final hardness with: A) Initial hardness and B) total percentage of solids emptied for various foods.

Table 3.3. Predicted and experimental values calculated from initial hardness

	Croutons		Shrimps	
	Predicted	**Experimental**	**Predicted**	**Experimental**
Initial Hardness	40.00 ±2.00	40.00 ±2.00	122.00 ±11.00	122.00 ±11.00
Final Hardness	0.86 ± 0.02	1.00 ±0.00	3.63 ±0.58	4.00 ±0.00
Rates of Hardness Reduction	0.80 ± 0.01	0.88 ±0.02	0.73 ±0.02	0.71 ±0.01
Total percentages of solids emptied	15.10 ± 0.16	20.0 ±0.40	8.65 ±0.53	8.90 ±0.30

CHAPTER 4

INFLUENCES OF VISCOSITY ON GASTRIC DISINTEGRATION AND EMPTYING OF FOOD IN A DYNAMIC GASTRIC SIMULATION MODEL

Do, D.H., AND F. KONG. To be submitted to: The Journal of Food Science.

4.0. Abstract:

In this study, an *in vitro* Dynamic Gastric Simulation Model (DGSM) to investigate the impact of viscosity on gastric disintegration kinetics and emptying patterns of foods. Peanuts, tofu, and carrots were tested in DGSM under different viscosity and their particle size fractions were determined. Results indicated that increasing the digesta viscosity to the range of 0.40-76.74 Pa·s, with guar gum concentrations of 0.0-2.0%, reduced the disintegration levels of peanuts, tofu, and carrots. To further investigate the influence of viscosity on the food emptying, both indigestible (amberlite beads) and digestible solids (carrots) were mixed with guar gum before being loaded in DGSM for simulated gastric digestion. The results indicated that increasing viscosity up to values 8.20 Pa·s for amberlite and carrots improved the particle dispersion and increased rates of solids emptying. Increasing the viscosity of the digesta beyond the critical viscosity hindered emptying of amberlite and carrot solids from the DGSM. The emptying rates of both indigestible and digestible solids were described with a mathematical model based on Particle-Emptying Coefficient (PEC). Modification of the equation allowed for the prediction of emptying rates based on the tested viscosity of the digesta.

Key Words: Dynamic Gastric Simulation Model, gastric viscosity, gastric emptying rate, Particle-Emptying Coefficient, gastric disintegration

4.1. Introduction

The disintegration of food within the stomach is thought to be critical, affecting both the release and absorption of nutrients (Kong and Singh, 2008). Food is masticated, swallowed, transported down the esophagus, and the contents are deposited in the stomach. Within the stomach, ingested food encounters gastric juice that softens and promotes the leaching of nutrients. The secreted hydrochloric acid (HCl) from Parietal cells hydrolyzes food via acid hydrolysis while the secreted pepsinogen from Chief cells eventually hydrolyzes the protein components (Gritti et al., 2000). Contractions within the stomach facilitate the disintegration of food through peristaltic movements that mix and grind particles. The greatest reported speed of mixing occurs within the center region of the stomach where retropropulsive speeds reach a range of 3.6-5.2 cm/s (Bouldby et al., 1999). Hydrodynamic mixing of food within the human stomach enhanced particle interactions while encouraging the disintegration of food through erosion. Greater contraction strength occurs near the narrow pylorus where food is disintegrated by the grinding of particles. The strong contraction strength overcomes the cohesive forces within the food resulting in the fracturing of food particles (Quo et al., 2014). In addition to hormones and other feedback mechanisms, the peristaltic contraction waves influence the rate of gastric emptying. With the help of the pylorus, the peristaltic contraction moves the particles to the emptying site to facilitate the removal of particles smaller than one millimeter while retaining larger particles for further disintegration within the stomach (Hellström et al., 2006).

Recent studies have suggested that the changes in stomach digesta viscosity may influence both the rates of gastric disintegration and the rate of gastric emptying (Prove & Ehrlein, 1982). The viscosity of digesta may vary from a low viscosity of 0.001 Pa·s after consumption of water. The viscosity of the digesta can be increased with the incorporation of dietary fibers with a

maximum viscosity about 29.5 Pa·s, as reported in one *in vivo* digestion trial (Marciani et al., 2001). Once in the stomach, the gastric environment may reduce the viscosity of the digesta. For example, the secretion of gastric juice has been known to hydrolyze and dilute the digesta to reduce the viscosity, as one study show the decrease of digesta viscosity from 11 Pa·s to 2 Pa·s immediately after the food moved into the stomach (Marciani et al., 2000). The same research also pointed out that the gastric juice further reduced the viscosity as the value dropped to 0.3 Pa·s after 30 minutes into the gastric digestion. Other researchers showed similar results indicating that the decrease in viscosity is attributed to the gush of gastric juice that further dilutes and acid hydrolyzes the dietary fiber (Versantvoort et al., 2004). The influence of viscosity on the rate of gastric disintegration and the rate of gastric emptying are debatable. Conflicting evidence shows that increasing viscosity may positively or negatively affect the rate of digestion. For example, one study showed that increased viscosity slowed down the emptying rate and promoted food disintegration within the stomach (Marciani et al., 2001). Another study showed that an increase in viscosity had caused an increased emptying rate of poorly disintegrated solids with particle sizes larger than 4.0 mm leaving the stomach (Paulson et al., 2001). Further investigation is needed to clarify the effects of viscosity on both the disintegration kinetics and the gastric emptying rate.

In vivo models, such as humans, rats, pigs, and canines, have been used to study the influence of viscosity on the digestion of food (Meyer et al., 1986; Sirois et al., 1990). However, the reproducibility and the high cost of these trials may not be feasible for all investigators. Simplified *in vitro* methods are often deployed to simulate digestion. *In vitro* static digestion models incorporate constant conditions, including hydrodynamic mixing, amount of enzymes, and amount of acid or base. A more realistic approach is to use a dynamic digestion model that simulates the digestive environment with the incorporation of contractions that mimic the

peristaltic movements (Hur et al., 2011). An example is the Dynamic Gastric Simulation Model (DGSM) that simulates gastric secretion, gastric peristaltic contractions, and gastric emptying (Duc, et al 2015). The objective of this study was to use the DGSM to investigate the influence of viscosity on gastric disintegration kinetics and gastric emptying rates. Carrots, peanuts, and tofu, with varying degree of hardness were subjected to digestion in the DGSM to investigate the effect of viscosity on the gastric disintegration. Indigestible solids including polystyrene, glass, and amberlite beads were used to understand the mechanisms involved in food emptying. An empirical equation was used to describe the emptying rate of the indigestible solids and the results were compared with carrot emptying as influenced by viscosity.

4.2. Materials and Methods

Porcine mucin, porcine pepsin (CAS: 47641, Lot: BCBM 7678V), guar gum, and amberlite were obtained from Sigma–Aldrich Chemical Company (St. Louis, MO). Carrots, tofu, and roasted peanuts were purchased at a local supermarket (Athens, GA). Indigestible solids including amberlite beads, glass beads and polystyrene foam were purchased at a local craft store (Athens, GA).

4.2.1. Preparation of samples and solutions

Guar gum was used to increase the viscosity of the digesta because of its stability in an acidic environment. Simulated gastric juice was prepared with various salts, mucin, pepsin, and hydrochloric acid (Donhowe et al., 2014). The simulated gastric juice solution (200 mL) was mixed with 0.0, 0.5, 1.0, 1.5, 2.0% w/w of guar gum, and the viscosity were measured at shear rates from 1-200 /s by using a Texas Instrument Rheometer DHR3 (New Castle, DE) with a vane attachment. The viscosity measurements were performed at constant temperature (37°C) maintained with a water circulating jacketed vessel. Particles of food entering the stomach varied

from 0.82 mm for peanuts to 8.7 mm for carrots, and were highly dependent on the amount of time these foods spent in the oral phase (Jalabert-Malbos et al., 2007, Lucas and Luke, 1986). Based on this information, an average particle size of 3.35-2.00 mm was used in these experiments. Tofu and peanuts were first placed in a Ninja food processor to reduce the particle size (Chino, CA). The food was subsequently filtered through two sieves with pore sizes of 3.35-2.00 mm. The food was added into simulated gastric juice with pH adjusted to 1.5, 3.0, or 5.0 to simulate the various conditions that may exist during human gastric environment.

4.2.2. Food disintegration at low viscosity gastric environment

Carrots, peanuts, or tofu (20g) were added to the simulated gastric juice mixture with no guar gum at the various pH to serve as the control group. Each solution was loaded into the DGSM, the peristaltic contractions were initiated and the simulated gastric digestion continued for 120 min. A full description of the model may be found in Do et al (2016) with slight modifications. The continuous gastric secretion or continuous gastric emptying were not included in the digestion trials to help reduce confounding factors in this portion of the experiment. After 120 min, the entire contents were removed from the DGSM. The samples were filtered by wet sieving under hot (~60°C) running tap water with pore sizes of 3.35, 2.00, 1.40, 1.14, 1.00, 0.50, and 0.30 mm. Each fraction was collected, and vacuum filtered with Fisherbrand Qualitative P8 Grade Plain Filter Paper circles (Waltham, MA). After filtration, the contents were dried in a vacuum oven at 65°C for 24 hours under vacuum pressure of -20 in Hg. The weight differences were calculated, and the results indicate the percentage of solids found in each particle size fraction. The DGSM measured the real-time resistance of the gastric mixture throughout the 120 minutes of simulated digestion. A minimum gap of 1.5 cm between the probe and the base of the stomach chamber was set for the contraction simulation, in which the maximum resistance was recorded, and defined as “bulk

hardness" of the gastric mixture. The profiles of the bulk hardness reduction were recorded for each food and used to signify the rate of food softening and food disintegration resulting from acid penetration and simulated peristaltic contractions.

4.2.3. Influence of viscosity on gastric disintegration

Carrots, peanuts, or tofu (20g) were added to the simulated gastric juice mixture with 0.0, 0.5, 1.0, 1.5, 2.0% w/w of gastric guar gum solution (200 mL) at various pHs. Each solution was loaded into the DGSM before the peristaltic contractions were initiated, and the simulated gastric digestion continued for 120 minutes. Similar to the procedure described above, the entire contents were removed from the DGSM. The samples were subsequently filtered by wet sieving under hot (~60°C) running tap water for 60 seconds to solubilize and remove most of the guar gum while isolating solids within sieve pans with pore sizes of 3.35, 2.00, 1.40, 1.14, 1.00, 0.50, and 0.30 mm. Each fraction was filtered and dried as described above. The weight differences were calculated to express the percentage of solids in each particle size fraction.

4.2.4. Influence of viscosity on the gastric emptying rate of carrots

Trials were performed on carrots with guar gum concentrations of 0.5, 1.0, 1.5, and 2.0% w/w. The guar gum was dispersed in simulated gastric juice with the initial pH of 3.0. The viscosity was measured as described above. Carrots were processed, and sieved to obtain particle size range of 1.40 -1.00mm. The carrots (20 gram) were added to the guar gum solution (200 mL) before being loaded into the DGSM. During digestion, the rate of secretion of the simulated gastric juice was set as 1.0 mL/min with the same viscosity gastric fluid being pumped into the DGSM. The initial rate of gastric emptying was set at 3.0 mL/min. Five emptied digesta samples were taken during the 60 min of gastric simulation trials. As described previously, the digesta samples were wet sieved to remove the guar gum. The solids were collected, vacuum filtered, and then dried in

a vacuum oven. The solids content in the emptied digesta was measured and the values signify the average amount being emptied during the 60 min.

4.2.5. Influence of viscosity on gastric emptying of amberlite

The objective of this study was to understand the mechanisms involved in gastric emptying of solids. Indigestible beads were used to avoid physical chemical changes in the solids during simulated digestion, so that the emptying rates are only affected by the initial physical characteristics (density and particle size). Guar gum solutions were prepared by dispersing 0.0, 0.2, 0.4, 0.6, 0.8, and 1.0% w/w in 200 mL water and mixing for 2 h to allow for complete hydration. The viscosities of these fluids were measured using the method described above. Amberlite, polystyrene foam, and glass beads (5.0 g) with corresponding densities of 300, 1250, and 2400 kg/m^3 were mixed with the guar gum solutions. The mixtures were loaded into the DGSM and peristaltic contractions were initiated with 3 per min. Gastric secretion was simulated at a rate of 1.0 mL/min with the same viscosity as for the gastric mixture. Gastric emptying was simulated by placing an emptying tube 3.0 cm above the base of the DGSM to pump out digesta. The emptying site was chosen to mimic the height difference between the base of the stomach and the pylorus, the site of gastric emptying (Liding et al., 2016). Digesta were removed at the rate of 1.0 mL/min as set by the control trial without guar gum. Naturally, increasing in viscosity above a certain point reduced the overall rate of gastric fluid (digesta) leaving the DGSM. Samples (10 mL) were collected every 10 minutes, and wet filtered through a pan sieve with a pore size of 0.80 mm. Samples were transferred and vacuumed filtered before being vacuum dried under the conditions described above. The emptying profiles of indigestible solids were used to fit empirical model and compared to the profiles for carrots. Additional trials were performed with increasing number of substrates, higher viscosities, and greater removal speed to reflect the upper limits of

factors that may exist in the stomach. The amount of amberlite was increased to 20 g, 4X from the previous amount, to reflect the average amount of solids ingested. The viscosities range being tested was increased to 0.01-76.74 Pa·s with 0.0-2.0% w/w guar gum mixed simulated gastric juice. The digesta removal rates were also increased to the initial value of 3.0 mL/min to allow for the removal of digesta at high viscosity up to 76.74 Pa·s. Both the amount of digesta and the solid content emptied were measured with similar procedure found in the trails that investigated the influence of viscosity on the gastric emptying rate of carrots. The results were compared between the emptying profile of amberlite and carrots upon increasing the viscosity of the digesta.

4.2.6. Statistical analysis

Trials were performed in triplicate. Comparisons between samples with various viscosities were analyzed using Fisher's least significant difference test at a statistical significance of $p < 0.05$ with SAS® software (version 9.3, SAS Institute Inc., Cary, NC). The regression equation and goodness of fit (R^2) were derived using Microsoft™ Excel 2010.

4.3.0 Results

4.3.2. Food disintegration at low viscosity gastric environment

This study was conducted to reveal the hardness and particle size changes of carrot, peanut and tofu in simulated gastric environment without addition of guar gum. The results will be used as a control to compare the digestion of the three foods at high viscosity gastric environment. At first, the rheological properties of the simulated gastric juice with/without addition of guar gum were measured. Figure 4.1 shows the shear stress vs shear rate profile for guar gum solutions with different concentration. The consistency, which reflects apparent viscosity, of each guar gum solution in water or simulated gastric juice was calculated and shown in Figure 4.1 and Table 4.1. The Power Law Equation ($\eta = K\gamma^{n-1}$) was applied to relate shear rate (γ) to shear stress (η).

Increasing the guar gum concentrations increased the consistency (K) while decreasing the power law index (n), which is indicative of greater shear thinning behaviors. The inclusion of mucin, enzymes, and salt to the simulated gastric juice further increased the viscosity of the guar gum solution.

Figure 4.2 indicates the overall decrease in bulk hardness of the gastric mixture at a viscosity of 0.0011 Pa·s (without addition of guar gum) when carrots, peanuts, and tofu were digested in DGSM incorporating simulated contraction and constant pH. Three separate pH conditions, 5.0, 3.0, and 1.5, were selected to simulate initial, middle, and final stages of gastric pH, respectively. The decline in hardness follows the Power Law equation with a high goodness of fit coefficient (R^2= 0.82-0.99), and the exponential value describes the rate of hardness reduction. Figure 4.2 further show that the higher acidic conditions caused quicker reductions in hardness. The highest hardness reduction in tofu, peanuts, and carrots were observed at pH 1.5, where tofu had the quickest hardness reduction among the three with a rate of 0.330 N/min. Further increasing the pH of the simulated gastric juice to 3.0 and 5.0 decreased the rates of hardness reduction in tofu to the values of 0.256 N/min and 0.244N/min, respectively. Although carrots and peanuts have higher initial harnesses than tofu, similar patterns of softening occurred at low pH of 1.5. Carrot has the biggest hardness reductions with a rate of 0.232 N/min at the pH 1.5, as compared to lower rates of hardness reduction at pH 3.0 and 5.0 with rates of 0.088 N/min and 0.065 N/min, respectively. The greater acidity in stomach enhanced food softening by promoting the food degradation through acid and enzymatic hydrolysis (Johnston et al., 2007).

In addition to the greater hardness reduction at pH 1.5, Figure 4.3 indicates that highly acidic gastric conditions promoted the greater disintegration of the three foods. Digestion of tofu at pH 5.0 generated 41.0 % particles that were smaller than 0.30 mm while retaining 42.8%

particles larger than 2 mm. Acidification of the digesta to pH 3.0 and 1.5 resulted in increased disintegration, and the particles < 0.30mm increased from 49.3 ± 3.4 % to 95.9 ±4.1 %, while the particles > 2.00 mm decreased from 29.2± 1.7 % to 2.0± 0.0%. Similar effect of pH on tofu disintegration were reported by other researchers using dynamic digestion model (Kozu et al., 2013) who showed that the increased small particles were highly correlated with the increased protein digestion due to synergistic effect of acid, enzymes, and peristaltic contractions. The rigid texture in peanut and carrot helped slow down their disintegration. At pH 5.0, digestion of peanuts generated 20.0% particles < 0.30 mm while retaining 67.7% particles > 2.00 mm. Acidification to the pH of 3.0 did not cause significant differences in the particle size distribution ($p>0.05$). However, further acidification of the digesta to pH 1.5 improved peanut disintegration by generating a significantly higher percentage of particles < 0.30mm (35.2%) and reducing the particles > 2.00 mm (51.8%). Digestion of carrots at pH 1.5 generated 47.62 % of particles < 0.30 mm. Increasing the pH to 3.0 and 5.0 reduced the disintegration of carrots to dismal level with only 8.5% and 9.5% of solids having sizes < 0.30 mm. These results indicate that the acidic gastric conditions promoted the softening and disintegration of tofu, peanuts, and carrots in the DGSM.

4.3.3. Influence of viscosity on gastric disintegration

DGSM was used to study the influence of viscosity on the disintegration of the three foods with constant pH and simulated continuous contractions similar to above. Figures 4.4, 4.5, and 4.6 show the particle size distribution of tofu, peanuts, and carrots after varying the viscosity of the digesta from 0.01 Pa·s to 76.74 Pa·s by adding 0.0% to 2.0% w/w guar gum. In general, the disintegration of the three foods were reduced (or not significantly changed) when the viscosity of the digesta was increased. When compared to the control, increasing the viscosity to the maximum level of 76.74 Pa·s decreased the tofu disintegration with the percentage of particles < 0.30 mm

decreased by 6.85% and 8.57% at pH of 5.0 and 3.0, respectively. The viscosity had no significant effect ($p > 0.05$) in the digestion of peanuts at pH 5.0 and 3.0, but significantly affected peanut disintegration at pH 1.5. Compared to the control, increasing the viscosity to 76.74 Pa·s decreased the peanut particles < 0.30 mm by 8.4% while increasing particles > 2.00 mm by 12.1%. Similarly, a great reduction in carrot disintegration was noticed at the pH of 1.5. When the viscosity was increased to the maximum value, a decrease of 7.5% was observed in the particles < 0.30 mm. Altogether, increasing the viscosity of the gastric environment reduced disintegration of the three foods with varying hardness, but the level of reduction decreased at high viscosity.

Increasing viscosity is thought to slow down hydrodynamic mixing of gastric fluid subsequently reducing the gastric disintegration of food. An increase in viscosity of gastric content from 0.01 Pa·s to 1 Pa·s has been shown to reduce retropropulsive jet velocity by 40% and diminish the strength of eddy circulation, which are critical in the mixing, rubbing, and grinding of gastric contents to reduce the particle sizes of the food (Schulze, 2006). The inadequate mixing caused by high viscosity also delays the penetration of gastric juice to further soften the ingested food for disintegration (Van De Abeele et al., 2017). Research in the pharmaceutical area also indicated that increasing viscosity reduced disintegration rate of drug capsules and tablets (Brouwers et al., 2011). In another study, increased passage of poorly disintegrated foods through the pylorus was observed after consumption of a meal with added guar gum (Meyer and Doty, 1988).

4.3.4. Influence of viscosity on the gastric emptying rate of carrots

Figure 4.7A-E shows the dispersion of carrot particles in simulated stomach chamber with different viscosities. The control trial (without guar gum addition, Fig. 4.7A) showed a limited amount of solids emptying with a rate of 6.54 mg/min. While the rate of the fluid being emptied was kept at 3.0 mL/min, the sedimentation of the carrot particles shown in Figure 4.7A reduced

the emptying of carrot solids from the DGSM. Increasing the viscosity to 0.40 Pa·s by adding 0.5% w/w guar gum improved the carrot solid emptying rate to 23.99 mg/ min. Furthermore, adding 1.0% w/w guar gum to the gastric juice (corresponding to viscosity 8.20 Pa·s) increased the carrot emptying rate to a maximum value of 35.98 mg/min. The solid emptying rate then started to decrease when more guar gum was added. Addition of 1.5% of guar gum (corresponding to the viscosity of 25.72 Pa·s) reduced the emptying of carrot solids to 27.26 mg/min. Additionally, increasing the viscosity to 76.74 Pa·s by adding 2.0% of guar gum further reduced the emptying of carrot solids to the rate of 16.35 mg/min. Less carrots solids were emptied at high viscosity (>8.20 Pa·s) due to the high resistance of the gastric fluid to flow that led to decreased emptying rate of gastric fluid with 1.68 mL/min and 1.00 mL/min at viscosities of 25.72 Pa·s and 76.74 Pa·s, respectively. The effect of viscosity on food emptying rates has been highly debated. Several researchers reported that increasing viscosity with pectin delayed the gastric emptying process by requiring twice the time necessary to remove half of the gastric content (Di Lorenzo et al. 1988, Meyer et al. 1986). Other researchers demonstrated that increasing viscosity with dietary fibers, including pectin, results in an increased removal of gastric contents (Marciani et al., 2000; Shimoyama et al., 2007). Results from this study supports both arguments as the data showed both increasing and decreasing trends relating the emptying rate of solids at various viscosities, and the emptying rate of solid carrots reached a maximum rate of at 8.20 Pa·s.

4.3.5.1. Influence of viscosity on gastric emptying of amberlite

The test with plastic foam and glass beads indicated these two materials are too light and too heavy to be used for digestion simulation. Food entering the stomach have a diverse range of densities from 600-1600 kg/m^3 (Hoelzel, 1930). Polystyrene and glass beads are out of this range. Eventually, only Amberlite with a density of 1250 kg/m^3 was used to study the mechanism

involved in solids emptying as affected by viscosity. Figures 4.7F-K shows the dispersion of amberlite solids in gastric fluid with various viscosities, indicates an improved suspension of the beads at high viscosity, and shows the solids emptying rates at various viscosities. Increasing the viscosity of digesta from 0.001 Pa·s to 0.644 Pa·s (corresponding to 0.0% to 0.80% w/w guar gum) increased the rate of amberlite emptying from 0.01 to 4.20 mg/min. Further increasing of the digesta viscosity from 0.644 Pa·s (0.8% guar gum) to 1.870 Pa·s (1.0% guar gum) decreased the overall emptying rate of gastric fluid from 1.00 mL/min to 0.92 mL/min, and eventually decreased the solids emptying rate from 4.20 mg/min to 4.05 mg/min. As shown in Figure 4.7F, the control trial had the lowest rate of solids emptying. Due to the greater density differences between amberlite and gastric fluid, the particles settled at the base of the DGSM with limited amount of solids emptied. Increasing the viscosity of the digesta improved the dispersion of particles, and allowed the solids to be emptied at higher rates. However, increasing the viscosity to 1.87 Pa·s slowed down the overall emptying of the gastric digesta due to the high flow resistance. This reduction in the removal of the overall digesta also reduced the rates of solids being emptied from the DGSM.

Ingested foods have varying physical properties including particle size, viscosity, and density, which can significantly affect their gastric emptying rate. Upon interacting with the gastric environment, the initial physical state of the stomach including fluid viscosity, fluid density, and rates of mixing further influences the rate of gastric emptying (Sirois et al., 1990). Sirois and others proposed a mathematical model that accounts for the physical properties of the food and the gastric fluid to calculate emptying rate of solids. The mathematical model, also called Particle Emptying Coefficient (PEC) model, as described in Equation 2, was used to explain the change of solids emptying rate of amberlite beads resulting from the increase in viscosity.

$$PEC = \frac{g(\rho f - \rho p)(Dp\text{^}2)}{\mu(v)} = \frac{Vt}{Vs} = \frac{Terminal\ Velocity}{Maximum\ upward\ velocity} \qquad [1]$$

where g is gravitational constant (m/s^2), $\boldsymbol{\rho}_f$ is fluid density (Kg/m^3), $\boldsymbol{\rho}_p$ is particle density (Kg/m^3), D_p is particle size (m), μ is viscosity (kg/(s·m)), and *v* is maximum upward velocity (m/s). The PEC model indicates the ratio between the downward sedimentation velocity (terminal velocity) (Vt, m/s) and the maximum upward velocity (Vs, m/s). Keeping the upward velocity constant, altering the viscosity decreases the downward sedimentation velocity and allows more particles to be suspended. The increase in particle suspension improved the solids emptying rate for amberlite beads from DGSM. Higher PEC values signify low solids emptying rate while lower PEC values signify a fast rate of solids emptying. Several assumptions were needed to use this equation to correlate the rate of gastric emptying of amberlite. The assumptions include that the particle shape is spherical with no lift forces, the particles have low density, and no electrostatic charges are present on the surface of particles.

PEC values were calculated using Equation 2 for amberlite beads. The maximum upward force of the fluid and particle size may be calculated by accounting for the radius of the probes compared to the radius of the insulated vessel within the DGSM (Chen et al. 2012).

$$V_{max} = \frac{Rb\ \text{^}2}{Ro\ \text{^}2 - Rb\text{^}2} \text{ x } V_b \qquad [2]$$

R_b is the radius of the probe, R_o is the radius of the vessel, and V_b is the speed of the probe. The DGSM contains a probe with a radius of 30.5 mm, an insulated vessel with a radius of 35.5mm, and a probe seed of 16.67 mm/s. The calculated maximum upward speed for the DGSM is 0.047 m/s. This value is like the maximum velocities reported in the literature, which ranging from 0.043 m/s to 0.052 m/s at the center of the stomach observed through MRI imaging following an ingested meal during *in vivo* digestion trials (Bouldby et al., 1999). PEC values were calculated using Equation 2 with a gravitation factor (g) of 9.8 m/s^2, fluid density (ρf) of 1000 kg/ m^3, particle

density (ρp) of 1250 kg/ m^3, particle size (Dp) of 0.0008 m, upward velocity (v) of 0.04698 m/s, and liquid viscosity (μ) of 0.0011, 0.0037, 0.0353, 0.1659, 0.6443, and 1.868 (kg/m*s). The PEC values calculated are within a range of 34.160 to 0.020 for the viscosity values ranging between 0.001 to 1.870 Pa·s. Plotting the PEC values as a function of the rates of amberlite solids emptied at various viscosities generated a logarithmic curve with a downward trend as shown in Figure 4.8 (R^2=0.943). This was used to derive Equation 3 and indicates the relationship between PEC and the solids emptying rate of amberlite.

$$Y=-0.554*(\ln(x)) + 2.058 \qquad [3]$$

Where Y is the solids emptying rate and x is PEC values.

In separate trials, several parameters were altered to reflect the upper limits of substrates, viscosity, and digesta removal rates that may exist in the stomach. The amount of amberlite was increased to 20 g, 4X from the previous amount, to reflect the average amount of solids ingested within a meal. The viscosities range were increased to a range of 0.01-76.74 Pa·s with 0.0-2.0% w/w guar gum mixed simulated gastric juice. The digesta removal rates were also increased to the initial value of 3.0 mL/min to resemble the flow rate set in the digestion of carrots. The results from the digestion of amberlite showed similar trends to the emptying profile of carrots with both increasing and decreasing sections when viscosity was increased. The control amberlite digestion trials (without guar gum) showed limited solid emptying rate of 5.10 mg/mL. Increasing the viscosity to 0.41 and 8.20 Pa·s allowed the amount of solids amberlite to emptied at increasing rates of 44.1 and 51.6 mg/mL, respectively. Viscosities greater than 8.20 Pa·s showed a steady decline both in the amount of digesta and solid amberlite being emptied. The increase of the digesta viscosity to 25.72 and 76.74 Pa·s reduced the digesta removal rate to 1.5 and 0.93 mL/min, respectively, and subsequently reduced the solids emptying rate of amberlite to 32.2 and 15.1

mg/mL, respectively. Furthermore, it is observed that there is an exponential decline in the rates of digesta being removed with increasing viscosity as shown in Figure 4.9A&B. Taking the average rates of both amberlite and carrots trials generate a derived equation that was further incorporated into equation 3 to account for the influence of viscosity on the flow rate. Note that these rates specific reflect the flow rate of the digesta being removed through a tube that has a 2 mm diameter, which may need to be modified to reflect the actual pylorus. Equation 4 was developed to predict the rates of solids emptying for amberlite (Z).

$$Z = 4\times(2.67e^{-0.014x})[-0.554 * (ln(PEC)) + 2.058] \quad [4]$$

Where the constant value of 4 indicates the increasing ratio of substrates concentration, $(2.67e^{-0.014x})$ is the rate of digesta emptied with dependency on viscosity (x), and $[-0.554 * (ln(PEC)) + 2.058]$is the original rate of solids emptying (Y). Shown on Figure 4.10A and Table 4.2 are the changes of amberlite emptying rate with various viscosities. The predicted values were calculated using the physical properties of amberlite with the viscosity ranging from 0.01 Pa·s to 76.74 Pa·s. Both the values and trend showed similar results between the predicted and experimental trials.

4.3.5.2 Using equation 4 to predict carrot emptying

Equation 4 was utilized to describe the carrot solids emptying pattern with the relationship between PEC values and the rates of amberlite solids emptying. The appropriate physical properties of carrots and gastric digesta fluid were combined to calculate the PEC values using Equation 1. With viscosities ranging from 76.74 Pa·s to 0.01 Pa·s, the calculated PEC values for carrots had a range of 0.002 to 13.490. Utilizing Equation 4, the predicted solids emptying rates were determined. Figure 4.10B indicates that the values and pattern are similar between the predicted and the experimental emptying rates of the carrot solids. The predicted and experimental

emptying rates of carrot resembled in values. In addition, the data showed that the experimental values are generally smaller than the predicted emptying values of carrots. This is attributed to the greater density and larger particles of carrots that increased the PEC values. Shown through the logarithmic relationship between PEC and rates of solids being emptied, the increasing in PEC values generate lower rates of carrot solids being emptied than the predicted values.

The mathematical model used to calculate PEC also explains the critical viscosity of amberlite and carrots where the solids emptying started to decrease. In the tested parameters, both amberlite and carrot have a critical value of at 8.20 Pa·s where the maximum emptying rates of solids occurred. The control trials for amberlite and carrots (without guar gum) had PEC values greater than 1 with results indicating greater terminal velocities when compared to the upward velocity. The greater terminal velocities allowed the particles to settle at the base of the model, aggregate, and reduce the overall rates of solids being emptied from the DGSM. Upon increasing the viscosity of the digesta, the terminal velocities were reduced, which improved the suspension of particles. The phenomenon creates a homogenous mixture that is known to greatly improve the rate of solids emptying (Sirois et al., 1990). The overall flow rates of the digesta decreased as the viscosity of the digesta increase as shown in Figure 4.9A&B. Beyond the critical viscosity, the overall rate of digesta emptying decline greatly as the viscous solution became harder to flow. The reduction in digesta being removed subsequently decreased the rate of solids being emptied from the DGSM. The differences in the physical characteristics between the two particles types impact the overall PEC value and influence the rates of solids emptying. Compared to amberlite, carrots had larger particle sizes and the bigger density differences between carrots and gastric fluid. The greater values inflate the numerator of the PEC model. With greater PEC values corresponding to lower rates of solids emptying, carrots showed less solids emptied at the critical viscosities than

amberlite. The PEC model indicated that modifying the physical characteristics (density, particle size, and viscosity) of food can regulate the rate of solids emptying from the stomach. To use the model, one can simply input physical properties of food (particle size, density) and the viscosity of gastric fluid into Equation 1 to calculate PEC values. Substitute the PEC values into Equation 4 will allow for the prediction of the solid emptying rate at that viscosity.

The emptying patterns of amberlite and carrots closely resembled each other using the PEC model. However, the complexity in the food and the gastric digestion process may limit the applicability of the current model. It is suggested that the model may only be applicable to the food that is hard to disintegrate in stomach including fruits and vegetables. The PEC equation and prediction of food emptying rate become more complex as the rates of disintegration increase. Greater disintegration generates a wider range of particle size that will influence the terminal velocity with larger particles settling to the base, and smaller particles floating to the top. Furthermore, greater disintegration promotes faster dissolution while altering the density of the fluid. In addition, high disintegration of food may increase the overall viscosity of the digesta by increasing the production of smaller particles with overall greater surface areas. Further research will be conducted to account for these factors to improve the model for better prediction of the rate of gastric emptying of solids.

4.4. Conclusion

The increase in digesta viscosity generally reduced the rate of disintegration of carrots, peanuts, and tofu in this study. The greatest amount of disintegration occurred at low viscosity due to high levels of hydrodynamic mixing and mechanical force resulting from gastric grinding of the particles. The increasing in viscosity further improved gastric removal of solids initially. However, increasing digesta viscosity above a certain critical value reduced the emptying rate of both digesta

and solids. A mathematical model was derived based on the PEC values and the emptying rate of gastric fluid to predict the rates of emptying for amberlite and carrot with a good fit. The information from this study indicates that altering viscosity through the consumption of dietary fiber with changing physical characteristics of food (density, particle size) have great potential in modulating the rate of gastric emptying.

References

Boulby, P., Moore, R., Gowland, P., & Spiller, R. (1999). Fat delays emptying but increases forward and backward antral flow as assessed by flow-sensitive magnetic resonance imaging. *Neurogastroenterology & Motility*, 11, 27-36.

Brouwers, J., & Augustijns, P. (2014). Resolving intraluminal drug and formulation behavior: gastrointestinal concentration profiling in humans. *European Journal of Pharmaceutical Sciences,* 61, 2-10.

Chen, J., Gaikwad, V., Holmes, M., Murray, B., Povey, M., Wang, Y., & Zhang, Y. (2011). Development of a simple model device for in vitro gastric digestion investigation. *Food & Function*, 2(3-4), 174-182.

Diorenzo, C., Williams, C. M., Hajnal, F., & Valenzuela, J. E. (1988). Pectin delays gastric emptying and increases satiety in obese subjects. *Gastroenterology*, 95,1211-1215.

Do, D. H., Fanbin, K., Penet, C., Winetzky, D., & Gregory, K. (2016). Using a dynamic stomach model to study efficacy of supplemental enzymes during simulated digestion. *LWT -- Food Science and Technology, 65,* 580-588.

Donhowe, E., Flores, F., Kerr, W., Wicker, L., & Kong, F. (2014). Characterization and in vitro bioavailability of β-carotene: Effects of microencapsulation method and food matrix. *LWT-Food Science & Technology.*, 57(1), 42-48.

Ferrua, M., &Singh, R. (2010). Modeling the fluid dynamics in a human stomach to gain insight of food digestion. *Journal of Food Science*, 75(7), R151-R162.

Gritti, I., Banfi, G., & Roi, G, (2000). Pepsinogens: physiology, pharmacology pathophysiology and exercise. *Pharmacological Research*. 41, 265–281.

Hellström, P., Grybäck, P., & Jacobsson, H. (2006). The physiology of gastric emptying. *Best Practice & Research Clinical Anaesthesiology*, 20(3), 397-407.

Hoelzel, F. "The rate of passage of inert materials through the digestive tract." (1930): *American Journal of Physiology*--Legacy Content 92.2 466-497.

Hur, S., Lim, B., Decker, E., & McClements, D. (2011). In vitro human digestion models for food applications. *Food Chemistry,*125(1), 1-12.

Jalabert-Malbos, M., Mishellany-Dutour, A., Woda, A., & Peyron, M. (2007). Particle size distribution in the food bolus after mastication of natural foods. *Food Quality and Preference*, 18,803-812.

Johnston, N., Dettmar, P. W., Bishwokarma, B., Lively, M. O., & Koufman, J. A. (2007). Activity/stability of human pepsin: implications for reflux attributed laryngeal disease. *Laryngoscope, 117*(6), 1036-1039.

Kong, F., & Singh, R. P. (2008). Disintegration of solid foods in human stomach. *Journal of Food Science* .73(5): R67-R80.

Liding C., Yufen, X., Tingting, F., Zhenkai, L., Peng, W., Xuee, W., & Xiao Dong, C. (2016). Gastric emptying and morphology of a "near real" in vitro human stomach model (RD-IV-HSM). *Journal of Food Engineering*, 1831-1838.

Lucas, P., Luke, D. (1984). Optimum mouthful for food comminution in human mastication. *Archives of Oral Biology*, 29(3), 205-210.

Marciani, L., Gowland, P., Spiller, R., Manoj, P., Moore, R., Young, P., & ... Fillery-Travis, A. (2000). Gastric response to increased meal viscosity assessed by echo-planar magnetic resonance imaging in humans. *Journal of Nutrition,* 130(1), 122-127.

Meyer, J., & Doty, J. (1988). GI transit and absorption of solid food: multiple effects of guar. *American Journal of Clinical Nutrition*, 48(2), 267-273.

Meyer, J. H., Gu, Y., Elashoff, J., Reedy, T., Dressman, J., & Amidon, G. (1986). Effects of viscosity and fluid outflow on postcibal gastric emptying of solids. A*merican Journal of Physiology: Gastrointestinal & Liver Physiology* 250(2), G161-G164.

Paulson, S., Vaughn, M., Jessen, S., Lawal, Y., Gresk, C., Yan, B., & ... Karim, A. (2001). Pharmacokinetics of celecoxib after oral administration in dogs and humans: Effect of food and site of absorption. *Journal of Pharmacology and Experimental Therapeutics*, 297(2), 638-645.

Prove, J., & Ehrlein, H. (1982). Motor functions of the gastric antrum and pylorus for evacuation of low and high viscosity meals in dogs. *Gut,* 23: 150-156.

Shimoyama, Y., Kusano, M., Kawamura, O., Zai, H., Kuribayashi, S., Higuchi, T., & ... Mori, M.(2007). High-viscosity liquid meal accelerates gastric emptying. *Neurogastroenterology & Motility*, 19(11), 879-886.

Schulze, K. (2006). Imaging and modelling of digestion in the stomach and the duodenum. *Neurogastroenterology & Motility*, 18(3), 172-183.

Sirois P., Amidon, G., Meyer, J., Doty, J., & Dressman, J. (1990). Gastric emptying of nondigestiblesolids in dogs: a hydrodynamic correlation. *American Journal of Physiology,* 258, G65-G72.

Van Den Abeele, J., Brouwers, J., Tack, J., & Augustijns, P. (2017). Research paper: Exploring the link between gastric motility and intragastric drug distribution in man. *European Journal of Pharmaceutics and Biopharmaceutics*, 11275-11284.

Vardaou, M., Mercuri, A., Barker, S., Craig, D., Faulks, R., & Wickham, M. (2011). Achieving Antral Grinding Forces in Biorelevant *In Vitro* Models: Comparing the Dissolution Apparatus II and the Dynamic Gastric Model with Human In Vivo Data. *Aaps Pharmscitech*, 12(2), 620-626.

Versantvoort, C. H., Van de Kamp, E., & Rompelberg, C. J. (2004). Development and applicability of an in vitro digestion model in assessing the bioaccessibility of contaminants from food. *Bilthoven, Inspectorate of Health Inspection*, 1–87.

Results

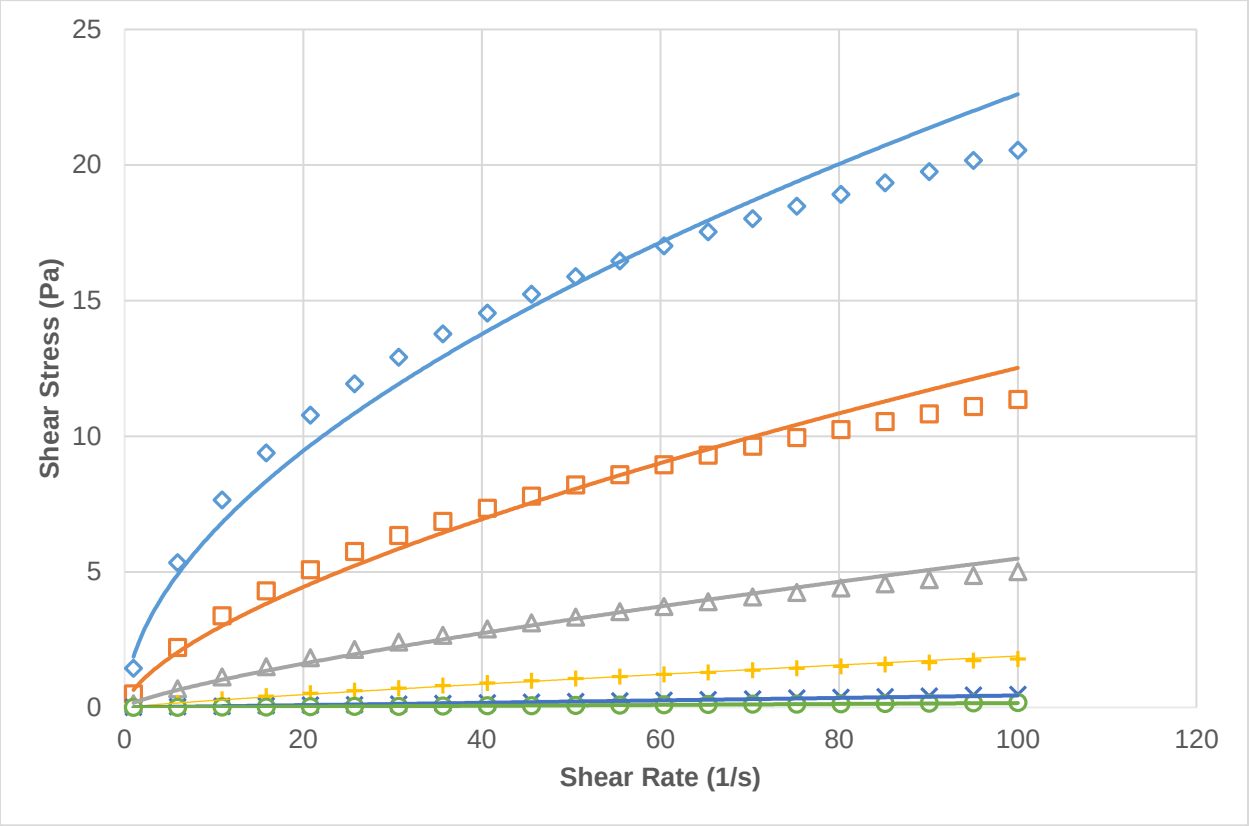

Figure 4.1. Rheological profiles of aqueous guar gum solutions at (◊) 1.00%, (□) 0.80%, (Δ) 0.60 %, (+), 0.40%, (x) 0.20%, and (o) 0.00%. The values for shear stress and shear rate were used to calculate the Consistency Index (K) and Flow Behavior Index (n) constants used in the power equation ($\eta = K\gamma^{n-1}$).

Table 4.1. Consistency & flow behavior index of guar gum dissolved in water and gastric juice

Guar Guam Dissolved in DI Water			Guar Guam Dissolved in Simulated Gastric Juice		
Percent Guar Gum (%w/w)	Consistency Index (Pa·s) [kg/m·s)	Flow Behavior Index (n)	Percent Guar Gum (%w/w	Consistency Index (Pa·s) [kg/m·s)	Flow Behavior Index (n)
0.00	0.001±0.00	1.00±0.00	0.00%	0.011 ±0.00	0.71±0.09
0.20	0.003±0.00	1.00±0.00	0.50%	0.401 ±0.09	0.55±0.05
0.40	0.035±0.04	0.86±0.06	1.00%	8.210 ±3.11	0.27±0.01
0.60	0.166±0.05	0.76±0.03	1.50%	25.720 ±1.49	0.23±0.01
0.80	0.644±0.09	0.64±0.04	2.00%	76.741 ±2.68	0.12±0.04
1.00	1.868±0.14	0.54±0.01			

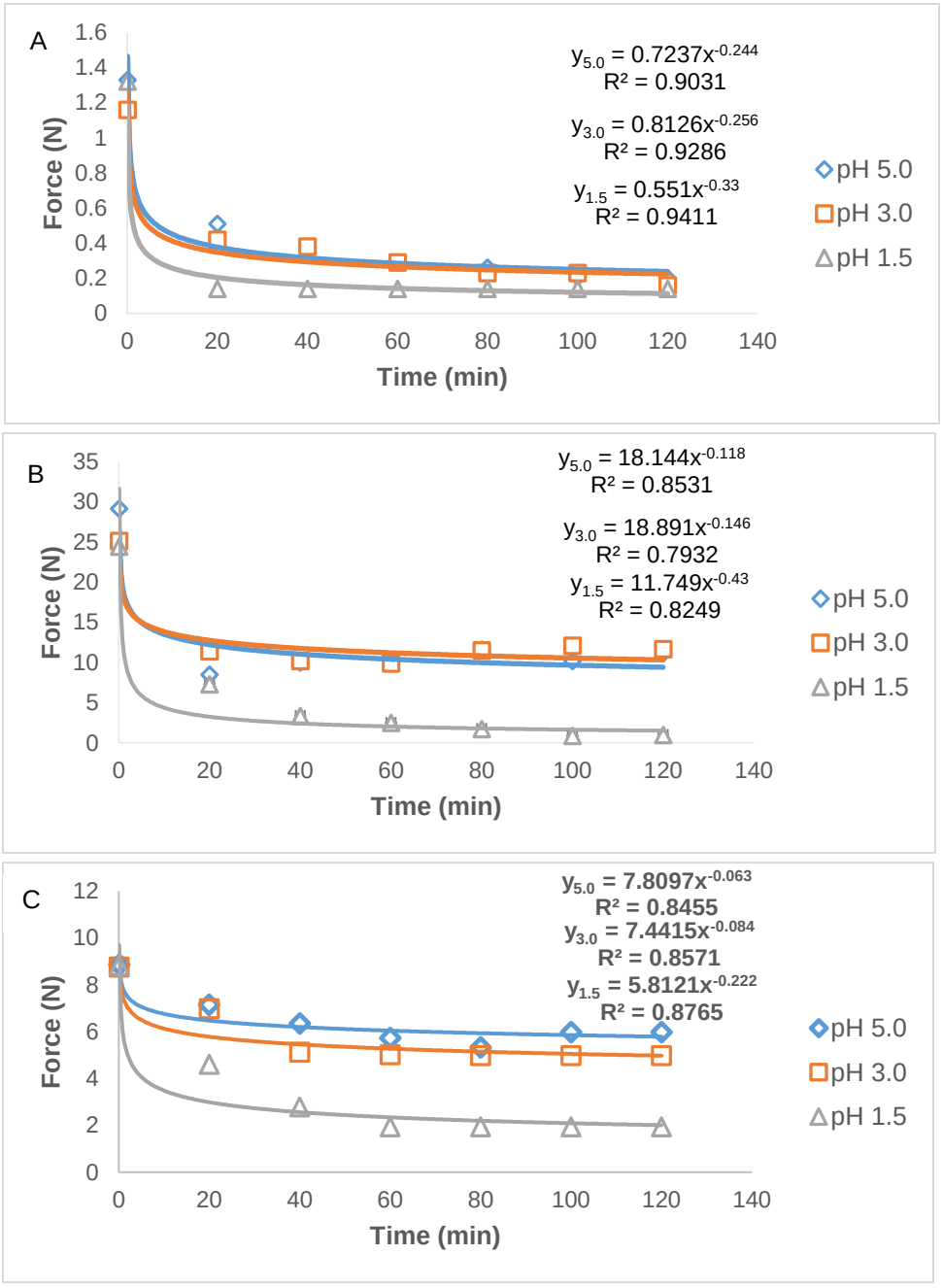

Figure 4.2. The initial hardness and the hardness reduction profiles of: (A) tofu, (B) peanut, and (C) carrots at the pH (◊) 5.0, (□) 3.0, and (Δ) 1.5.

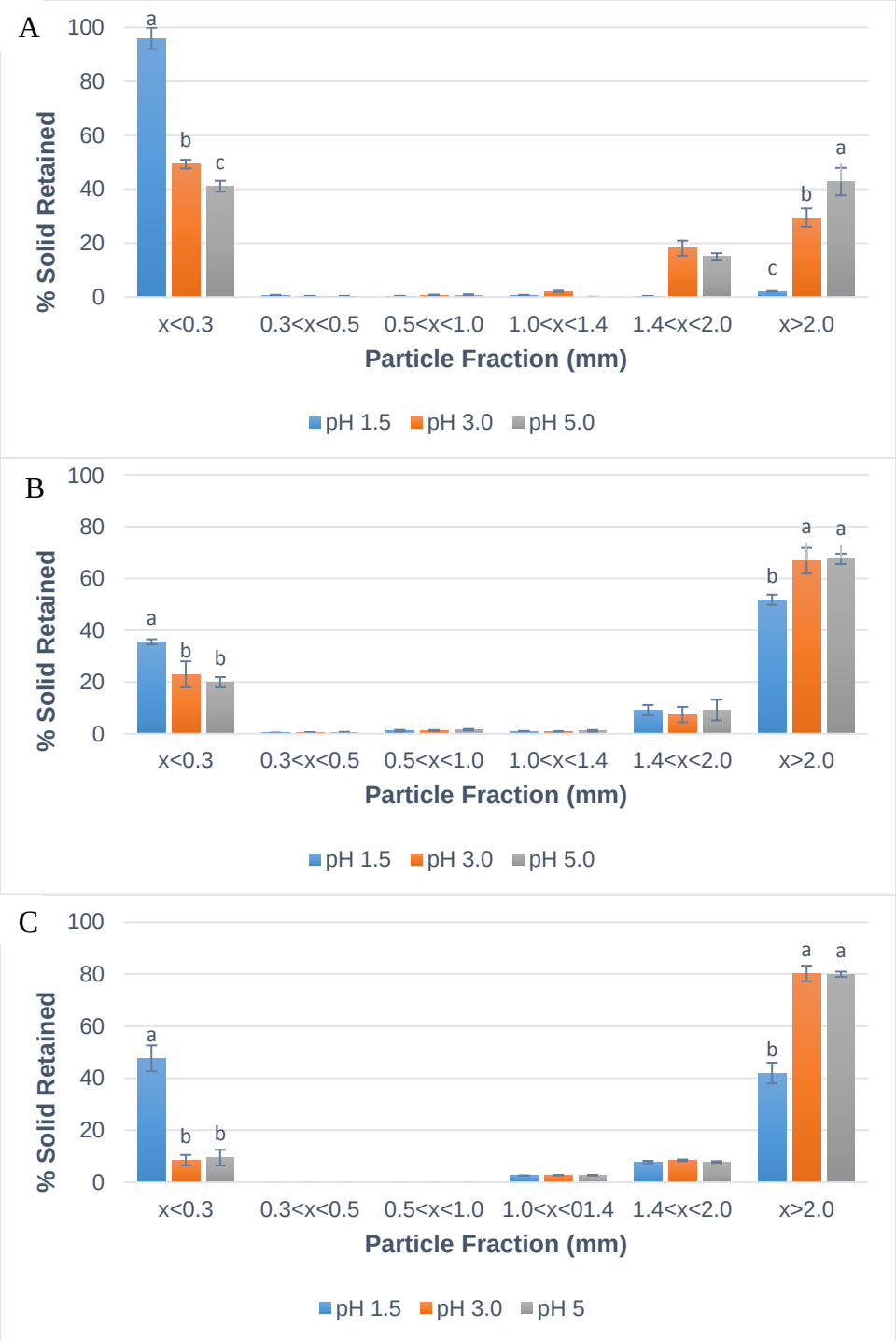

Figure 4.3. The particle size distribution after 120 min of gastric digestion of (A) tofu, (B) peanuts, and (C) carrots at various pH. Subscripts with different letters indicate significant differences at $p<0.05$.

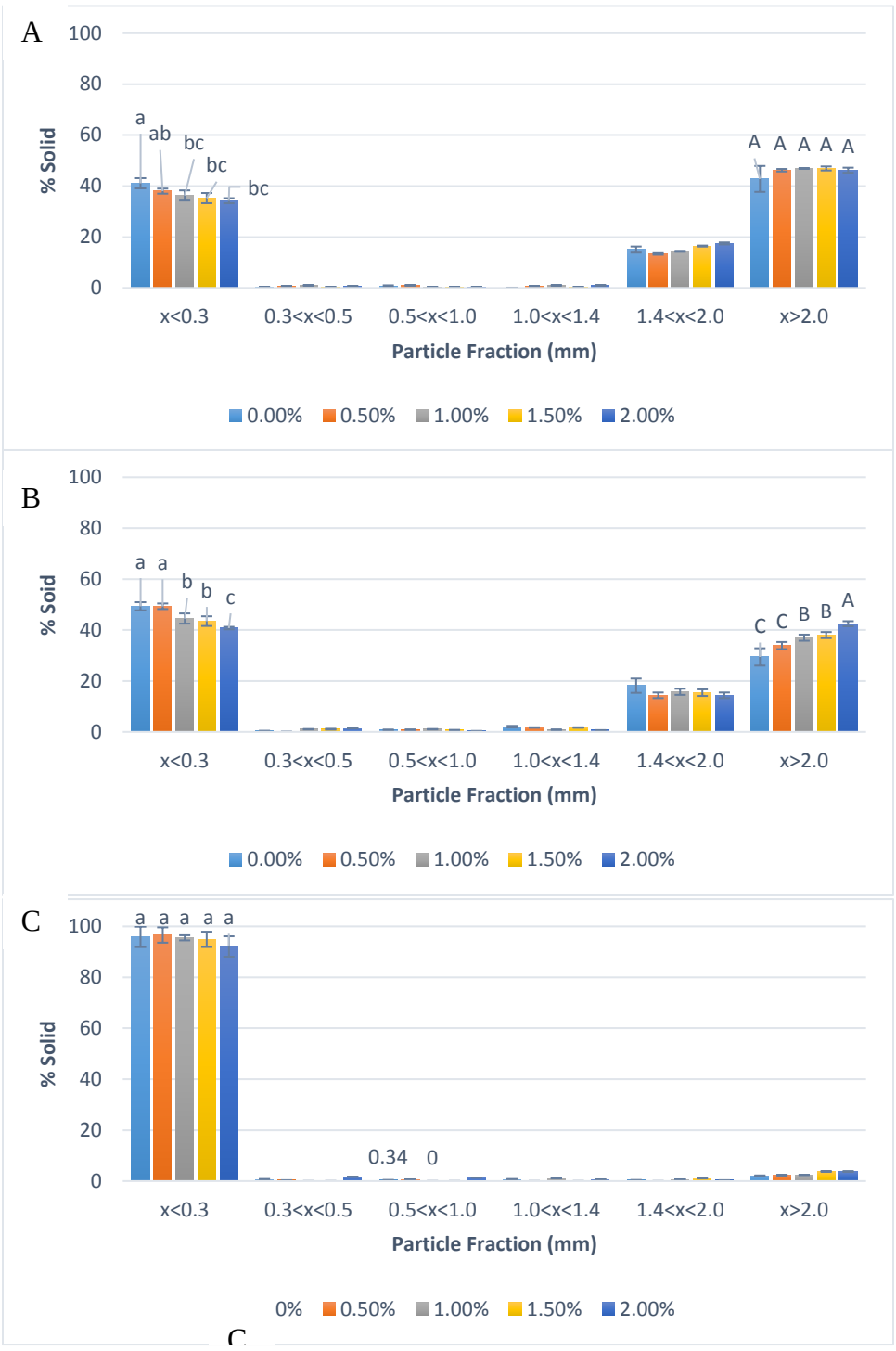

Figure 4.4. The particle size distribution after 120 min of gastric digestion of tofu at pH (A) 5.0, (B) 3.0, and (C) 1.5. Columns with different letters indicate significant differences between the various viscosities at $p<0.05$ with error bars representing the standard deviation (n=3).

Figure 4.5. The particle size distribution after 120 min of gastric digestion of peanuts at pH s (A) 5.0, (B) 3.0, and (C) 1.5. Columns with different letters indicate significant differences between the various viscosities at $p<0.05$ with error bars representing the standard deviation (n=3).

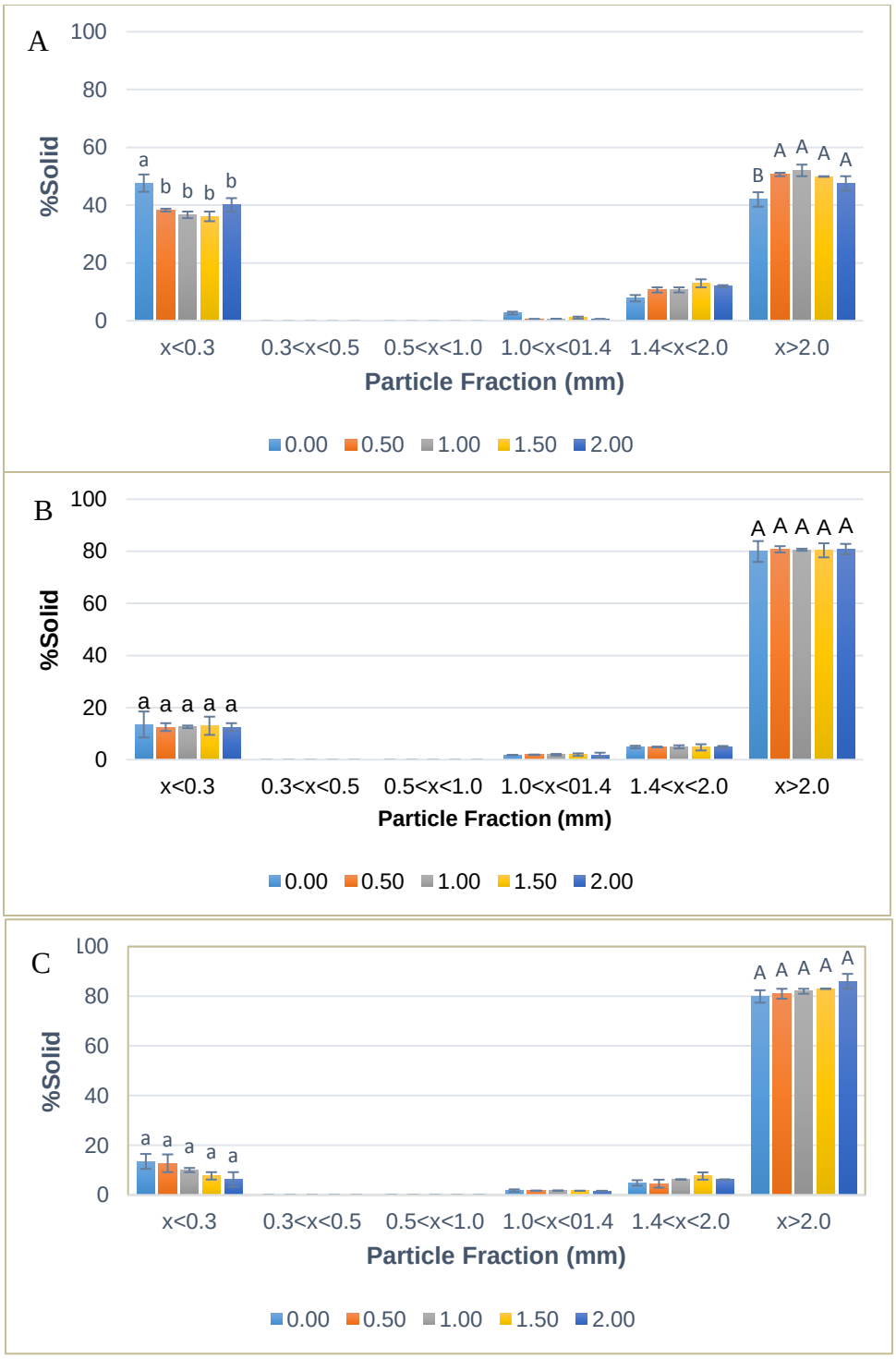

Figure 4.6. The particle size distribution after 120 min of gastric digestion of carrots at pH (A) 5.0, (B) 3.0, and (C) 1.5. Columns with different letters indicate significant differences between the various viscosities at $p<0.05$ with error bars representing the standard deviation (n=3).

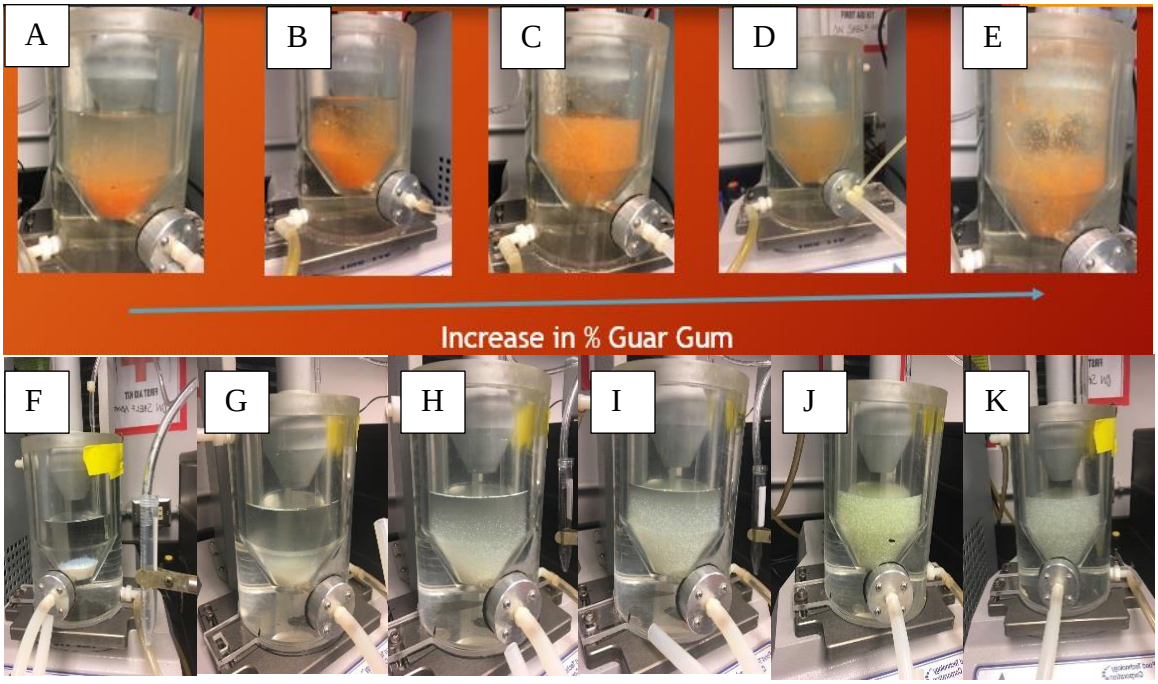

Figure 4.7. Top row indicates the dispersion of carrots loaded into the DGSM at increasing levels of guar gum: (A) 0.0%, (B) 0.5%, (C) 1.0%, (D) 1.5%, and (E) 2.0%. The bottom row indicates the dispersion of amberlite loaded into the DGSM at increasing levels of guar gum: (F) 0.0%, (G) 0.2%, (H) 0.4%, (I) 0.6%, (J) 0.8%, and (K) 1.0%.

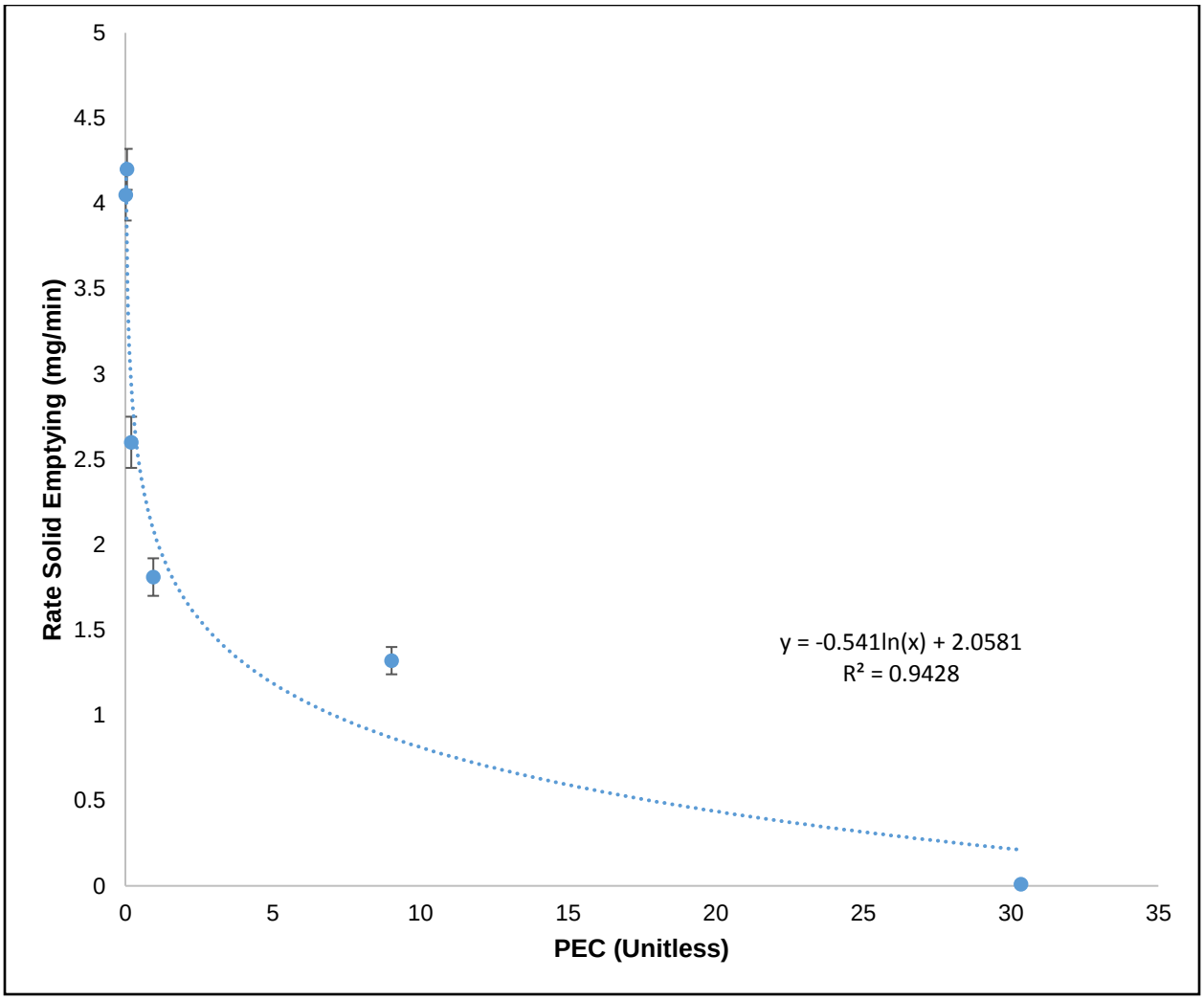

Figure 4.8. Relationship between PEC values and rate of solids emptying for amberlite. PEC values were calculated using Equation 1.

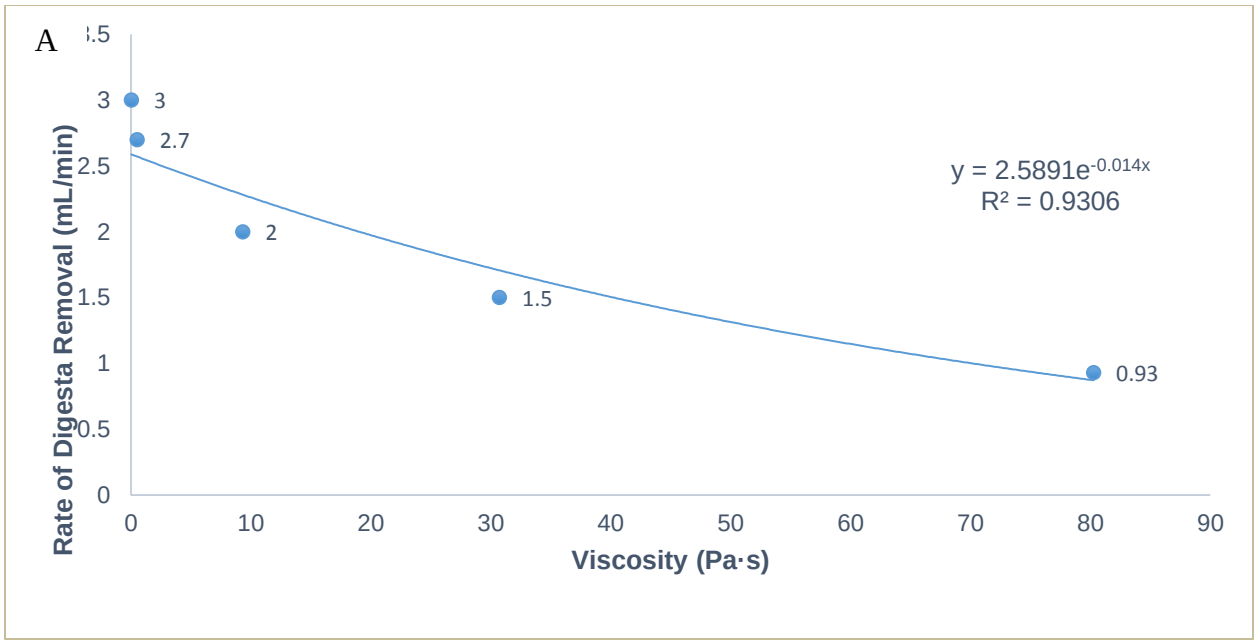

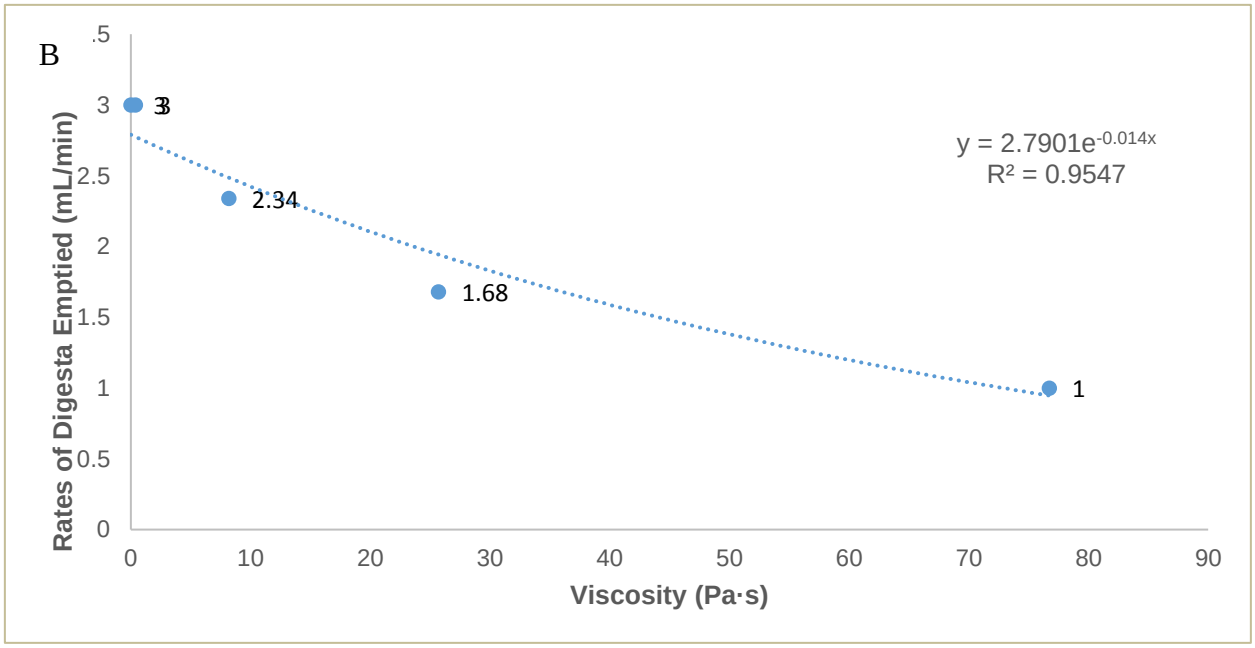

Figure 4.9. Relationship between viscosity and the rate of gastric fluid (digesta) being emptied from the DGSM with amberlite (A) and carrots (B). The values from the two experiments were average to generate an equation of $y = 2.67e^{-0.014x}$.

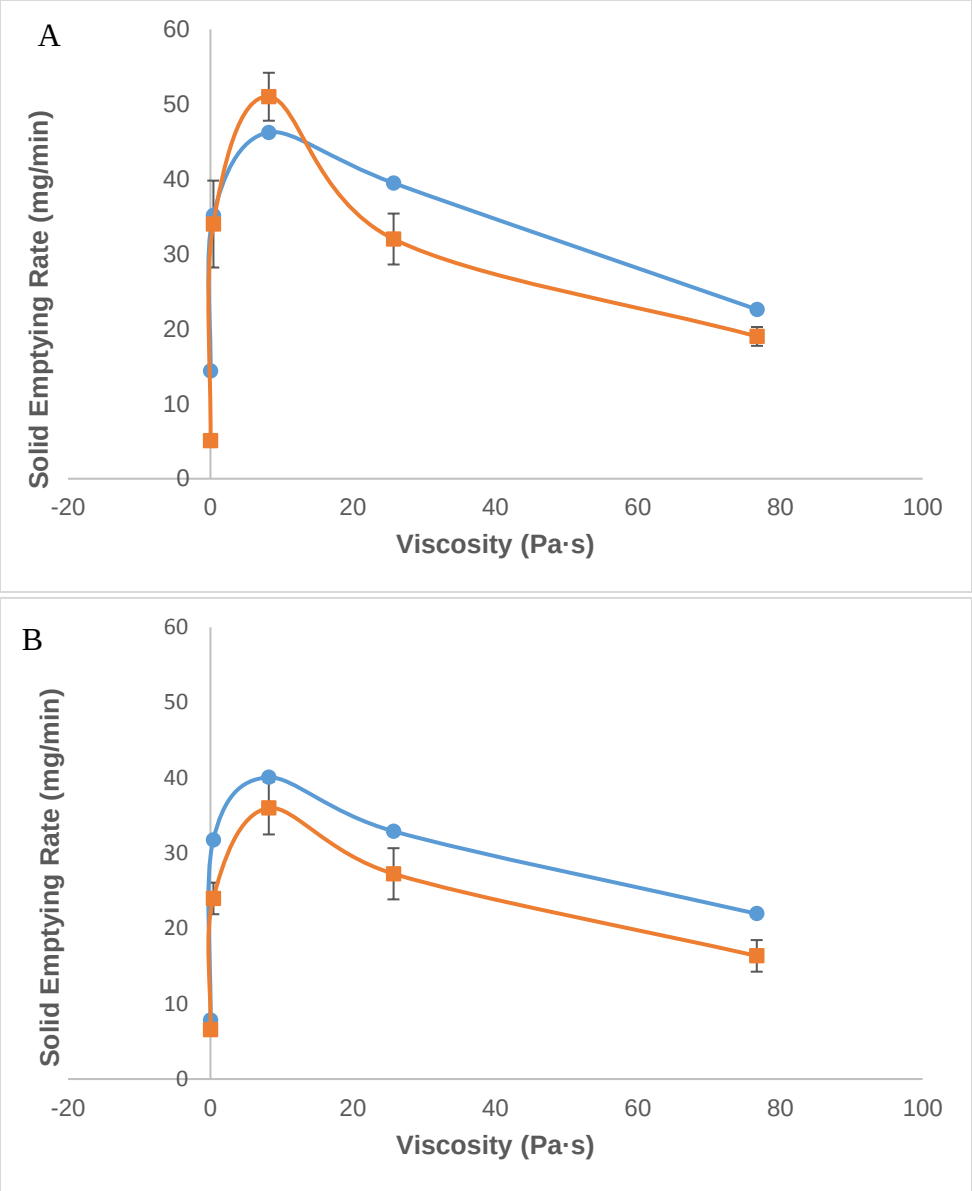

Figure 4.10. Emptying profiles of amberlite (A) and carrots (B) with predicted value (●) and experimental values (■).

Table 4.2. Predicted and experimental data of amberlite and carrot solids emptying rate

Gaur Gum Percentage (%)	**Apparent Viscosity (Pa·s)**	**Calculated PEC***	**Theoretical Rate of Solids Emptying**	**Ratio of the amount of carrot to the amount of amberlite**	**Rates of content emptied (mL/min) $y = 2.671e^{-0.014x}$ ** **	**Adjusted Rate of Solids Emptying**	**Experimental Rate of Carrot Solids Emptying**
Amberlite							
0.0	0.01	3.3376	1.41	4:1	2.67	15.09	5.10
0.5	0.40	0.0417	3.78	4:1	2.65	36.29	34.12
1.0	8.20	0.0036	5.11	4:1	2.37	48.54	51.61
1.5	25.72	0.0011	5.75	4:1	1.84	43.39	32.22
2.0	76.74	0.0004	6.27	4:1	0.88	24.68	15.15
Carrots							
0.0	0.01	13.49	0.650	4:1	2.67	9.34	6.54
0.5	0.40	0.337	2.646	4:1	2.65	30.48	23.99
1.0	8.20	0.016	4.280	4:1	2.37	42.76	35.98
1.5	25.72	0.005	4.898	4:1	1.84	37.81	27.26
2.0	76.74	0.002	5.489	4:1	0.88	20.26	16.35

* PEC values for carrot were calculated using Equation 2 with a gravitation factor (g) of 9.8 m/s^2, fluid density ($\boldsymbol{\rho}_f$) of 1000 kg/ m^3, particle density ($\boldsymbol{\rho}_p$) of 670 kg/ m^3, particle size (Dp) of 0.0014 m, upward velocity (v) of 0.04698 m/s, and apparent viscosity of the liquid (μ) listed on the table.

** Accounting for the rate of digesta being emptied from the DGSM with relationship between the amount emptied and the various viscosities shown in Figure 4.9

CHAPTER 5

TEXTURE CHANGES AND PROTEIN HYDROLYSIS OF DIFFERENT CHEESES UNDER SIMULATED GASTRIC ENVIRONMENT

Do, D.H., AND F. KONG. To be submitted to: The Journal of Food Science.

5.0. Abstract

The structure of cheese plays an important role in determining the rate of digestion by influencing the disintegration rate and affecting the release of bioaccessible components. Once in the stomach, the physical and chemical break down of food structure occurs through mechanical peristaltic forces and hydrolysis of macronutrients. Recent findings indicate the resistance of cheese disintegration in the gastric environment. The objective of these studies was to investigate the influence of the gastric environment on the digestion of Cheddar, Mozzarella, and Parmesan cheeses using both static and dynamic *in vitro* gastric digestion model. During static gastric incubation at pH 1.5, Mozzarella cheese had the lowest rate of nutrient leaching due to aggregation of the protein matrix as observed under the Scanning Electron Microscope, while Parmesan cheese had the highest rate of nutrient leaching. During dynamic gastric simulation, Mozzarella cheese showed the most resistance to protein hydrolysis by generating only 6.81 g/L amino acids when compared to 12.70 g/L and 24.3 g/L amino acids released by Cheddar and Parmesan cheese, respectively. The resistance of Mozzarella cheese was attributed to the dense outside layer formed at highly acidic environment that encapsulated the cheese particles and prevented gastric juice from further digesting the protein.

Key Words: *In vitro* gastric digestion, texture change, food structure degradation, disintegration rate, protein digestion.

5.1. Introduction

Foods entering the human digestive tract have different structures, which are based on their composition, the arrangement of compounds in the matrix, and processing techniques (Hu et al., 2011). The structural behavior of the ingested food inside the digestive tract influences both the release of bioaccessible components and the absorption of bioavailable compounds. One method for measuring the structural breakdown of food is through the quantification of texture and the rate of food softening under the conditions of the human digestive tract. The initial hardness and the rate of hardness reduction have been used as indicators of food disintegration and digestion (Bornhorst, Ferrua, and Singh, 2015). Foods, like carrots, with greater initial hardness values and lower rates of food softening have been shown to resist disintegration and digestion (Kong & Singh, 2009). In contrast, food with lower initial hardness values and faster rates of softening have been shown to have fast disintegration rates and digestion (Kozu et al., 2015). The breakdown of structures in peanuts, carrots, and potatoes have been reported in the literature, but limited research has been found regarding the structural behavior of cheese inside the human digestive system (Xixi et al., 2016).

The variations in cheese structure are governed by the composition of the cheese, the arrangement of the macronutrients in the cheese matrix with influences from the processing techniques. Cheeses are mainly composed of casein, fat, water, and minerals. The majority of the structure is attributed to the casein matrix that provides the main hardness of the cheese while the water and fat globules gives it smoothness (Mistry et al., 1993). In addition, the arrangement of compounds in the cheese matrix also contributes to the structure of cheese. For example, the hardness of Mozzarella cheese is influenced by the fibrous protein matrix and a low amount of fat globules (Gunasekaran & Ak, 2003). The hardness of Cheddar cheese is mainly governed by the

protein aggregates that have a combination of globular and sub-micellar shapes. Furthermore, the large coalesced fat globules found in Cheddar cheese reduces its hardness. Parmesan cheese has a non-cohesive structure that is mainly composed of protein aggregates arranged in chains and strands. The high amount of fat globules weakens the structure of Parmesan cheese (Michalski et al., 2007). The processing of cheeses further influences their structures. The stretching process during the production of Mozzarella cheese gives the cheese a fibrous and compact structure (Gunasekaran & Ak, 2003). The Cheddaring process of stacking one cheese on top of another creates larger coalesced fat globules that gives Cheddar cheese its distinct hardness (Guinee, Auty, and Fenelon, 2000). The aging process in Parmesan cheese impacts structure through protein degradation and reduction of moisture content (Fox et al., 1993). The variations in the structure permit cheese to be an excellent model food for the study of structural breakdown kinetics under human digestive conditions.

One of the major organs in the human digestive system is the stomach, which breaks down the structure of food both physically and chemically (Chen et al., 2011). The peristaltic movement physically reduces the size of food particles through grinding while a mixing effect increases the shear interactions between particles (Kong and Singh, 2009). In addition, the secretion of gastric juice containing hydrochloric acid (HCl) and Pepsin are thought to degrade the structure of food chemically through the hydrolysis of macronutrients (Malagelada et al., 1976; Dean and Ma, 2007). Using human subjects for the direct study of food structure breakdown in the digestive system can be costly, and it may be considered unethical in certain instances. Thus, in vitro simulation models are often used to investigate the effect of the gastric environment on food structure. One type of in vitro simulation is a static digestion model in which the volume, pH, temperature, and forces within the simulation are kept constant (Kong and Singh, 2010). The

second type of in vitro simulation is a dynamic digestion model in which the volume, pH, temperature and forces within the simulation are continuously changing. Dynamic models are more complex because continuous gastric juice secretion, cycling gastric forces, and gastric emptying create a dynamic environment similar to the human digestive tract (Kong and Singh, 2010).

The aim of this study was to understand the influence of the gastric environment on both the physical and chemical breakdown of cheese structures. Three cheeses were chosen to represent a semisoft cheese (Mozzarella), a hard cheese (Cheddar), and very hard cheese (Parmesan) (Han & Spradlin, 2000). Two types of in vitro gastric digestion models were used to investigate the digestion of cheeses. Trials were conducted in a static model to gain a basic understanding of cheese disintegration and digestion behavior under various controlled gastric environments. Trials were also conducted in a dynamic model, Dynamic Gastric Simulation Model (DGSM), to understand the behavior of cheese digestion under more realistic physiological conditions. It is expected that utilizing both static and dynamic models to study cheese digestion will provide a more comprehensive understanding of the way in which cheese behaves during digestion.

5.2. Materials and Methods

Chemicals

Simulated gastric juices were prepared according to the method of Donhowe, Flores, Kerr, Wicker, and Kong (2014) containing 6.0 mg/mL mucin, 5.0 mg/mL porcine pepsin, and various salts. Enzymes were added on the day of the experiment to preserve enzymatic activities. Porcine pepsin, porcine mucin, glutaraldehyde, hexamethyldisilazane, and Osmium tetroxide were obtained from Sigma–Aldrich Chemical Company (St. Louis, MO). Cheddar, Mozzarella, Parmesan cheese were purchased locally in Athens, GA.

5.2.1. Contents of moisture, protein, and fat in three cheeses

Mozzarella cheese, Mild Cheddar cheese, and Parmesan cheese were processed in a Ninja Master Prep Professional processor (Chino, CA). Each cheese was dry sieved through two sieves with mesh sizes of 1.0 mm and 1.4 mm. The sieved fractions were placed into an oven set at 65°C with a vacuum pressure of -20 in Hg. After 24 h, the moisture content was determined by weight difference. The fat content was quantified using a Soxhlet hexane extraction method. Hexane was subsequently removed using a Buchi model R-210 Rotary Evaporator (New Castle, DE). Crude protein content was measured by the Dumas method in a LECO FP-628 system (Saint Joseph, MI), and calculated using a factor of 6.38.

5.2.2. Static in vitro gastric digestion

Mozzarella cheese was cut into 3 mm cubes (5.0 gram), and placed into Erlenmeyer flasks containing simulated gastric juice (50 mL) adjusted to pH 1.5, 3.0, or 5.0 (six replicate flasks per pH), respectively. The flasks were placed in a water bath and incubated at 37°C for 120 minutes without any agitation. At increments of 20 min, one flask at each pH was removed from the water bath, and the contents were filtered. The cheese cubes were subjected to a compression test with 50% strain to measure their harness (n=8). Filtered samples were collected and vacuumed dried to measure percent solids. The data were used to evaluate the loss in solids due to leaching over 120 min. Comparative trials were performed on Parmesan and Cheddar cheese.

5.2.3. Imaging of Cheese

The cheese cubes incubated in gastric juice, as detailed above, were collected and cut in half to examine their internal structures. The microstructures of the un-cut digested cheese cubes were evaluated using a Zeiss 1450EP Scanning Electron Microscope (Scotts Valley, CA). The cheese cubes were fixed for 120 min in 2.0% glutaraldehyde solution (pH 7.3, solubilized in 0.1

M Phosphate Buffer Solution) at room temperature. The cheese cubes were washed three times for 30 min in PBS, and post-fixed in 1.0 % osmium tetroxide at room temperature for 1 hour. The samples were washed for additional 3 times with buffer solution followed by dehydration using 20% increments of ethanol with the last 3 washes containing 100% ethanol. Finally, samples were washed twice in hexamethyldisilazane, and air dried overnight. Grooves were created in the samples before fracturing to reduced misleading artifacts. Fractured and dehydrated samples were coated with gold using SPI-Module Sputter Coater (West Chester, PA) before being observed under the SEM.

5.2.4. Digestion of cheeses in the Dynamic Gastric Simulation Model (DGSM)

Major components and dimensions of the Dynamic Gastric Simulation Model are described in Do et al (2015). Briefly, the model consists of an insulated vessel to maintain an internal temperature of 37°C throughout the experiment. The standard protocol includes the pumping of simulated gastric juice with a pH of 1.5 at a rate of 1.0 mL/min. Gastric emptying were simulated by removing the digesta at the rate of 3.0 mL/ min. Gastric contractions were simulated through compressions forces that move the probe at a speed of 16.7 mm/s into the insulated vessel. A gap of 1 cm was left between the bottom of the probe and the base of the vessel before the probe returned to its starting position. Three compression cycles were applied per minute, and the digestion trials were carried out for 120 minutes. The force was measured in real time utilizing the Food Technology Corporation TMS-Pro Texture Analyzer (Sterling, Virginia).

Upon consumption of a large meal, the pH of the stomach increases up to 7.3 due to the dilution and absorption of acids by ingested constituents (Dressman et al., 1990). However, the sporadic secretion of gastric juice at the initial stage may increase to 50 mL/min (Versantvoort et al., 2005). The interactions between the ingested food and gastric juice generate various initial

pH's. Subsequently, the variations in initial pH may influence both the rate of acid and enzyme hydrolysis of the cheeses. Trials were performed with ascending amounts of initial simulated gastric juice to accommodate the high rates of initial gastric secretion. The goal of these trials was to investigate the effect of the initial and the dynamic gastric environments on the chemical digestion of Mozzarella, Cheddar, and Parmesan cheeses. Cheese cubes (30 g) were placed in 200 mL DI water. The mixture was placed in the DGSM and digested using the standard protocol. Comparative trials were performed by incubating each of the cheeses with 50 mL of simulated gastric juice (pH 1.5) for two minutes before adding 150 mL of DI water to have comparable volumes. Additional trials were performed with 100 mL of simulated gastric juice before addition of 100 mL of water. The amounts of initial simulated gastric juice were 0, 50, and 100mL and classified as Low, Medium, and High, respectively. The emptied contents were collected continuously for 120 minutes, and the samples were grouped together in increments of 15 minutes. Hexane was added to the aliquots and the samples were centrifuged at 6,000 x g for 5 minutes. The top layer of hexane was discarded, and the supernatant was collected to quantify the amount of amino acid present using the NOPA (o-phthaldialdehyde/N-acetyl-l-cysteine) method of Butzke and Dukes (1998). In addition, percent solids were also measured by vacuum drying. The pH of the emptied contents was monitored, and the overall rate of hardness reduction in the cheese mixture were monitored in real time.

5.2.5. Statistical analysis

Trials were conducted in duplicate. All average and total values were analyzed using Fisher's Least Significant Difference test at statistical significance of $P < 0.05$ with SAS® software (version 9.3, SAS Institute Inc., Cary, NC).

5.3. Results and discussion:

5.3. 1. Contents of moisture, protein, and fat in three cheeses

The percentage of moisture, fat, and crude protein were significantly different among the three cheeses used in the digestion studies. Table 5.1 shows the percentage of moisture, protein, and fats, which are generally in agreement with values reported in the literature (Lamothe et al., 2012). Parmesan cheese has the lowest moisture content of 20.8% mainly due to the aging process. During aging, moisture is removed through controlled storage temperature. Further protein hydrolysis also reduces the moisture content by allowing the ionic groups to compete and bond with available water in the system (Fox et al., 1993). The crude protein contents are also significantly different, with Cheddar cheese having the lowest percentage of protein with an average value of 27.4%. In addition, significant differences in the percentage of fat were also observed among the cheeses with Mozzarella having the lowest amount of fat with an average value of 15.98%. Ayala-Bribiesca and other researchers noted that higher amount of fat globules present in the cheese disrupts the protein matrix and reduces the hardness (2016). The composition of the cheese and the various protein matrices give the individual cheeses their distinct structures. The behavior of these structures in the gastric environment may affect the disintegration and digestion of the different cheeses.

5.3.2. Static digestion of cheeses

Static simulation trials were performed by incubation of each cheese at pH 1.5, 3.0, and 5.0 since the pH of the stomach during digestion may vary between 1 and 5 (Malagelada et al., 1976). Typically, food hardness directly correlates with gastric pH. At low pH, acid and enzymatic hydrolysis reduce the hardness of the ingested food. Lower pH values decreased the hardness in carrots and ham as the acids and enzymes further breakdown the structural cell walls and protein

matrix, respectively (Lentle and Janssen, 2011; Kong and Singh, 2008). However, Figure 5.1 shows the inverse relationships between cheese hardness and the pH of the simulated gastric juice. The digested cheeses had the highest hardness at pH 1.5 and lowest hardness at pH 5. This is opposite from conventional results. The reason for the higher hardness of the cheese at the lower pH is attributed to the more acidic environment that encourages greater enzymatic activities of pepsin. Similar to the cheese making enzyme of chymosin, pepsin has been shown to hydrolyze the kappa- casein in milk at the peptide Phe 105-Met 106 (Rolet-Repecaud et al., 2017). Greater enzymatic hydrolysis of the casein enables hydrophobic regions of the micelle to aggregate and form stronger network (Sousa, Ardo, & MicSweeney, 2001). In addition, hydrochloric acid found in gastric juice has been shown to further harden the cheese through the acidic precipitation of the casein (Robinson et al., 1998). The acidic environment further influences the rates of hardness reduction. Unconventionally, the low pH hardened the exterior of the three cheeses, and protected the cheese matrix from being further hydrolyzed by acids and enzymes. This phenomenon allowed all three cheeses to resist the highly acidic gastric environment with lower hardness reduction rates at low pH. The trend was more significant for Mozzarella cheese as the low pH even increased the hardness in Mozzarella cheese above the initial hardness. Conversely, Figure 5.1 shows that the higher pH generated faster rates of hardness reduction. Ultimately, the various gastric environments affected the hardness of the cheeses differently. Greater acid contents in the gastric juice helped the cheeses to resist hardness reduction with the capability of even increasing the hardness of cheeses beyond the initial hardness.

5.3.3. Nutrient leaching and structure changes of cheese during static gastric digestion

The solids content of the cheese after various gastric incubation times were used as indicator of nutrients leaching. Figure 5.2 indicates the loss in solids from the cheese cubes over

time in simulated gastric juice at pH 1.5. Parmesan had a 60% loss of solids, the fastest solid loss rate within the first 20 minutes. Due to the processing of Parmesan cheese, which required vigorously stirring during cooking, much of the water was exuded out of the Parmesan curd grain. While this allows the curd grain to retain their individuality, the overall curd grains become relatively wrinkled with very poor cohesive capability (Fobbetti and Di Cagno, 2002). The poorly cohesive Parmesan cheese matrix causes a quick rate of solids loss as the penetration of acid and enzymes into the voided space further encourages the degradation of protein matrix. Comparatively, Cheddar cheese has a relatively linear decreasing trend in solids loss as the fat migrates out of the cheese with s 60% loss at the end of incubation. Other studies found that fats are the main nutrient leached from Cheddar cheese during gastric digestion (Xixi et al., 2016). Figure 5.2 shows the resistance of nutrient leaching found in the digestion of Mozzarella resulting in only 15% solid loss at the end of 120 minutes.

Further sampling of cheese every 20 minutes showed signs of gastric juice migration into the cheese. Figure5.3 shows the whole cheese cubes on the top row followed by a cross section of each cube. Unlike the migration of gastric juice that degrades the structure of carrots, the migration of gastric juice inside the cheese strengthens the structure by forming a protective outer layer while keeping the interior of the cheese relatively moist. Further incubation of the cheese allowed for greater migration of gastric juice inside the cheese, which eventually hardened the whole cheese cube. Moreover, the Scanning Electron Microscope (SEM) results in Figure 5.4 show the dense and compact regions of protein on the exterior of Mozzarella cheese cube. After 120 minutes of static incubation at pH 1.5, the interior structure of the cheese cubes retained their original structure with remnants of fat globule cavities. As a result, the outer layer of the cheese cube hardened and

reduced the leaching of nutrients as shown by the higher retention of solids inside the Mozzarella cheese cubes.

5.3.4. Digestion of cheeses using the Dynamic Gastric Simulation Model (DGSM)

5.3.4.1. Rate of cheese hardness reduction

The pH profiles for Mozzarella Cheese are shown in Figure 5.5 to demonstrate the continuous acidification of the digesta under dynamic gastric simulation. The other two cheeses follow a similar trend. There is a steady decline in pH as more acid and enzymes were introduced into the DGSM for the trials classified as Low. The initial pH of the digesta for the Medium and High trials started at 3.69 and 2.96 respectively. The pH increased initially for the latter two experiments, and this may have been the result of continuous compressions that fractured the cheese releasing calcium phosphate (Johnson, 2002). Phosphate buffer, a known buffering agent, kept the pH relatively stable before a further decline in pH after 20 minutes. The interactions between pH and enzymes further influenced the disintegration rate of the digested cheese.

In a previous research, bulk hardness was defined as the hardness of the mixture containing food and simulated gastric juice. The reduction in bulk hardness was attributed to both the softening rates and the reduction in particle size of the food mixture. The overall hardness in the gastric mixture was recorded by the texture analyzer, is shown in Figure 5.6 for the dynamic digestion of Mozzarella cheese in varying amounts of initial simulated gastric juice. As in static gastric digestion trials, high pH yielded the lowest initial hardness while the low pH yielded the highest initial hardness. The increasing amounts of simulated gastric juice from 0, 50, and 100 mL produced initial pH of 5.76, 3.69, and 2.96, respectively. Furthermore, decreasing the pH produced an increase in initial hardness of the cheese mixture to values of 130, 150, and 180N, respectively. The results agreed with the static digestion trials as greater acid and enzyme

hydrolysis showed a resistance in hardness reduction of Mozzarella cheese during the period of 10-80 minutes when greater amounts of simulated gastric juice were used. Unlike static digestion, the continuous contractions and removal of digesta in the dynamic simulation trials showed decreasing rates of hardness reduction over time. The rates of hardness reduction were not different between the Low and Medium levels of simulated gastric juice.

Figure 5.7 shows the overall rates of hardness decrease in the mixture of the three tested cheeses. Unlike Mozzarella, Cheddar and Parmesan cheese showed limited resistance to the hardness reduction. Cheddar cheese gave the lowest initial force with a mixture hardness of 85N. In the dynamic gastric environment with greater simulated gastric juice, the degradation of the Cheddar cheese protein matrix allows for the liberation of fat globules. This liberation of fat globules weakens the cheese by leaving large cavities in the cheddar cheese protein matrix (Lamothe et al., 2012). The continuous peristaltic simulation further disintegrates and reduces the hardness of the Cheddar cheese mixture. Parmesan cheese experienced a similar pattern with quick rates of hardness reduction in cheese mixture, especially at the high level of simulated gastric juice. It is suggested by researchers that the minimum 9 months aging process hydrolyze the protein and further weaken the overall protein matrix of Parmesan (Barbieri et al., 1994). In agreement with the static digestion results, the influx of gastric juice into the dried and poorly structural protein matrix of Parmesan allowed for a fast rate of hardness reduction.

5.3.4.2. Disintegration Rate of cheese

Figure 5.8 shows the various disintegration patterns of the unemptied contents after 120 minutes. Greater disintegration is shown in the unemptied contents of both Mozzarella and Cheddar cheese were observed when high amounts of gastric juice were used (Fig. 8A&B). On the contrary, larger Cheddar and Mozzarella cheese particles remained when low amounts of

simulated gastric juice were used. In addition, the graphs in Figure 5.9A&B indicate the rates of disintegration as the percent of solids emptied, from the dynamic digestion of Mozzarella and Cheddar cheese, respectively. When comparing the digestion of Mozzarella cheese, the low amount of gastric juice trial had 56.3% solids emptied after 120 minutes of dynamic digestion. When the simulated gastric juice was increased to 50 mL and 100 mL the amount of solids removed increased to 75.7% and 79.4%, respectively. Similarly, addition of 0, 50 or 100 mL simulated gastric juice at the initial point generated increasing emptied solids with percentages of 46.7%, 62.7%, and 74.9% for Cheddar cheese, respectively. The same pattern of higher amount of simulated gastric juice generating greater disintegration is also found in the digestion of Parmesan cheese. However, the fast rates of disintegration in Parmesan cheese allowed similar percentages of solids to be emptied with results shown in Figure 5.9C. Other researchers reported that increasing amounts of gastric juice enhances food disintegration through enzymes and acid hydrolysis. The use of enzymes in the earlier cheese digestion study showed improvements in the hydrolysis of the casein matrix and increased disintegration values from 14% to 24% (Xixi et al., 2016). The data indicate similar disintegration patterns but for different reasons. The static trials showed hardening of Mozzarella cheese upon further acidification. This hardening of Mozzarella cheese occurred again in the DGSM as the digesta were further acidified in the trials at high levels of simulated gastric juice. The hardening process stiffens Mozzarella particles to further influence the interactions between particles. Upon the simulated peristaltic contractions in the DGSM, the movement of the probe to the base of the model compressed and allowed stiff mozzarella particles to further grind neighboring cheese particles. The grinding of stiff Mozzarella particles produced greater disintegration as monitored through the production of much smaller cheese fragments and greater solids emptied as shown in Figure 5.8.

5.3.4.3 Protein hydrolysis under DGSM.

The amino acid content of the emptied digesta from the dynamic gastric trials was evaluated to further investigate their bioaccessibility. Figure 5.10A shows the amino acid concentration profiles with high amounts of amino acids generated in the digestion of Parmesan cheese. Both Mozzarella and Cheddar cheeses showed increasing linear trends in the amount of amino acids generated with the highest concentrations of 1.8 g/L and 2.3 g/L, respectively. Figure 5.10B shows the influence of various concentrations of simulated gastric juice on the protein hydrolysis of Cheddar, Mozzarella, and Parmesan cheeses. At all three gastric juice levels, the total amount of amino acids generated remained consistently high, and the highest was produced by Parmesan cheese at 24.0 g/L. The high amount of protein hydrolysis of Parmesan cheese was expected as much of the protein was hydrolyzed during the aging process. In the Cheddar cheese digestion trials, the increasing amount of simulated gastric juice from 0 mL to 100 mL improved protein hydrolysis from 9.6 g/L to 12.7 g/L. However, the increasing amount of simulated gastric juice from 0 mL to 100 mL reduced protein hydrolysis in Mozzarella from 10.6 g/L to 6.8 g/L. When comparing among the cheeses, simulated gastric juice (100 mL) degraded Cheddar cheese and generated close to twice the amount of amino acids found in the digestion of Mozzarella cheese. Similar observations were noted during the gastric digestion of milk. Milk formed protein gels with compact matrices capable of slowing down protein hydrolysis (Morris and Cunning, 2008). Even though the crude protein content of Mozzarella cheese is significantly higher, the combination of the dense protein structure and the high concentration of acid and enzymes that enabled the development of a protective layer. As a result, the protective layer impeded the diffusion of enzymes and acid resulting in slower protein hydrolysis.

5.4. Conclusion

The acid and enzymes in the gastric environment are generally thought to affect the structures of ingested food by reducing hardness and increasing disintegration rate. Unconventionally, the greater acidic gastric environment allowed the three cheeses to develop a protective layer. This protective layer allowed the cheeses to resist hardness reduction with the lowest hardness reducing rate at the low pH and a high hardness reducing rate at high pH. Our study also demonstrated that the greater acid and enzyme concentrations during static gastric simulation led to an increase in the hardness of Mozzarella cheese while decreasing nutrient leaching. Furthermore, the resistance of Mozzarella cheese to hardening was also found in the dynamic gastric digestion simulation. Higher hardness regions were noticeable when greater amounts of simulated gastric juice were used at the start of digestion. The continuous acidification process through the dynamic simulation of gastric secretion allowed an increase in hardening of Mozzarella particles, and further grinding of stiff mozzarella cheese particles improved disintegration rate. In contrast, the greater hardening and the formation of a protective layer in Mozzarella cheese reduced protein hydrolysis by generating much lower concentrations of amino acids when compared to Cheddar cheese. Ultimately, the combination the composition and the arrangement of compounds creates food structure. More importantly is the behavior of the food in the digestive tract that will dictate both the release of bioaccesssible nutrients and their absorption.

References

Ayala-Bribiesca, E., Lussier, M., Chabot, D., Turgeon, S. L., & Britten, M. (2016). Effect of calcium enrichment of Cheddar cheese on its structure, in vitro digestion and lipid bioaccessibility. *International Dairy Journal*, 531-9.

Barbieri, G., Bolzoni, L., Careri, M., Mangia, A., Parolari, G., Spagnoli, S., & Virgili, R. (1994). Study of the volatile fraction of Parmesan cheese. *Journal of Agricultural and Food Chemistry*, *42*(5), 1170-1176.

Bornhorst, G. M., Ferrua, M. J., & Singh, R. P. (2015). A proposed food breakdown classification system to predict food behavior during gastric digestion. *Journal of Food Science, 80*(5), R924-934.

Chen, J., Vishwajeet, G., Holmes, M., Murray, B., Povey, M., Wang, Y., & Zhang, Y. (2011). Development of a simple model device for in vitro gastric digestion investigation. *Food & Function*, *2*(3--4), 174-182.

Dean, J. R., & Ma, R. (2007). Approaches to assess the oral bioaccessibility of persistent organic pollutants: a critical review. *Chemosphere*, 68(8), 1399-407.

Do, . H., Fanbin, K., Penet, C., Winetzky, D., & Gregory, K. (2016). Using a dynamic stomach model to study efficacy of supplemental enzymes during simulated digestion. *LWT -- Food Science and Technology*, *65*, 580-588.

Donhowe, E. G., Flores, F. P., Kerr, W. L., Wicker, L., & Fabin, K. (2014). Characterization and in vitro bioavailability of β-carotene: effects of microencapsulation method and food matrix. *LWT -- Food Science and Technology, 57*(1), 42-48.

Dressman, J. B., Berardi, R. R., Dermentzoglou, L. C., Russell, T. L., Schmaltz, S. P., Barnett, J. L., & Jarvenpaa, K. M. (1990). Upper gastrointestinal (GI) pH in young, healthy men and women. *Pharmaceutics Research, 7*(7), 756-761.

Dukes, B. C., & Butzke, C. E. (1998). Rapid determination of primary amino acids in grape juice using an o-phthaldialdehyde/N-acetyl-l-cysteine spectrophotometric assay. *American Journal of Enology and Viticulture, 49*(2), 125-134.

Fobbetti, M., & Di Cagno, R. (2002). Hard Italian cheeses, in Encyclopedia of Dairy Science. Academic Press, London, 378-385.

Fox, P. Paul, L. McSweeney, H. Timothy, M. Cogan, P. & Timothy P., G. (1993). Cheese: Chemistry, Physics and Microbiology (2nd ed.). London, UK, Chapman & Hall.

Guinee, T. P., Auty, M. A. E., & Fenelon, M. A. (2000). The effect of fat content on the rheology, microstructure and heat-induced functional characteristics of Cheddar cheese. *International Dairy Journal, 10*(4), 277-288.

Gunasekaran, S., & Ak, M. (2003). Factors affecting functional properties of cheese. *Cheese rheology and texture*, 409–439

Han, X., & Spradlin, J. (2000). U.S. Patent No. 6,093,424. Washington, DC: U.S. Patent and Trademark Office.

Hu, M. Li, Y. Decker, E. A., & McClements, D. J. (2010). Role of calcium and calcium binding agents on the lipase digestibility of emulsified lipids using an in vitro digestion model. *Food Hydrocolloids*, 24, 719-725.

Johnson, M. (2002). Cheese pH-What's behind the rise and falls? *Dairy Pipeline*, 14(4), 6-12.

Kong, F., & Singh, R. P. (2008). Disintegration of solid foods in human stomach. *Journal of Food Science, 73*(5), R67-80.

Kong, F., & Singh, R. P. (2009). Modes of disintegration of solid foods in simulated gastric environment. *Food Biophysics*, *4*(3), 180-190.

Kong, F., & Singh, R. P. (2010). A human gastric simulator (HGS) to study food digestion in human stomach. *Journal of Food Science, 75*(9), E627-E635.

Kozu, H., Nakata, Y., Nakajima, M., Neves, M. A., Uemura, K., Sato, S., Kobayashi, I., & Ichikawa, S. (2014). Development of a human gastric digestion simulator equipped with peristalsis function for the direct observation and analysis of the food digestion process. *Food Science and Technology Research, 20*(2), 225-233.

Lamothe, S., Remillard, N., Tremblay, J., & Britten, M. (2017). Influence of dairy matrices on nutrient release in a simulated gastrointestinal environment. *Food Research International*, *92*, 138-146.

Lentle R. Janssen P. (Eds.), The physical processes of digestion, Springer, New York, NY, USA (2011), 47–61

Malagelada, J. R., Longstreth, G. F., Summerskill, W. H., & Go, V. L. (1976). Measurement of gastric functions during digestion of ordinary solid meals in man. *Gastroenterology, 70*(2), 203-210.

Michalski, M. C., Camier, B., Gassi, J. Y., Briard-Bion, V., Leconte, N., Famelart, M. H., & Lopez, C. (2007). Functionality of smaller vs control native milk fat globules in Emmental cheeses manufactured with adapted technologies. *Food Research International, 40*(1), 191-202.

Mistry, V. V., & Anderson, D. L. (1993). Composition and microstructure of commercial full-fat and low-fat cheeses. *Food Structure, 12*(2), 259-266.

Morris, V. J., & Gunning, A. P. (2008). Microscopy, microstructure and displacement of proteins from interfaces: implications for food quality and digestion. *Soft Matter, 4*(5), 943-951.

Robinson, R. K., Scott, R., & Wilbey R. A. (1998). Cheesemaking Practice. Gaithersburg, Md: Aspen. 161-163.

Rolet-Repecaud, O., Arnould, C., Dupont, D., Gavoye, S., Beuvier, E., & Achilleos, C. (2017). Quantification of pepsin in rennet using a monoclonal antibody-based inhibition ELISA. *LWT- Food Science and Technology, 76*(Part A), 190-196.

Sousa, M. J., Ardo, Y., & McSweeney, P. H. (2001). Advances in the study of proteolysis during cheese ripening. *International Dairy Journal*, 11, 327-345.

Versantvoort, C. H. M., Oomen, A. G., Kamp, E. v. d., Rompelberg, C. J. M., & Sips, A. J. A. M. (2005). Applicability of an in vitro digestion model in assessing the bioaccessibility of mycotoxins from food. *Food and Chemical Toxicology, 43*(1), 31-40.

Xixi, F., Rioux, L. E., Labrie, S., & Turgeon, S. L. (2016). Disintegration and nutrients release from cheese with different textural properties during in vitro digestion. *Food Research International, 88*(Part B), 276-283.

Results

Table 5.1. Contents of moisture, protein, and fat in three cheeses

	Moisture (%)	Proteins (%)	Fats (%)
Parmesan	20.80^{c} ±0.20	39.46^{a} + 0.29	30.82^{a} +0.71
Cheddar	33.60^{b} +1.40	27.42^{c} + 0.22	23.09^{b} +0.51
Mozzarella	46.60^{a} +0.10	31.68^{b} +0.13	15.98^{c} +.74

Analyses were carried out in triplicate. Different superscript letters are significantly different at $P<0.05$.

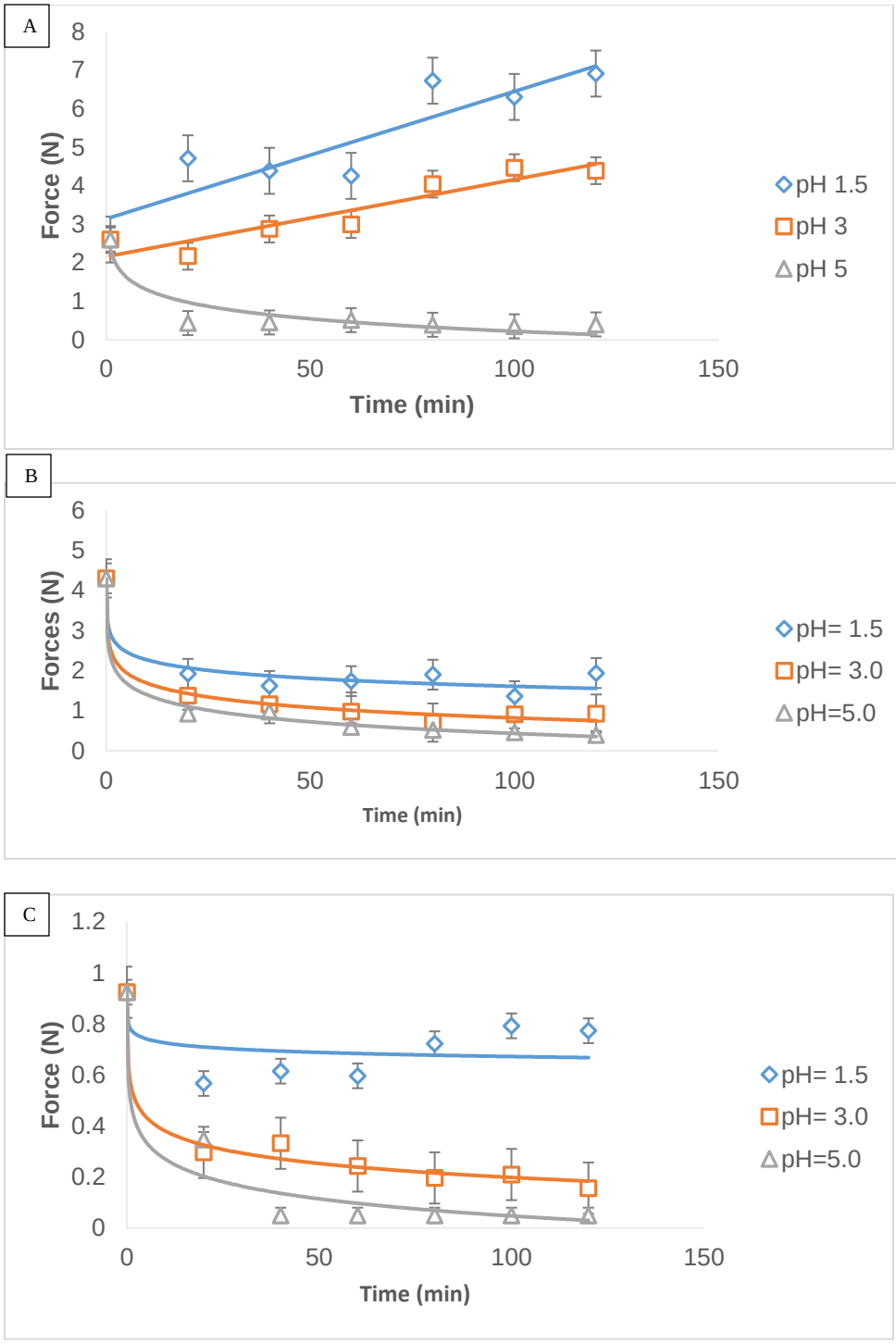

Figure 5.1. The cheese hardness and their softening rate during static incubation A) Mozzarella cheese, (B) Cheddar cheese, and (C) Parmesan cheese with simulated gastric juice (◊) pH 1.5, (□) pH 3.0, and (Δ) pH 1.5. n=8

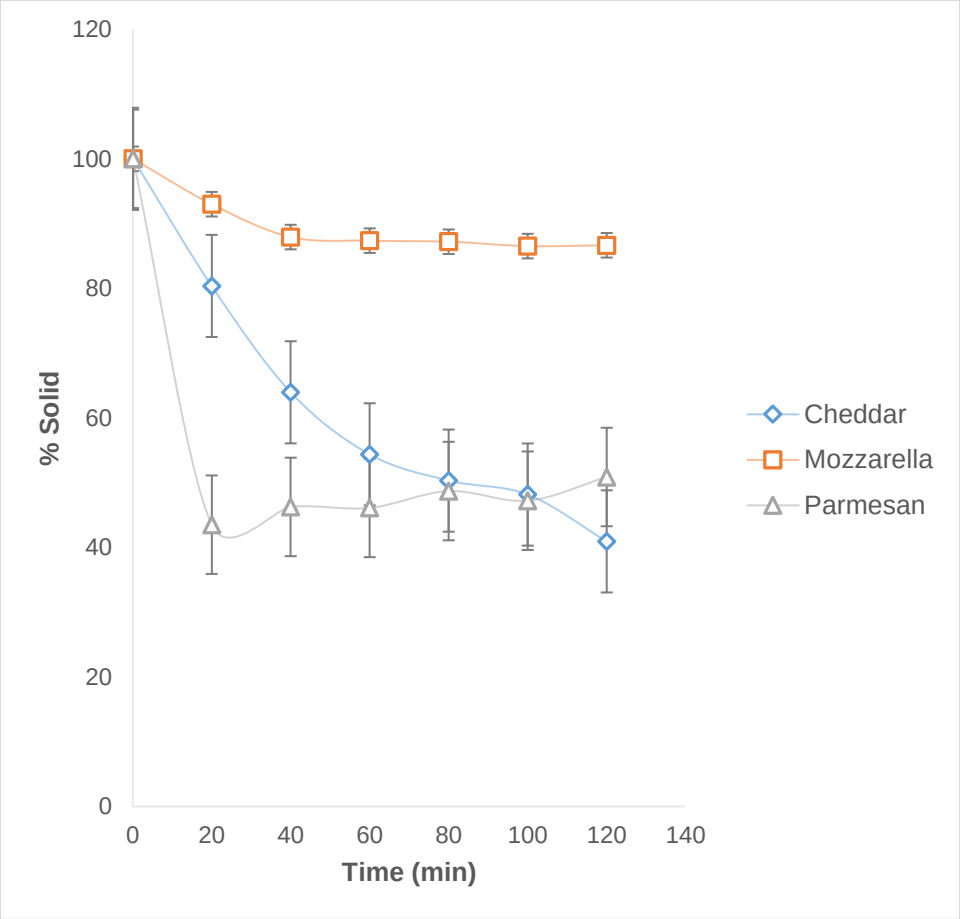

Figure 5.2. The percent solids content remained in cheese cubes after static incubation at pH of 1.5 for Cheddar (◊), Mozzarella (□), and Parmesan (Δ).

Figure 5.3. The migration of gastric juice into Mozzarella (A) and Cheddar cheese (B) during static soaking (pH 1.5). The top row of each picture represents the uncut cheese cubes soaked in simulated gastric juice. The bottom row of shows the cross section of the cubes and the migration of gastric juice into them.

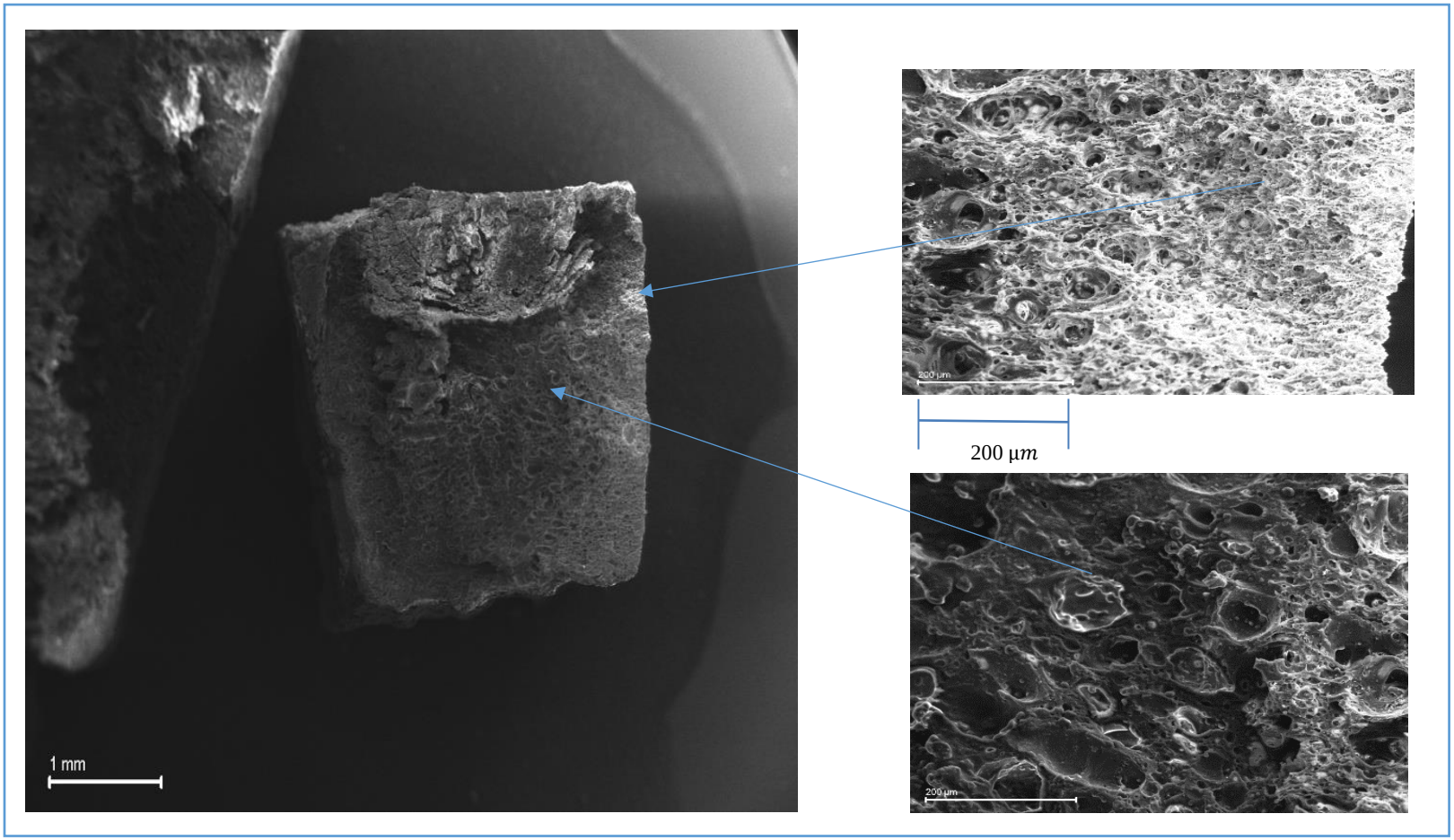

Figure 5.4. SEM images of Mozzarella cheese after 120 minutes of incubation with simulated gastric juice at pH of 1.5. The exterior of the Mozzarella formed a dense, compact protein matrix. The center of the cheese cube still contained relatively loose protein structures with large fat globule cavities

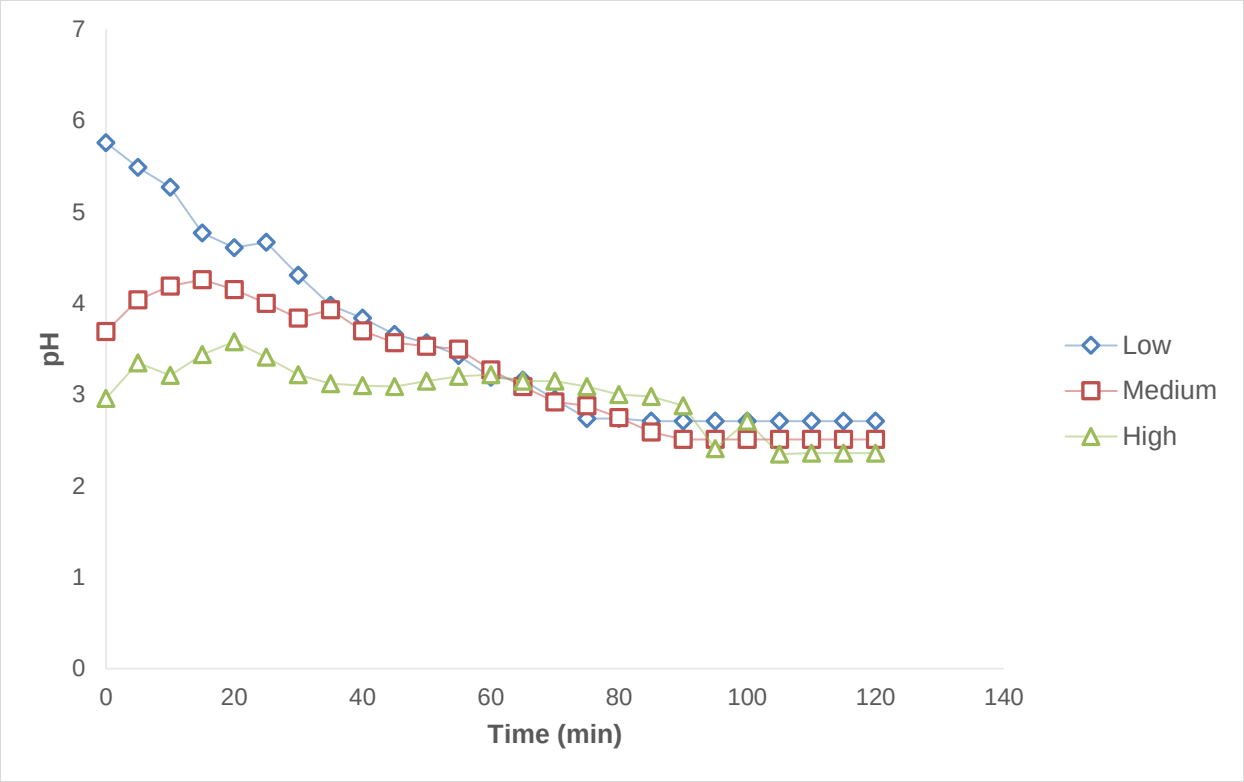

Figure 5.5. The pH profile of emptied digesta during incubation in Low -0 mL (◊), Medium- 50 mL (□), and High- 100 mL (Δ) levels of simulated gastric juices were used to incubated with Mozzarella cheese. Similar pattern was observed in in Cheddar and Parmesan cheese.

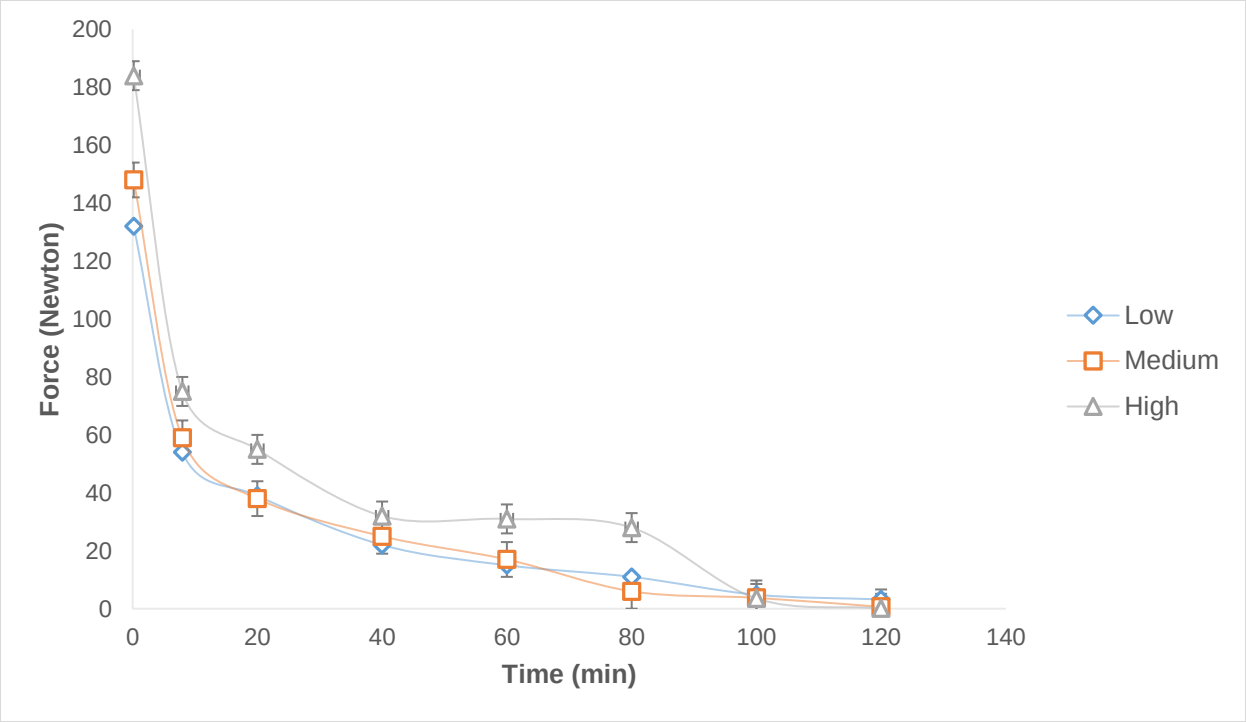

Figure 5.6. Force profiles obtained from simulated digestion of Mozzarella cheese in the DGSM. Different amounts of simulated gastric juice and water were added including (◊) Low (200 mL water), (□) Medium (50 mL simulated gastric juice plus 150 mL water), and (Δ) High (100 mL simulated gastric juice plus 100 mL water). Cheese samples were presoaked for 2 minutes before the DGSM was initiated at a secretion rate of 1.0 mL/min, 3 cycles/min peristaltic contractions, and gastric emptying at a rate at 3.0 mL/min.

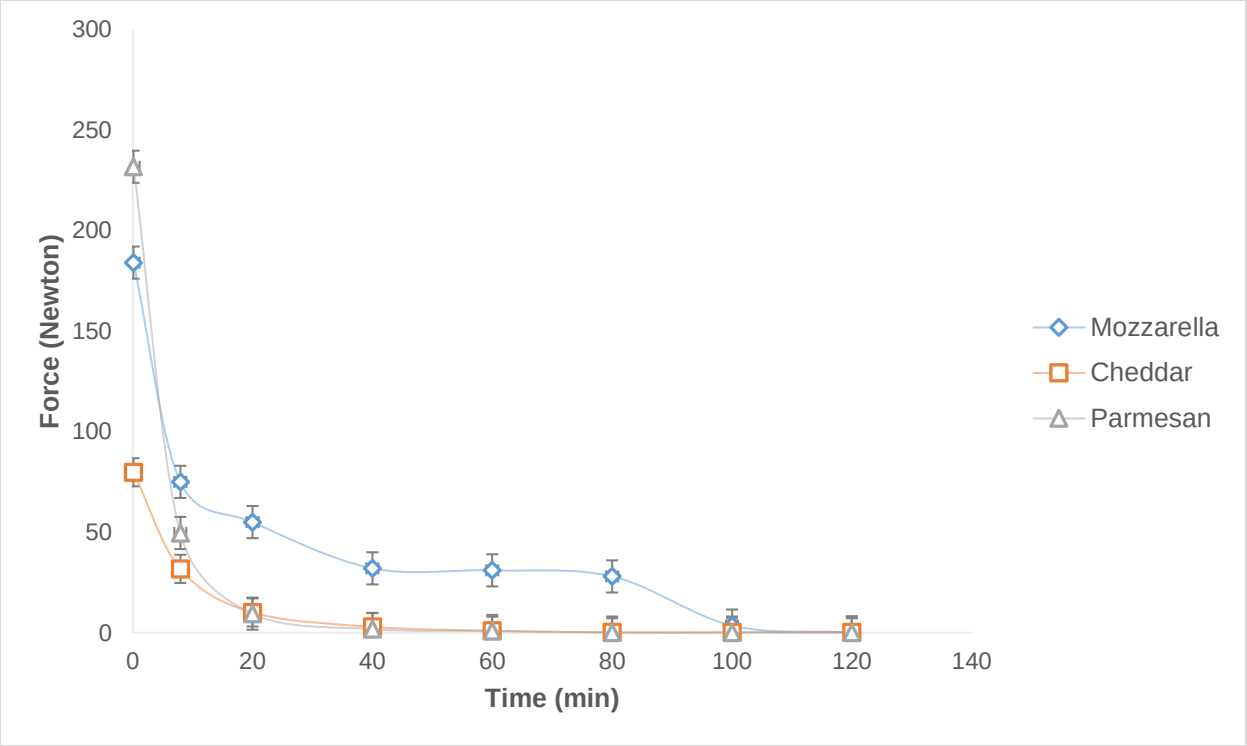

Figure 5.7. Force profiles for various cheeses during simulated digestion in DGSM with 100 mL of preloaded simulated gastric juice for (◊) Mozzarella, (□) Cheddar, and (Δ) Parmesan.

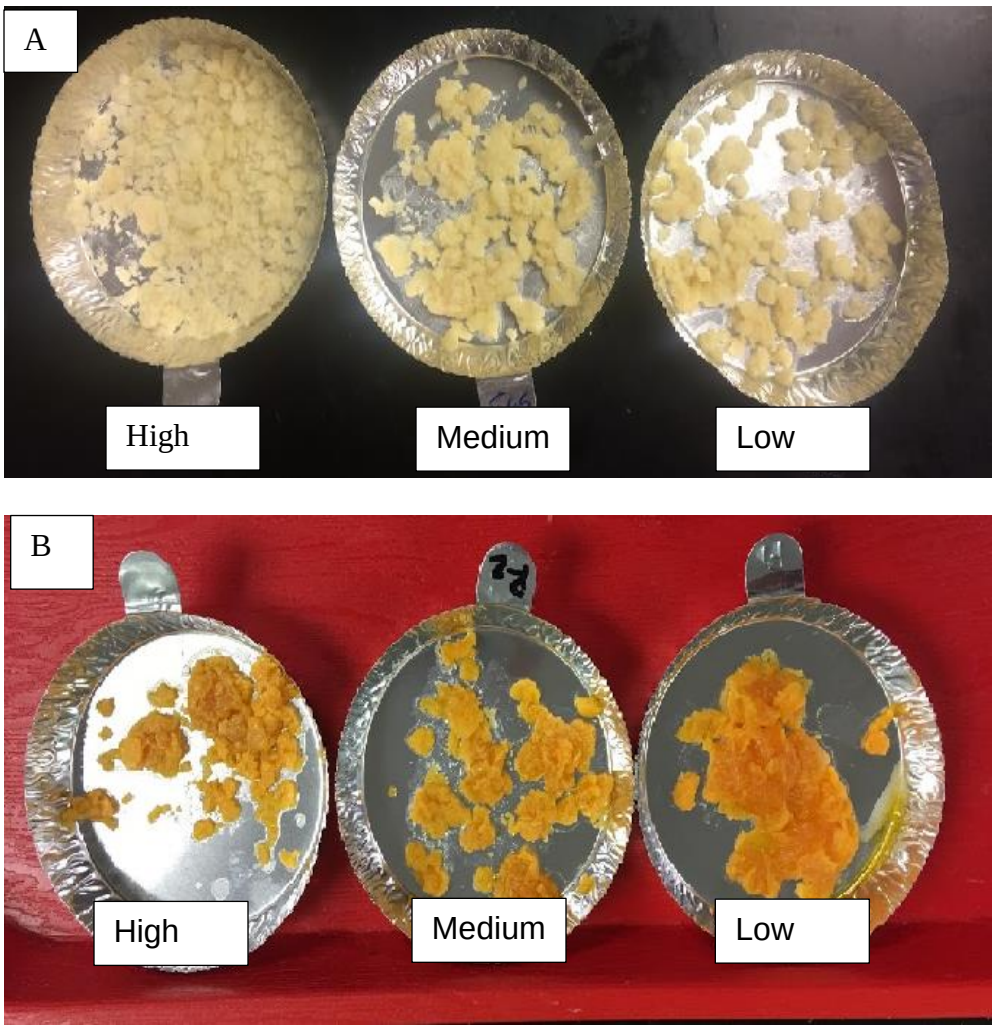

Figure 5.8. Cheese particles collected from unemptied digesta for (A) Mozzarella and (B) Cheddar cheese with High, Medium, and Low levels of gastric juice.

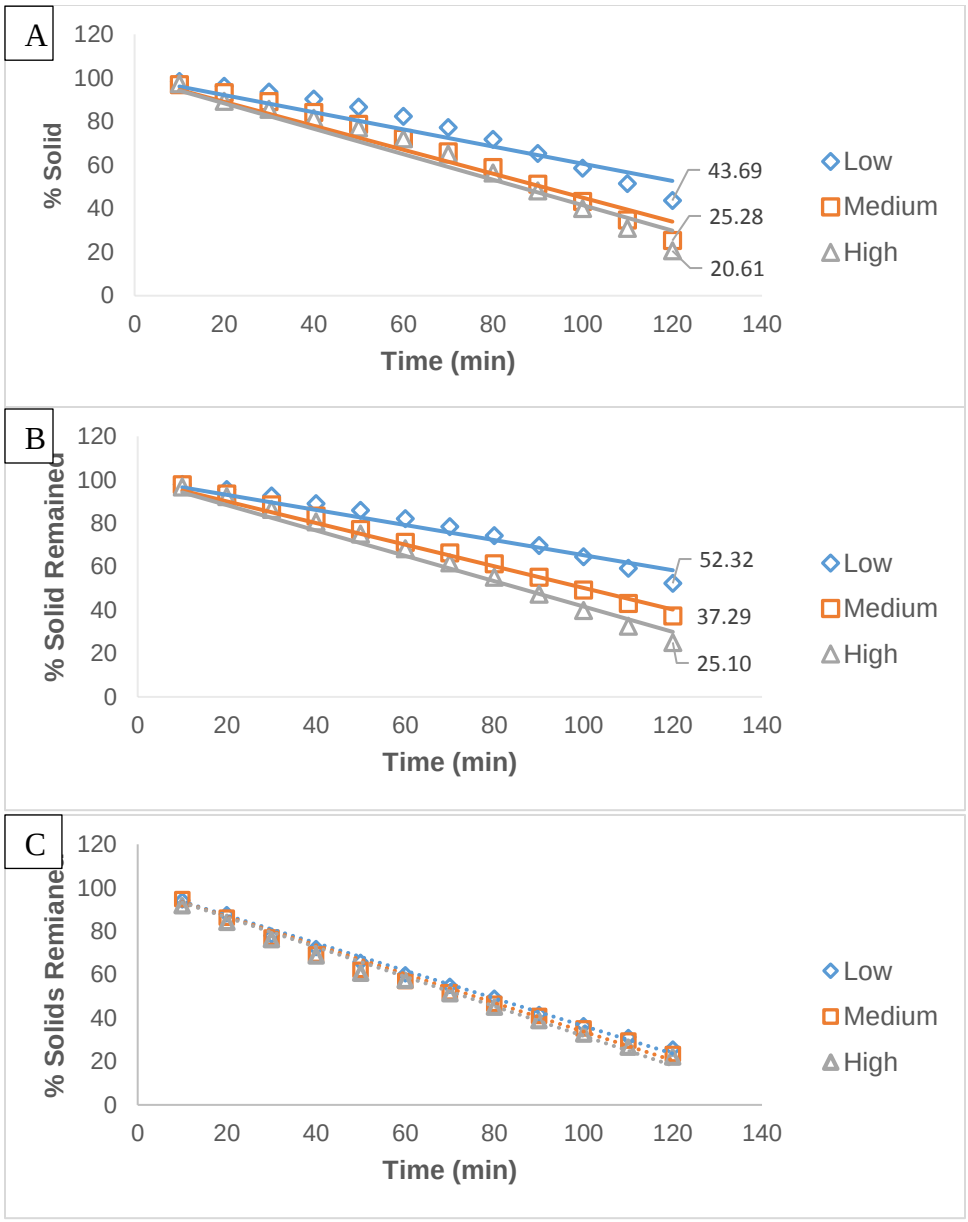

Figure 5.9. The gastric emptying profile for: A) Mozzarella, B) Cheddar, and C) Parmesan cheese at Low (◊), Medium (□), and High (Δ) initial levels of simulated gastric juice.

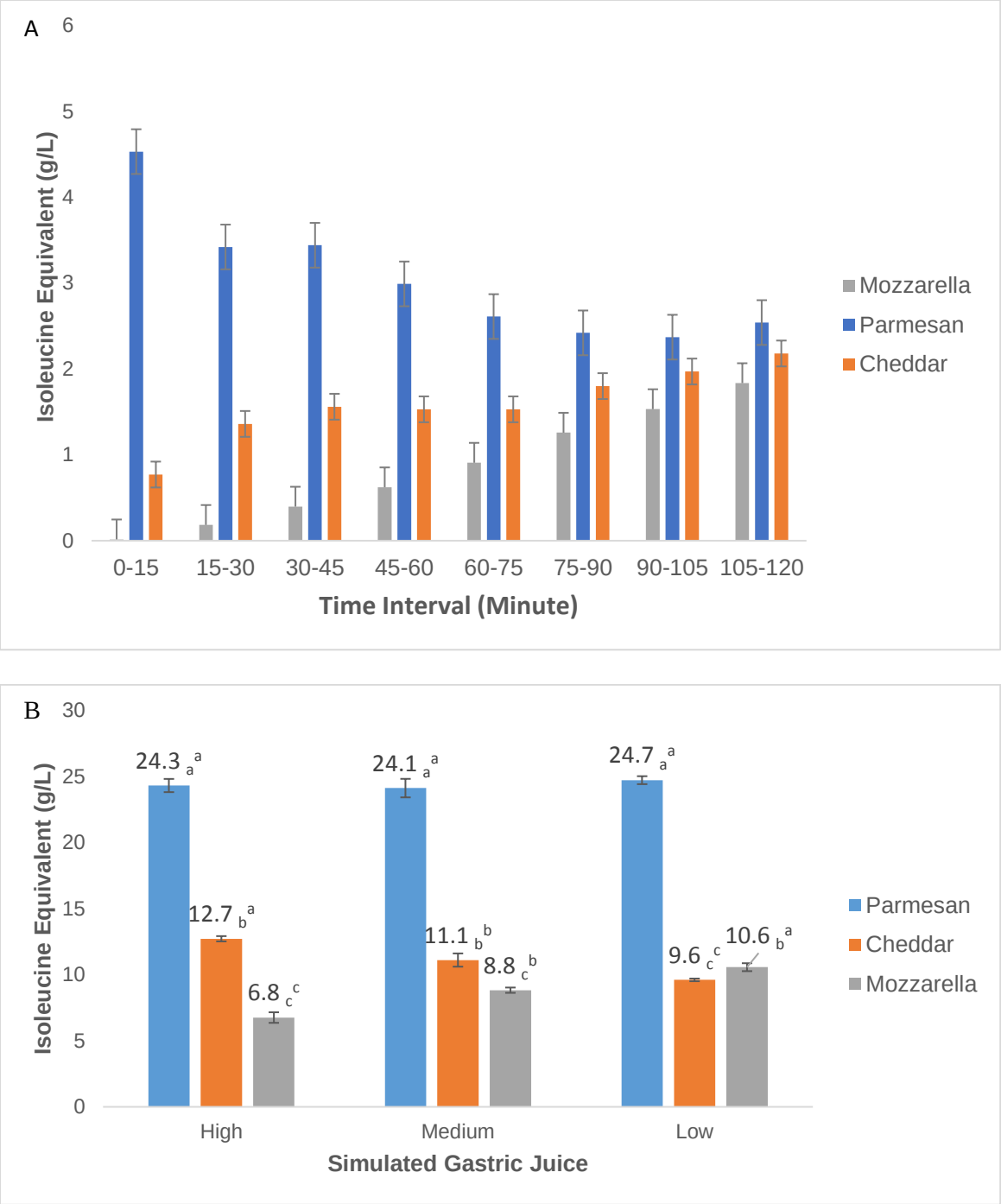

Figure 5.10. The amino acid content expressed as isoleucine equivalent in: A) the emptied digesta at various time point with the 100 mL of initial gastric juice, and B) the total concentration generated from the digestion cheeses for ( ) Cheddar, ( ) Mozzarella, and ( ) Parmesan.

CHAPTER 6

USING A DYNAMIC STOMACH MODEL TO STUDY THE EFFICACY OF SUPPLEMENTAL ENZYMES DURING SIMULATED DIGESTION

Do, D., Kong, F., Penet, C., Winetzky, D., & Gregory, K. 2015. *LWT-Food Science and Technology*, 65,580-588.

Reprinted here with permission from the publisher. Copyright 2015, with permission from Elsevier.

6.0. Abstract

In vitro static digestion models, with constant pH and volume, are commonly used to evaluate supplementary enzyme activity. The research objective was to apply a dynamic stomach model, Dynamic Gastric Simulating Model (DGSM), to evaluate the efficacy of supplementary enzymes in assisting food digestion. DGSM incorporates compressive forces to disintegrate food, mimics continuous gastric emptying, and simulates gastric secretion that generated pH profiles similar to human stomach. Static and dynamic models were used to evaluate supplementary proteases (SPs) efficacy. Additionally, acid-stable supplementary fungal enzyme blends were tested on food matrix containing oil, starch, and tuna using DGSM. A prescribed pancreatic enzyme drug, CREON, was used as a comparison. In static model, porcine pepsin (PP) had higher proteolytic activities generating significantly higher average Tyrosine Equivalent (TE) concentrations at pH 1.3 and 3. DS Proteases generated comparable TE concentrations to PP at pH 5. Under DGSM, addition of DS Proteases and Peptidases generated significantly greater TE and Primary Amino Nitrogen (PAN) than PP alone. Main findings indicate enhancements of food digestion upon adding supplementary enzymes and blends. Furthermore, DGSM showed great potential as being an alternative tool used to study enzyme performances inside the human stomach as affected by dynamic physiological conditions.

Key Words: Dynamic Gastric Simulating Model (DGSM), enzyme supplements, gastric digestion, simulation

6.1. Introduction

Supplementary digestive enzymes are commonly used to improve food digestion. Oral pancreatic enzyme supplements are often prescribed to treat patients suffering from chronic pancreatic insufficiency diseases including Crohn's diseases and Cystic Fibrosis (Scolapio et al., 1999). The sources of supplementary digestive enzymes are derived from animals, plants, and fungi. Examples include prancreas, bromelain, and β- galactosidase from porcine, pineapples, and *Aspergillus oryzae*, respectively (Roxas, 2008). Enzymes derived from microbes are often used to make supplementary digestive blends because the mean of extracting the enzymes are cost effective, and the enzymes possess wider pH range of activity when compared to animal and plant derived enzymes (Nakamura et al., 1998). Furthermore, synergistic effect in aiding digestion has been reported when microbial derived enzymes were combined with animal and plant derived enzymes (Schneider et al., 1985). However, the efficacy of enzymes to aid digestion is debatable as they are thought work more efficiently in a laboratory setting than in the actual human body (Dodge & Turck, 2006). *In vivo* digestion studies are the gold standard in testing the efficacy of supplementary digestive enzymes. Extensive time commitment, high cost, and relatively greater variations in the data are several disadvantages for using *in vivo* methods. *In vitro* digestion models are thus used to study the efficacy of supplementary enzymes as an alternative method (Boisen & Eggum, 1991).

The two main categories of *in vitro* digestion model are static model and dynamic model. Most *in vitro* models are considered static as the pH (ranging from 1-3) and the volume are kept constant (Kong & Singh, 2010). An example includes using an Erlenmeyer flask placed in temperature and speed controlled water bath. Researchers have used this model to examine food disintegration, the release of essential nutrients from food matrix, and the release of toxic mercury

after the digestion of fish (Cabanero et al.,2007; Kozu et al., 2014; Kulkarni et al., 2007). The convenience attribute makes this model preferable. However, static digestion trials are unable to adequately simulate the dynamic physiological conditions food encounters in the human stomach. The constant pH underestimates the enzymatic reactions of certain enzymes while overestimating product formation of other enzymes. Long incubation periods without changes in the digesta volume increases products formation due to high retention time of substrates and enzymes. The increases in products by the static model reiterate the point that supplementary enzymes may work better in the laboratory setting than in the human body.

The physical and chemical conditions inside the human stomach are more complex than those found in a static model. The mechanical forces from the gastric contractions physically breakdown the food structures through disintegration (Chessa et al., 2014). In addition, continuous gastric emptying physically removes food particles less than 2mm (Hellström et al., 2006). Furthermore, the stomach pH continuously declines as gastric juice secretions modify the chemical conditions of the stomach by releasing digestive enzymes and hydrochloric acid. Acidification of the human stomach contributes to the acid hydrolysis of food while assisting in digestion of food through the activation of proteolytic enzymes (Wey et al., 2014). Dynamic digestion models have been developed to better simulate the conditions of the human stomach. Examples include TNO (gastro-) Intestinal Models, (TIM) and Dynamic Gastric Model (DGM), and Human Gastric Simulator (HGS) developed by The Netherlands Organization for Applied Science Research and The Institute of Food Research, and researchers at The University of California Davis, respectively (Minekus et al., 1995; Chessa et al., 2014; Kong & Singh, 2010)

Researchers proposed a dynamic model simulating gastric digestion using a spherical Teflon probe attached to a texture analyzer that was used to mix and disintegrate food (Chen et al.,

2011). A similar stomach model was created in this research. The proposed model, Dynamic Gastric Simulation Model (DGSM), incorporates additional factors including the integration of continuous gastric secretions, gastric emptying, and a different probe design. The main benefit of the DGSM includes the simulation of a dynamic environment with changing volume, changing pH, and changing forces that resemble the conditions found in the human stomach. Thus, the objective of the research was to use the DGSM to further investigate the efficacy of selected supplementary digestive enzymes under dynamic simulated gastric conditions. Supplemental Proteases efficiencies were evaluated in digesting casein using both a static model and the DGSM. The DGSM was further used to test the efficacy of commercial supplementary enzyme blends in assisting the hydrolysis of a complex food matrix containing oil, starch, and tuna.

62. Materials and Methods

6.2.0. Materials

Porcine mucin, porcine pepsin, porcine alpha amylase, Folin & Ciocalteu's (CAS: 47641, Lot: BCBM 7678V), and solid bovine casein (CAS:9000-71-9, Lot: SLBJ3852V) were obtained from Sigma–Aldrich Chemical Company (St. Louis, MO). Acid Stable Protease (Lot:ASP-TW22), DS Protease (Lot:DSP-VW28), Peptidase (Lot: UMP-VW28), Fungal Protease (Lot: FP1MBC-OV14) were obtained from BIO-CAT (Troy, VA). The sources of the extracted proteases, optimum pH, and optimum temperatures for the enzymes activities are shown in Table 6.1. Two enzyme cocktails referred to High Activity Blend and Low Activity Blend were obtained from BIO-CAT (Troy, Virginia). The enzyme blends have proprietary concentrations of amylase, lipases, and proteases. CREON, a prescription pancreatic enzyme drug having low activity under gastric conditions, was used as a comparison (AbbVie Inc. Chicago, IL). Canned tuna in Water and pure canola oil were purchased at local store (Athens, GA).

6.2.1. Preparation of simulated juice

Simulated salivary and gastric juices were prepared according to the method described by previous researchers (Donhowe et al., 2014). Simulated salivary juice, with a pH 6.8, contains 1mg/mL of mucin, 2 mg/mL of porcine alpha amylase, and various salts. The simulated gastric juice with pH of 1.3 contains 6 mg/mL mucin, 5 mg/mL porcine pepsin, and various salts. Enzymes were added on the day of the experiment to preserve enzymatic activities.

6.2.2. Development of Dynamic Gastric Simulation Model (DGSM)

The proposed model consists of an acrylic water insulated vessel and a probe made of PVC attached to a TMS-Pro texture analyzer with a 500 N load cell (Food Technology Corporation, Virginia). The DGSM is shown in Figure 6.1. The probe and gastric chamber are shown in Figure 6.2. The water insulated vessel simulates the stomach chamber and it can accommodate up to 300 mL of food. The inner chamber has a 36 mm radius, and a 110 mm height. The bottom is a truncated cone with a 17 mm base radius, a 36 mm top radius, and a 17 mm height. The outer chamber has a 72 mm radius, and a 152 mm height. Plastic tubing (3.4 mm inner diameter) was placed at the bottom of the inner vessel to empty gastric contents. There are two ports on the outer chamber for water circulating to ensure the internal chamber remains 37˚C.

The gastric contractions were achieved by the up and down movements of a probe attached to a texture analyzer. The probe consists of two truncated cones separated by a cylinder with a 30 mm radius and 16 mm height, as shown in Figure 6.2. The bottom truncated cone has 13 mm small radius, 34 mm height, and 30 mm large radius. The top truncated cone has a 16 mm small radius, a 26 mm height, and a 30 mm large radius. A cylinder, with 16 mm radius and 144 mm height, allows the attachment of the probe head to the texture analyzer. The probe compresses food by moving down into the bottom of the inner water vessel chamber, leaving a 2 mm gap at the bottom,

before cycling back up. The 2 mm gap was chosen to generate food particles < 2 mm, as the stomach only empties small particles less than 1-2 mm particles (Hellström et al., 2006). The DGSM cycles three times per min applying corresponding compressive forces and gaps as shown in Figure 6.3A. The number of cycles mimics the 3 axial forces previously found by *in vivo* study of the human stomach (Vassallo et al., 1992). The texture analyzer program (TL-Pro) measures the forces observed at the smallest gap during simulation. A thin polyester mesh bag with 1.5 mm net pore size was placed inside the chamber to prevent large particles from entering the emptying tube.

A Variable Flow Mini-Pump (Neta Scientific INC. Hainesport, NJ 08036) added the simulated gastric juice into the gastric chamber using a plastic tube (3.0 mm ID). Simulated gastric juice was added at 1.0-1.5 mL/min generating a dynamic change in pH shown by Figure 6.3B. Another mini pump was connected to the model facilitating gastric emptying through a plastic tubing (3.4 mm ID). Previous studies indicate that the rate of emptying liquid food is faster than the rate of emptying of solid food. Half of the liquid meals emptied at 11-35 min while half of solid meals emptied at 75-90 min (Maddern et al., 1985). The rate of emptying was set at 3 mL/min to ensure half of the digesta emptied within 50-70 min of simulated digestion using DGSM, since the food being digested contained both solids and liquids.

6.2.3. Influence of dynamic changes of pH and volume on tuna digestion

During a typical digestion trial using the DGSM, the pH and digesta volume changed progressively due to the continuous secretion of simulated gastric juice and the emptying of digesta. To study the effects of dynamic changes in the stomach environment on food digestion, tuna digestion trials were conducted under both dynamic conditions (changing pH or volume or both) and constant conditions (with fixed pH or volume or both). Results of the measured forces

and the soluble solids were compared between constant conditions and dynamic conditions. The measured forces are directly related to the hardness of the tuna while the measured soluble solids reflect the level of tuna disintegration and solid release.

For trials with dynamic conditions, tuna (30 g) was dispersed in water (200 mL), and the solution was placed in DGSM with continuous simulated gastric juice secretion at the rate of 1.0 mL/min. The digesta was emptied continuously at 3 mL/min, and the entire amount of emptied digesta was collected every 30 min increments. Samples were placed in 80˚C water bath for ten min (heat) to inactivate the enzymes. To quantify insoluble solids, the samples were filtered with Whatman paper # 5, oven-dried, and weighted. Filtrates were centrifuged at 6,000 x g for 5 min, and 2 mL aliquots of the supernatant were dried to determine soluble solid content.

For trials under constant conditions, tuna (30 g) was placed in the simulated gastric solution (200 mL) already adjusted to pH 1.3. The solution was placed in the DGSM without continuous gastric secretion or continuous gastric emptying. Samples (5 mL) were collected every 15 min for 2 h, and replaced with an equal volume of simulated gastric juice to maintain constant volume. Samples were deactivated using heat, centrifuged, filtered, and oven dried to quantify soluble solids. Comparative trials to determine the influence of pH were performed with simulated gastric juice adjusted to pH 3 and pH 5.

6.2.4. Efficacy of Supplementary Proteases in casein digestion using a static digestion model

Casein was used as a substrate to investigate the performance of SPs in static stomach models. Simulated stock gastric juice (100 mL) with the adjusted of pH 1.3 was placed inside an Erlenmeyer flask. Porcine pepsin and mucin were then added, and the flask was placed inside shaking water bath at 37˚C. Solid bovine casein (3 g) was added, and mixed at 120 rpm for 120 min. Samples (5 mL) were collected at 10, 20, 30, 60, and 120 min, deactivated with heat, and

placed in the freezer for analysis later. Comparative trials replacing PP were conducted with four supplementary proteases (SPs): “Acid Stable Protease”, “DS Protease”, “Peptidase”, and “Fungal Protease”. The concentration of each SP was 0.5 mg/mL. Additional comparative static digestion trials using SPs were performed with simulated gastric juice adjusted to pH 3 and pH 5.

6.2.5. Efficacy of Supplementary Proteases in casein digestion using DGSM

Solid bovine casein was dissolved in potassium phosphate buffer at 0.03 g/mL. The solution (250 mL) was placed in the DGSM, and Acid Stable Protease was (0.5 g) added. The simulation was conducted using gastric juice secreted at 1.0 mL/min and gastric emptying at 3.0 mL/min. Samples (5 mL) of the continuously emptied digesta were collected the at 10, 20, 30, 60, and 120 min, deactivated with heat, and stored for analysis later. Comparative trials were conducted with 3 other SPs. The results were compared to control trials consisting of DI water (0.5 g) in place of the proteases.

6.2.6. Efficacy of enzyme blends on digestion of complex food matrix

A food matrix (~250 g) were prepared by mixing canola oil (20 g), 3g /100mL starch solution made by dissolving in boiling water (200 g), and canned tuna (30 g). The food matrix was mixed with simulated salivary juice (30 mL) for 5 min on a stir plate, and placed inside DGSM. The Low Enzyme blend (0.20 g) was added to the gastric chamber, and the DGSM simulation was initiated. Samples of the continuous emptying digesta were collected every 5 min, deactivated with heat, and stored in a freezer for analysis later. These samples were grouped together from 0-5, 5-60, 60-120, and 120-180 min. The High Enzyme blend (0.20 g) was subjected to the same dynamic digestion procedure. High and the Low Enzyme blends were compared to CREON (0.20 g), an enzyme blend available by prescription.

6.2.7. Chemical analysis

Samples were thawed at room temperature. Aliquots (1 mL) were obtained from the collected samples, and centrifuged at 6,000 x g. The supernatant were analyzed for L- Tyrosine Equivalent (TE) using the Universal Protease Activity Assay (Cupp-Enyard, 2008)with Folin & Ciocalteu's agent reacting with Free Tyrosine to form chromophores. Results were quantified using a spectrophotometer. The aliquots were further analyzed for concentrations of primary amino nitrogen (PAN), glucose, and glycerol. PAN concentrations were quantified using the NOPA (o-phthaldialdehyde/N-acetyI-L-cysteine) method (Dukes & Butzke, 1998). In this method, the primary amino groups react with O-phthaldialdehyde and N-acetyl cysteine to form chromophores that were quantified at 340 nm. HPLC (Agilent 1100 Series, Santa Clara, CA 95051) was used to measure glucose and glycerol concentrations with a refractive index detector, using a 30 cm x 7.8 mm SUPELCOGEL C-610H column (Sigma–Aldrich Chemical Company, St. Louis, MO), with 1 g/L phosphoric acid as mobile phase at a flow rate of 0.5 mL/min.

5.2.8 Statistical analysis

Trials were conducted in duplicates. The average TE and PAN generated by SPs at various pH were calculated and analyzed using Fisher's least significant difference test at statistical significance of $P<0.05$ with SAS® software (version 9.3, SAS Institute Inc., Cary, NC).

6.3. Results and Discussion

6.3.2. Influence of dynamic pH and volume on tuna digestion

The measured compressive forces and soluble solids were used to compare the constant and dynamic digestion of tuna using the DGSM. The measured forces correspond to the hardness of the tuna in the DGSM, and the reduction in hardness over time correlated with tuna softening

in simulated gastric environment. The measured soluble solid concentrations indicated the level of tuna disintegration and nutrient release. Figures 6.4 and 6.5 compare the changes in forces and soluble solids of the trials under constant versus dynamic conditions. At constant pH 5, the forces follow a descending curve indicating reduction in hardness while the soluble solid concentrations show an ascending curve after 2 h of digestion. Researchers reported that constant compressive forces fracture food particles and facilitate erosion through mixing of the digesta (Wey, et al., 2014). Varying pH values further altered tuna digestion. At a constant pH of 5, the forces were relatively high, attaining a 23 N maximum force, and the content of soluble solids was relatively low with a range of 1.75 – 2 g/100g. At pH 1.3, the forces decreased, attaining a 2.5 N maximum force, and the soluble solids content increased from 2.5 - 3.75 g/100g. These results show that low gastric pH further softening and disintegration of tuna, indicated by the reduction in compression forces, and leads to increased nutrient release. Similarly, researchers have reported that the absorption of acidic gastric juice caused tenderization of food structure due to both enzyme hydrolysis and acid hydrolysis, which facilitates the leaching of nutrients (Kong & Singh, 2010; Wey et al., 2014).

Unlike the stagnant pH in the constant conditions trials, the initial pH of the dynamic trials was 6-7 due to the buffering effect of food. Upon continuous secretion of acidic gastric juice, the pH of the digesta declined by a value of 1 every 30 min shown in Figure 6.3B. The linear pH decline is consistent with the pH change observed in *in vivo* measurements of human stomachs (Camilleri et al., 1985). The volume of the digesta also decline linearly as the contents were continuously emptied at the rate of 3.0 mL/min. The combination of continuous change in pH and volume of the digesta altered the detected compression forces and the content of released soluble solids when compared to constant pH and volume conditions. The detected compression forces

and the content of soluble solids are shown in Figures 6.4 and 6.5B. Figure 6.4 shows that the maximum force is 30 N, which is higher than under constant conditions, but declined rapidly to below 5 N after 40 min of tuna digestion in the DGSM. The forces were relatively high at the start of dynamic digestion due to limited softening in tuna caused by the neutral pH. Repeating compressive force mechanically softens and disintegrates the tuna, while continuous acidification of the stomach contents further softens and digests tuna through acid hydrolysis and enzyme hydrolysis. Adding to the reduction in forces is the continuous emptying that remove solids and liquid from the digesta. Based on Figure 6.5, fewer solids were left in the model as increasing trends of solids were found in the emptied digesta up to 150 min. As the time of digestion progressed, the reduction in solids led to drop-in forces sensed by the texture analyzer. In addition, the dynamic trials generated relatively lower initial soluble solids concentrations (0.75 g/100g), but increased rapidly to 2.4 g/100g after 2 h of digestion. The content of total solids (insoluble + soluble solids content) significantly increased from initially 0.8 g/100g to 2.7 g/100g after 2 h digestion (Fig. 5B), as liquids tended to be emptied first leading to an increased solids concentration. The high solid content should also affect the release of soluble solids. The results shown in Figs. 5.4 and 5.5 indicated the dynamic changes of pH and gastric empty significantly impact the textural changes of food and breakdown in the stomach, and the subsequent nutrient release.

6.3.3. Efficacy of SPs in casein digestion using a static digestion model.

Shown on Figure 6.6, Porcine Pepsin hydrolyzed casein and generated linear increases in Tyrosine Equivalent (TE) concentrations at the constant pH of 1.3, 3, and 5. The linear increases in TE are attributed to the 2 h of incubation, which allows for optimum interactions between enzymes and substrate. There were no differences in the proteolytic activity of Porcine Pepsin at

pH 1.3 and 3, but proteolytic activity was lower at the pH 5. This is consistent with the pH range for porcine pepsin, which has an optimum pH between 2- 4, as shown in Table 6.1. The proteolytic activities of the SPs were compared to PP at three selected pH, and the average concentrations of TE over 2 h of digestion are shown in Table 6.2. Porcine Pepsin generated 3-4 times greater product than the SPs at pH 1.3 and 3. The DS protease generated high concentrations of products that are not significantly different than PP at the pH 5. Researchers noted that temperature, pH, and incubation time are factors influencing the characterization of enzymatic activities using the *in vitro* digestion system (Boisen & Eggum, 1991). Since both incubation time and temperature were kept constant within the static model, the main contributing factor altering the proteolytic activities for SPs was the pH. When the pH corresponded to the optimum pH of the SPs, the proteolytic activities were relatively high. This is prominent as Acid Stable protease and DS protease produced relatively high TE concentrations at pH 1.3 and 5, respectively. In contrast, low proteolytic activities were observed due to enzyme inactivation when the pH were much higher or much lower than the optimum pH of the proteases. Consequently, Acid Stable Protease and DS protease generated relatively low concentrations of TE at the pH 5 and 1.3, respectively. Thus, the optimum pH of enzymes is highly correlated with the predicted efficiency for SPs in the static model.

6.3.4. Efficacy of SPs in caseinate digestion using DGSM

The DGSM was used to test the efficiency of SPs in digesting potassium caseinate under dynamic conditions. Figure 6.7 shows the concentrations of TE and PAN generated by continuous secreting Porcine Pepsin alone compared to adding SPs with the Porcine Pepsin secretion. The products concentrations were relatively low in the control trials mainly attributed to the low concentrations of gastric juice containing Porcine Pepsin being pumped into the model. When DS

protease or Peptidase was added, both TE and PAN concentrations were relatively high followed by decreases in the products generated. The reason for high initial product levels is due to the relatively neutral initial pH (6.8) of the casein solutions that encourages and maximizes the activity of the SPs with neutral optimum pH. Jung et al. showed the degree of protein hydrolysis is relatively fast with maximum product generated after 30 min of incubating fungal enzymes with soy flour (2004). As simulated digestion progressed, the contents in the DGSM had a decline in pH similar to the dynamic pH decline show in Figure 6.3B. The acidification of the digesta leads to the inactivation of SPs with relatively neutral optimum pH. In comparison, the SPs with relatively acidic optimum pH showed increasing proteolytic activities as the environment became more acidic. The main example is the Acid Stable Protease that generated relatively low concentrations of products initially, but the concentrations of TE and PAN increased as the environment become increasing acidic upon further digestion time. The pH of the stomach influences the efficacy of digestive enzymes. While extreme pH denatures the enzymes, the neutralization of emptied digesta into the intestine may further enhance the efficacy of these supplementary enzymes by reactivating the enzymes with optimum neutral pH inside the intestines.

The average product concentrations were calculated over the 2 h dynamic gastric simulation to compare the SPs' efficiencies. Table 6.3 shows the averages of TE and PAN produced by secretion PP alone compares to the addition of SPs along with simulated gastric secretions containing PP. The addition of Peptidase, DS protease, or Fungal Protease increases protein hydrolysis by generating significantly higher average concentrations of TE while Peptidase and DS Protease generated significantly greater average concentrations of PAN. Results from the dynamic trials shown in Table 6.2 indicate that the addition of SPs had greater effects on digestion

as demonstrated by the generation twice the concentrations of TE and PAN in most cases. The pH did not drop below 4 until the 80 min of digestion (Fig. 3A). Acid Stable Protease was not as efficient in aiding in the digestion of casein as the average TE and PAN concentrations were not significantly different from secreting gastric juice with PP alone. The low concentration of product by Acid Stable Protease is attributed to the dynamic change in pH and the continuous emptying of digesta. It took 80 min before the pH reached within the activity range of Acid Stable Protease. By that time, over 190 mL/250mL of the digesta had already emptied. The continuous emptying decreases the interaction time between substrate and enzymes as the process continuously remove enzymes, substrate, and products. This result further emphasizes the significant impact of dynamic physiological processes in the stomach on the digestion of food, which should be considered in the design of *in vitro* models to obtain accurate predictions of the enzyme activity.

6.3.5. Efficacy of enzyme blends on digestion of complex food matrix

The tested digestive blends consist of fungal derived amylases, lipases, and proteases that are acid stable. Ideally, the enzymes pre-digest macromolecules inside the human stomach and make the nutrient more bio-accessible for the small intestine to absorb. The blends were evaluated under gastric conditions simulated by the DGSM to determine their efficacy in aiding the digestion of a complex food matrix containing canola oil, starch, and tuna. Figure 6.8 shows the concentrations of PAN, glucose, and glycerol that indicate the hydrolysis of proteins, starch, and fats upon adding of enzymes blends to digestion the food matrix. Comparative trials with CREON generated 0.09-0.22 mg/L glucose, 0.01-0.05 mg/mL glycerol, and 327-467 mg/L PAN. Compared to CREON (Placebo), adding Low Enzyme blend generated 2X greater glucose, 8X glycerol, and 1.2X greater PAN. Figure 6.8 also shows that addition of both of the High Enzyme Blends improve

the release of bioaccessible components by generating 4X more Glucose, 10X more of Glycerol, and roughly 1.3X more FAN, respectively.

More important is the hydrolysis trend that occurs when the blends were placed in the DGSM. The degree of hydrolysis occurs at a relatively fast rate, especially when the environment favors the enzymes (Jung et al., 2004). The initial simulation conditions in the DGSM favor the lipase and amylase activities in the blends, since the environment of the digesta had relatively neutral pH. The linear increases are found in the production of amino acids, glucose, and glycerol as shown in all the graphs shown in Figure 6.8. Under DGSM, the blends showed efficiency at various points in the digestion of a complex food matrix. Further testing using different blends and greater enzyme concentrations are recommended to reiterate the efficiency of supplementary enzymes. Further investigation within the intestinal model may shows the improvement of consuming supplemental digestive enzymes.

6.4. Conclusion

The Dynamic Gastric Simulated Model mimics gastric digestion and was used to test the efficacy of supplementary digestive enzymes. DGSM incorporates compressive forces to disintegrate food, continuous gastric secretion that simulates the pH changes in the human stomach, and continuous gastric emptying to remove digesta. Findings indicated the dynamic changes of pH and digesta volume significantly impact the textural changes of food and breakdown in the stomach, and the subsequent release of nutrients. Using the static model, the optimum enzyme pH is highly correlated with the predicted efficiency of Supplementary Proteases. The results from DGSM emphasize the significant impact of the dynamic physiological processes inside the stomach on food digestion, which should be considered in designing *in vitro* models to obtain accurate predictions of the enzyme activity. In addition, the supplementary blends

demonstrated efficiency at varying degree in the digestion of a complex food matrix using the DGSM. Additional research in understanding the re-activation of enzymes, as food move from the stomach into the intestines, will further demonstrate the high efficiency of these supplementary digestive enzymes inside the whole human digestive system.

6.5. Acknowledgements

This study was partly supported by BIO-CAT (Troy, Virginia). The author also wishes to acknowledge Food Technology Corporation (Sterling, Virginia) for the generous donation of the TMS Pro Food Texture Analyzer.

References

Armand, M., Borel, P., Pasquier, B., Dubois, C., Senft, M., Andre, M., Peyrot, J., Salducci, J., & Lairon, D. (1996). Physicochemical characteristics of emulsions during fat digestion in human stomach and duodenum. *American Journal of Physiology*, 271, G172-183.

Boisen, S., & Eggum, B. O. (1991). Critical evaluation of in vitro methods for estimating digestibility in simple-stomach animals. *Nutrition Research Reviews, 4*(1), 141-162.

Cabanero, A. I., Madrid, Y., & Camara, C. (2007). Mercury-selenium species ratio in representative fish samples and their bioaccessibility by an in vitro digestion method. *Biological Trace Element Research, 119*(3), 195-211.

Camilleri, M., Malagelada, J. R., Brown, M. L., Becker, G., & Zinsmeister, A. R. (1985). Relation between antral motility and gastric emptying of solids and liquids in humans. *American Journal of Physiology, 249*(5), G580-585.

Chen, J., Gaikwad, V., Holmes, M., Murray, B., Povey, M., Wang, Y., & Shang, Y. (2011) Development of a simple model device for *in vitro* gastric digestion investigation. *Food. Function*, 2, 174-182.

Chessa, S., Huatan, H., Levina, M., Mehta, R. Y., Ferrizzi, D., & Rajabi-Siahboomi, A. R. (2014). Application of the Dynamic Gastric Model to evaluate the effect of food on the drug release characteristics of a hydrophilic matrix formulation. *International Journal of Pharmaveutics, 466*(1-2), 359-367.

Cupp-Enyard, C. (2008). Sigma's Non-specific Protease Activity Assay - Casein as a Substrate. *Journal of Visualized Ezperiments,* (19).

Dodge, J. A., & Turck, D. (2006). Cystic fibrosis: nutritional consequences and management. *Best Practice Researchear Clinical Gastroenterology, 20*(3), 531-546.

Donhowe, E. G., Flores, F. P., Kerr, W. L., Wicker, L., & Fabin, K. (2014). Characterization and in vitro bioavailability of β-carotene: effects of microencapsulation method and food matrix. *LWT -- Food Science and Technology, 57*(1), 42-48.

Dukes, B. C., & Butzke, C. E. (1998). Rapid determination of primary amino acids in grape juice using an o-phthaldialdehyde/N-acetyl-l-cysteine spectrophotometric assay. *American Journal of Enology and Viticulture, 49*(2), 125-134.

Hellström, P. M., Grybäck, P., & Jacobsson, H. (2006). 3: The physiology of gastric emptying. *Best Practice & Research Clinical Anaesthesiology, 20*, 397-407.

Jung, S., Roussel-Philippe, C., Briggs, J. L., Murphy, P. A., & Johnson, L. A. (2004). Limited hydrolysis of soy proteins with endo- and exoproteases. *Journal of the American Oil Chemists' Society, 81*(10), 953-960.

Kong, F., & Singh, R. P. (2010). A human gastric simulator (HGS) to study food digestion in human stomach. *Journal of Food Science, 75*(9), E627-E635.

Kozu, H., Nakata, Y., Nakajima, M., Neves, M. A., Uemura, K., Sato, S., Kobayashi, I., & Ichikawa, S. (2014). Development of a human gastric digestion simulator equipped with peristalsis function for the direct observation and analysis of the food digestion process. *Food Science and Technology Research, 20*(2), 225-233.

Kulkarni, S. D., Acharya, R., Rajurkar, N. S., & Reddy, A. V. R. (2007). Evaluation of bioaccessibility of some essential elements from wheatgrass (Triticum aestivum L.) by in vitro digestion method. *Food Chemistry, 103*(2), 681-688.

Maddern, G., Miners, J., Collins, P. J., & Jamieson, G. G. (1985). Liquid gastric emptying assessed by direct and indirect techniques: radionuclide labelled liquid emptying compared with a simple paracetamol marker method. *Australian and New Zealand Journal of Surgery*,*55*(2), 203-206.

Minekus, M., Huis in 't Veld, J. H. H., Havenaar, R., & Marteau, P. (1995). A multicompartmental dynamic computer-controlled model simulating the stomach and small intestine. *Alternatives to laboratory animals : ATLA*, *23*(2), 197-209.

Nakamura, T., Takeuchi, T., & Tando, Y. (1998). Pancreatic dysfunction and treatment options. *Pancreas*, *16*(3), 329-336.

Roxas, M. (2008). The Role of Enzyme Supplementation in Digestive Disorders. *Alternative Medicine Review*, *13*(4), 307-314.

Schneider, M. U., Knoll-Ruzicka, M. L., Domschke, S., Heptner, G., & Domschke, W. (1985). Pancreatic enzyme replacement therapy: comparative effects of conventional and enteric-coated microspheric pancreatin and acid-stable fungal enzyme preparations on steatorrhoea in chronic pancreatitis. *Hepato-Gastroenterology*, *32*(2), 97-102.

Scolapio, J. S., Malhi-Chowla, N., & Ukleja, A. (1999). Nutrition supplementation in patients with acute and chronic pancreatitis. *Gastroenterology Clinics of North America*, *28*(3), 695-707.

Vassallo, M. J., Camilleri, M., Prather, C. M., Hanson, R. B., & Thomforde, G. M. (1992). Measurement of axial forces during emptying from the human stomach. *American Journal of Physiology*, *263*(2), G230-G239.

\

Wey, A. S. v., Cookson, A. L., Roy, N. C., McNabb, W. C., Soboleva, T. K., Wieliczko, R. J., & Shorten, P. R. (2014). A mathematical model of the effect of pH and food matrix composition on fluid transport into foods: an application in gastric digestion and cheese brining. *Food Research International*, *57*, 34-43.

Table 6.1. Supplementary enzyme sources and optimum pH and temperature ranges

Enzymes Label	Derived From	pH range of Activity	Relative Optimum pH	Temperature Range of Activity	Relative Optimum Temperature
Porcine Pepsin	Swine	1.0-5.0	2.0-4.0	30˚C-60˚C	39˚C
Acid Stable Protease	*Aspergillus niger*	1.0-4.0	2.5	30˚C-70˚C	58˚C
Peptidase	*Aspergillus oryzae*	3.0-10.0	6.7-7	30˚C-70˚C	48˚C
Fungal Protease	*Aspergillus oryzae*	3.0-6.0	4.0	25˚C-60˚C	50˚C
DS Protease	*Aspergillus melleus*	5.0-8.0	5.0	30˚C-70˚C	45˚C

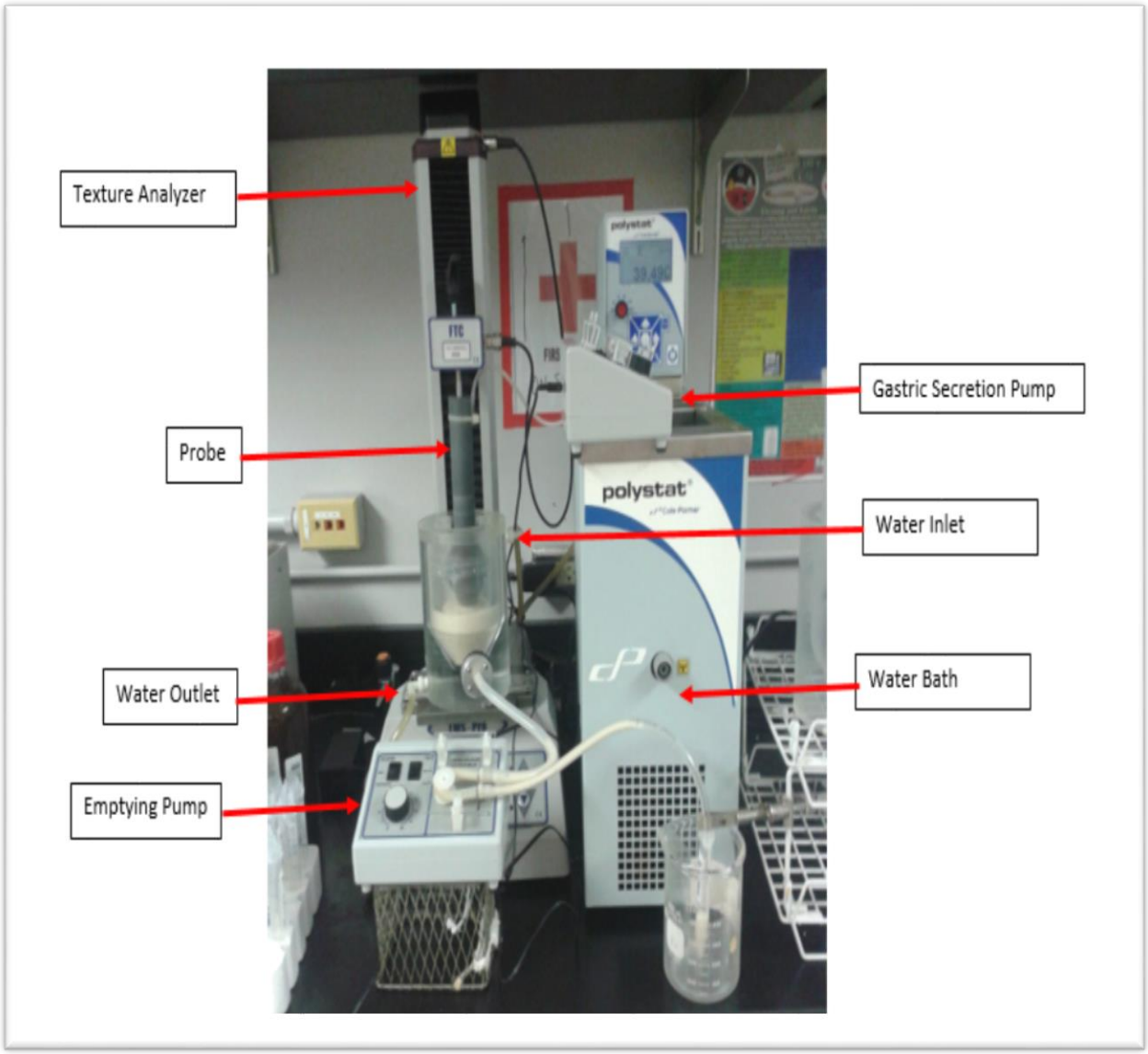

Figure 6.1. Schematic of the DGSM with pumps to simulate gastric secretion and gastric digestion. The probe is attached to the texture analyzer, and the gastric chamber is attached to a circulating water bath to ensure internal temperature of 37˚C

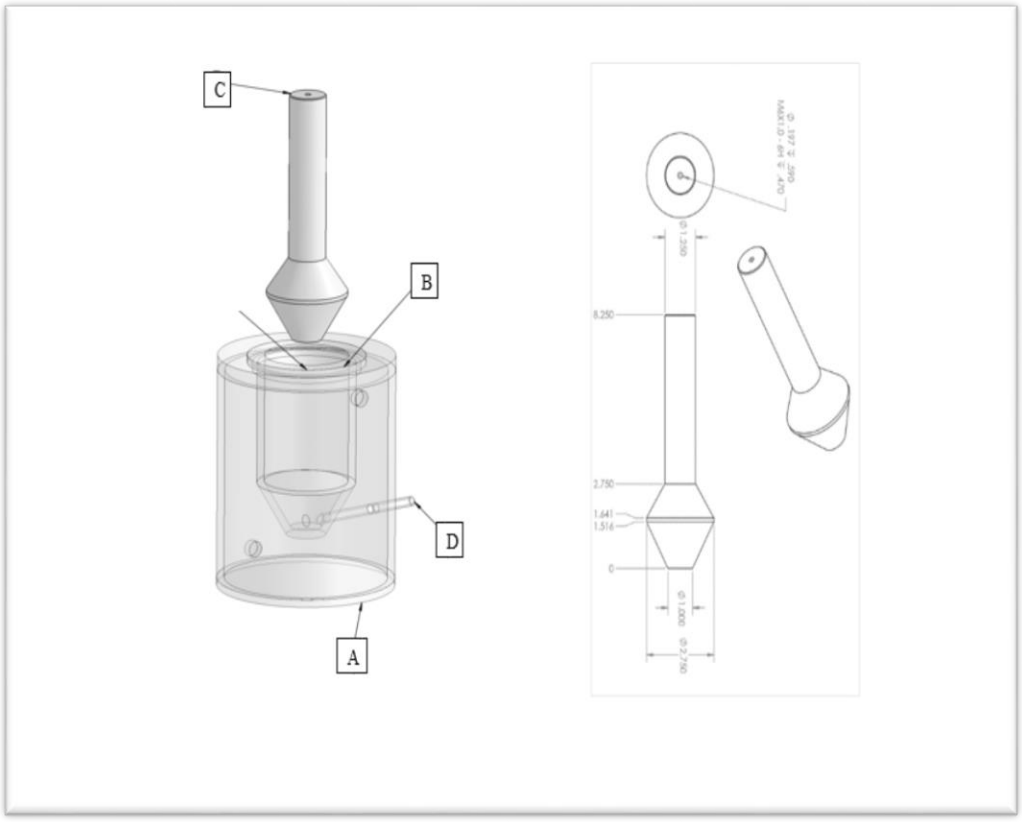

Figure 6.2. Composition of DGSM: A) Water Jacket; B) Internal gastric Chamber; C) Probe; and D) Food Tube.

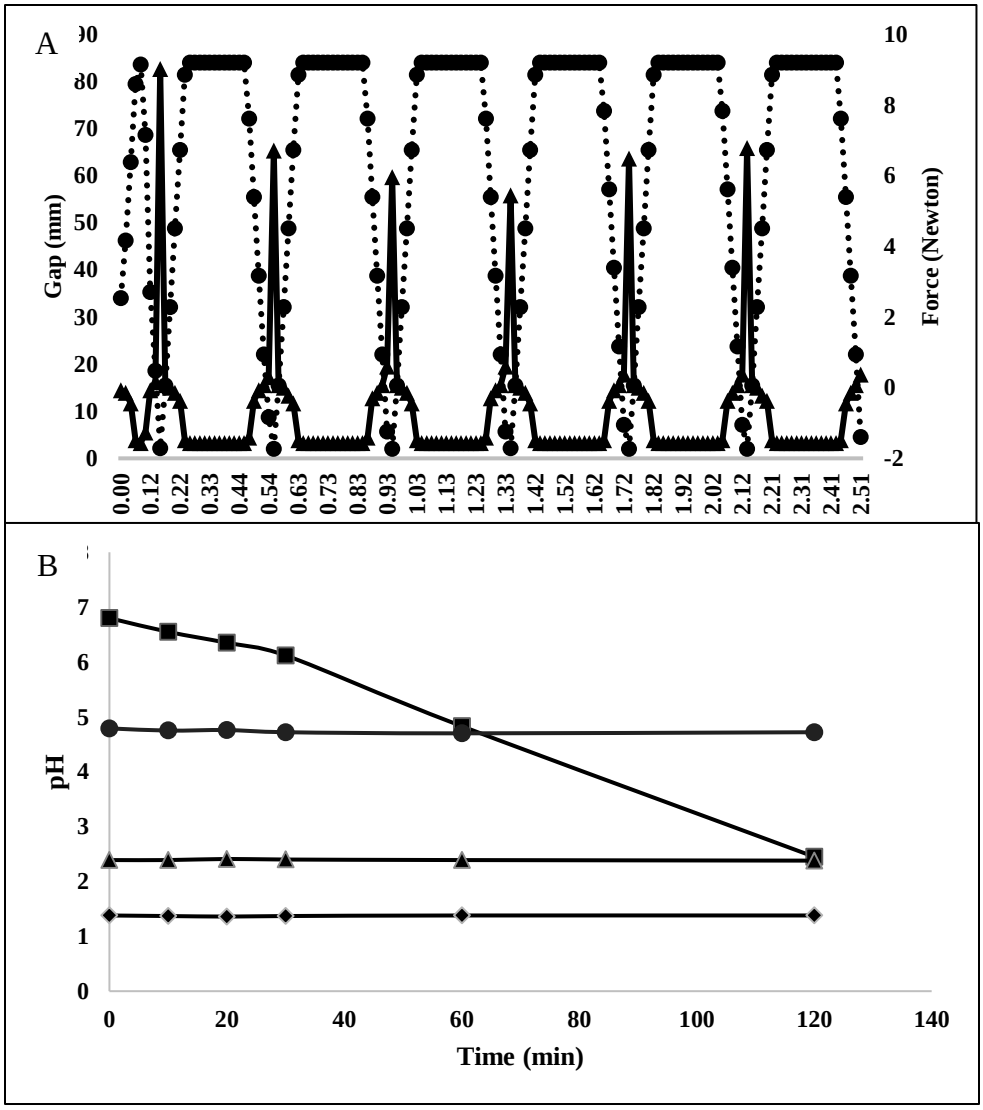

Figure 6.3. Contractions and pH profile of the DGSM. A) There are 3 contractions per minute, and the changing (··●··) gaps between the bottom of the internal stomach model and the probe is shown on the right axis. The initial gap (34 mm) was used for the zero point of compressive forces (—▲—), and the negative forces are indicator of the probe moving above the liquid (left axis). B) The pH profile for dynamic simulated digestion (■) using DGSM compared to the static simulated digestion at pH 1.3 (♦), pH 3 (▲), pH 5 (●).

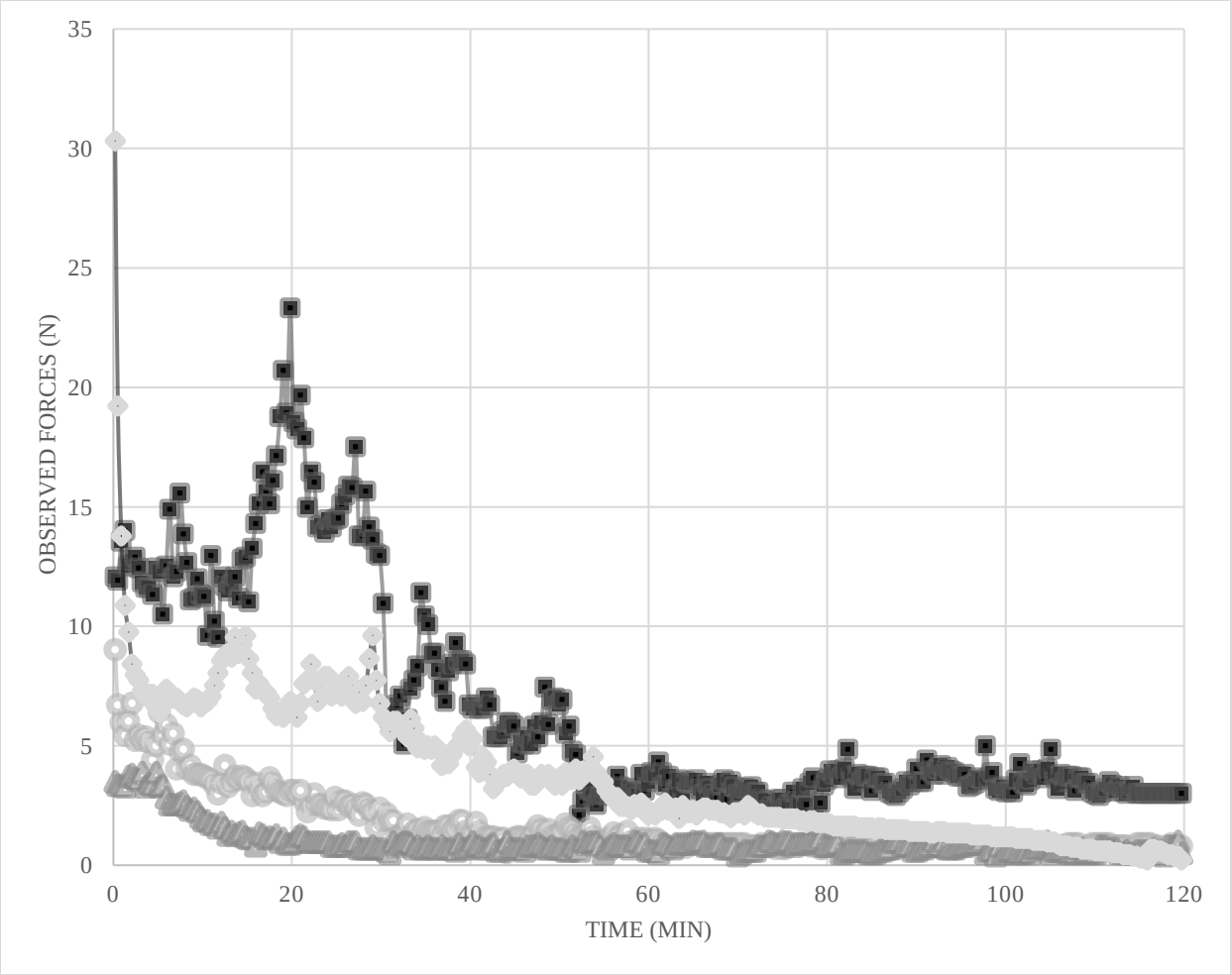

Figure 6.4. The measured force profile of tuna soaked in simulated gastric juice at the various constant pH 5 (■), pH 3 (♦), and 1.3 (●) in the DGSM without continuous gastric secretion nor gastric emptying. The continuous curve (▲) measured the tuna digestion under dynamic DGSM conditions with continuous gastric secretion addition at 1.5 mL/min and continuous gastric emptying at 3.0 mL/min.

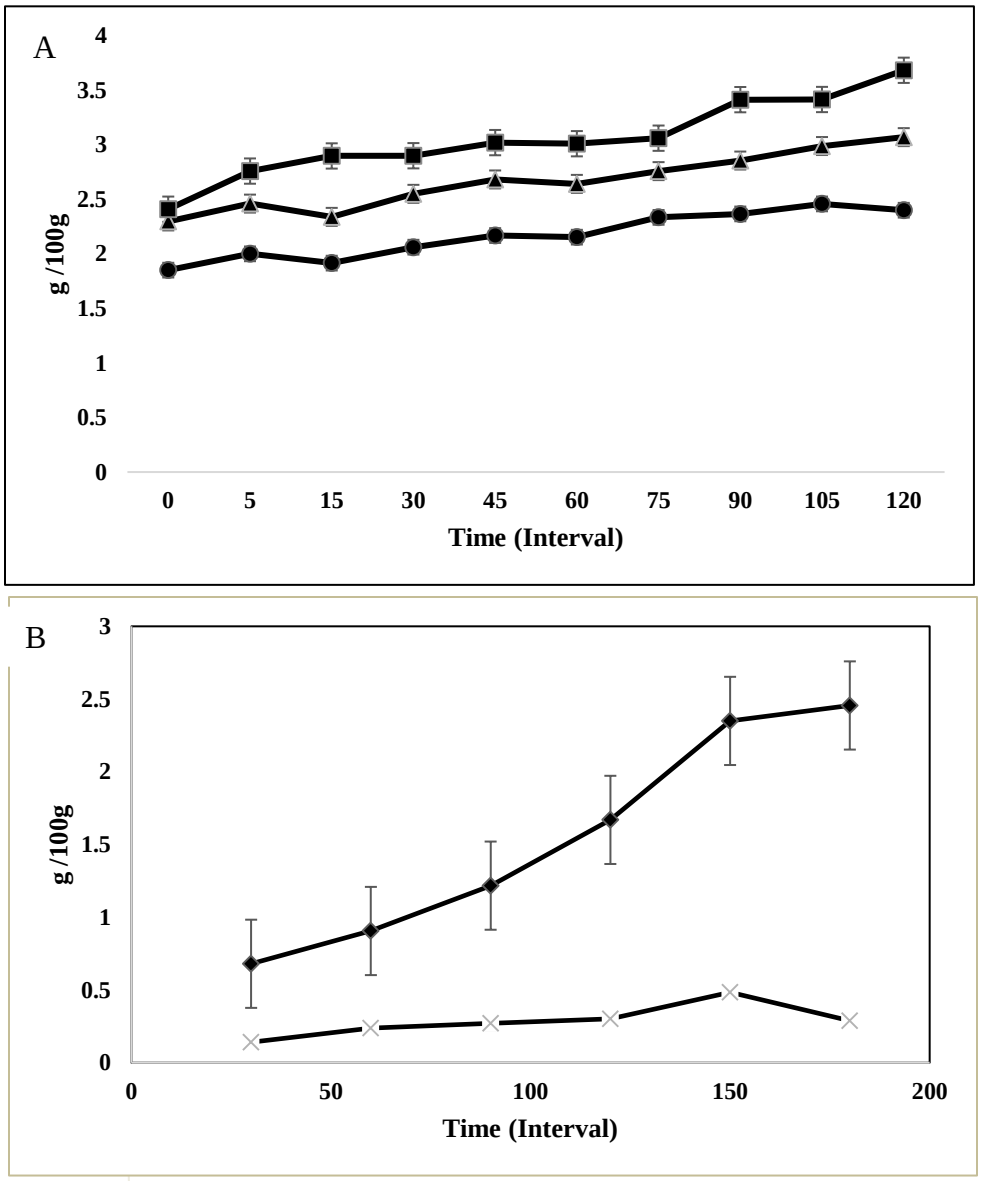

Figure 6.5. Percent Solids: A) Soluble solids measured in the static model with non-continuous removal of samples (5 mL) for the trials at constant pH 1.3 (■), pH 3 (▲), and pH 5 (●). B) Soluble (♦) and insoluble solids (x) measured from the accumulation of the continuous emptied digesta at 3 mL/min.

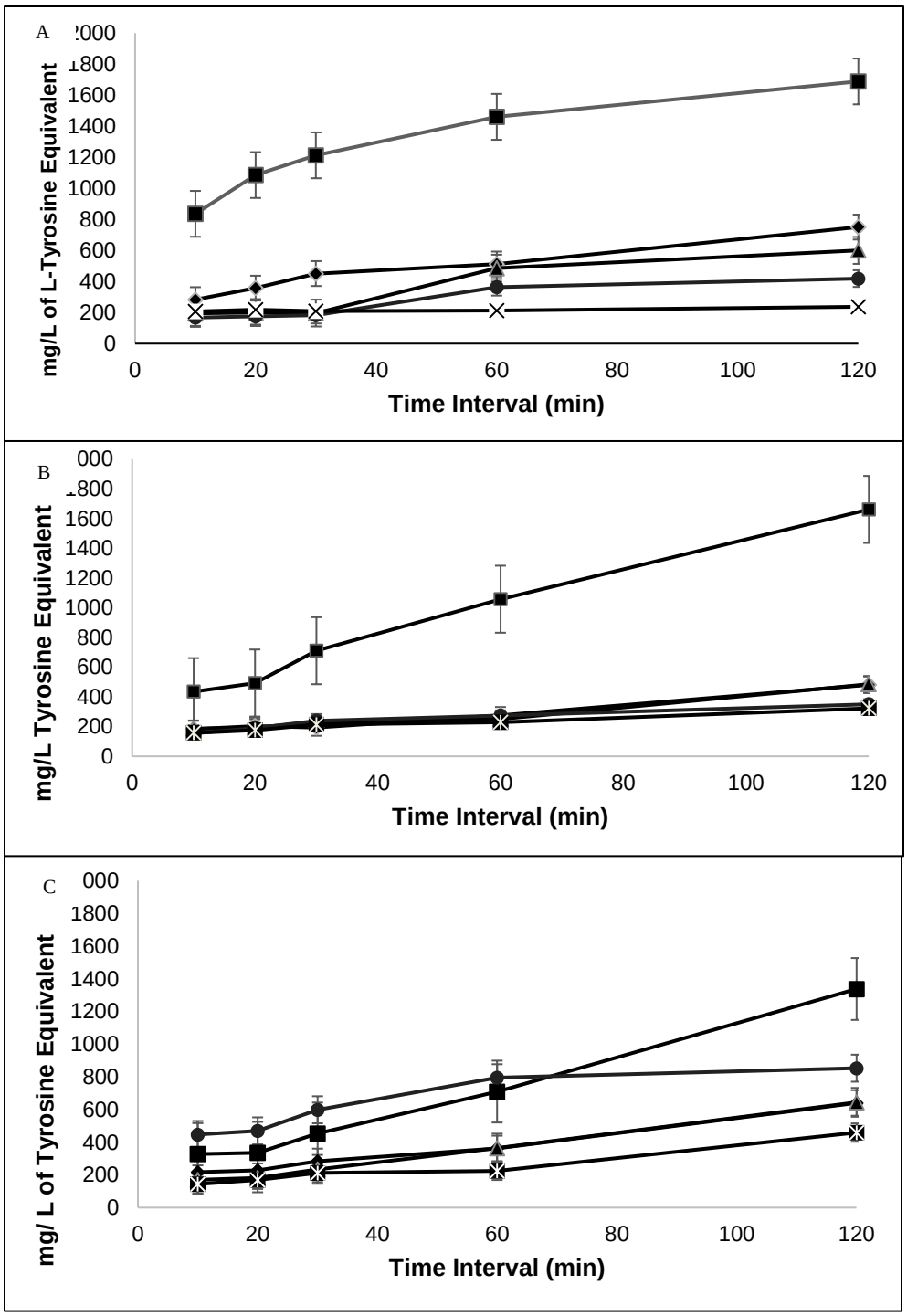

Figure 6.6. Changes of Tyrosine equivalent as an indicator of proteolytic activities of the porcine pepsin against porcine pepsin (■), fungal protease (▲), acid stable protease (♦), DS protease (●), Peptidase (x) under static digestion with constant pH value of: A) 1.3; B) 3; C) 5.

Table 6.2. Supplementary Protease performance as quantified by product formation under static digestion model conditions.

pH	Porcine Pepsin	DS Protease	Fungal Protease	Peptidase	Acid Stable Protease
1.3	1300±200[a]	260±100 [bc]	340 ± 150 [bc]	210 ± 60[c]	470 [b] ±150
3	870 ±390[a]	240±60[b]	270 ±90[b]	210±40[b]	210 ±20[b]
5	630 ±150[a]	630 ±130[a]	350 ±120[b]	320 ±150[b]	370 ±100[b]

All concentrations are expressed in mg/L of Tyrosine Equivalent. Means that do not share a common superscript within the same row are significantly different ($P<0.05$).

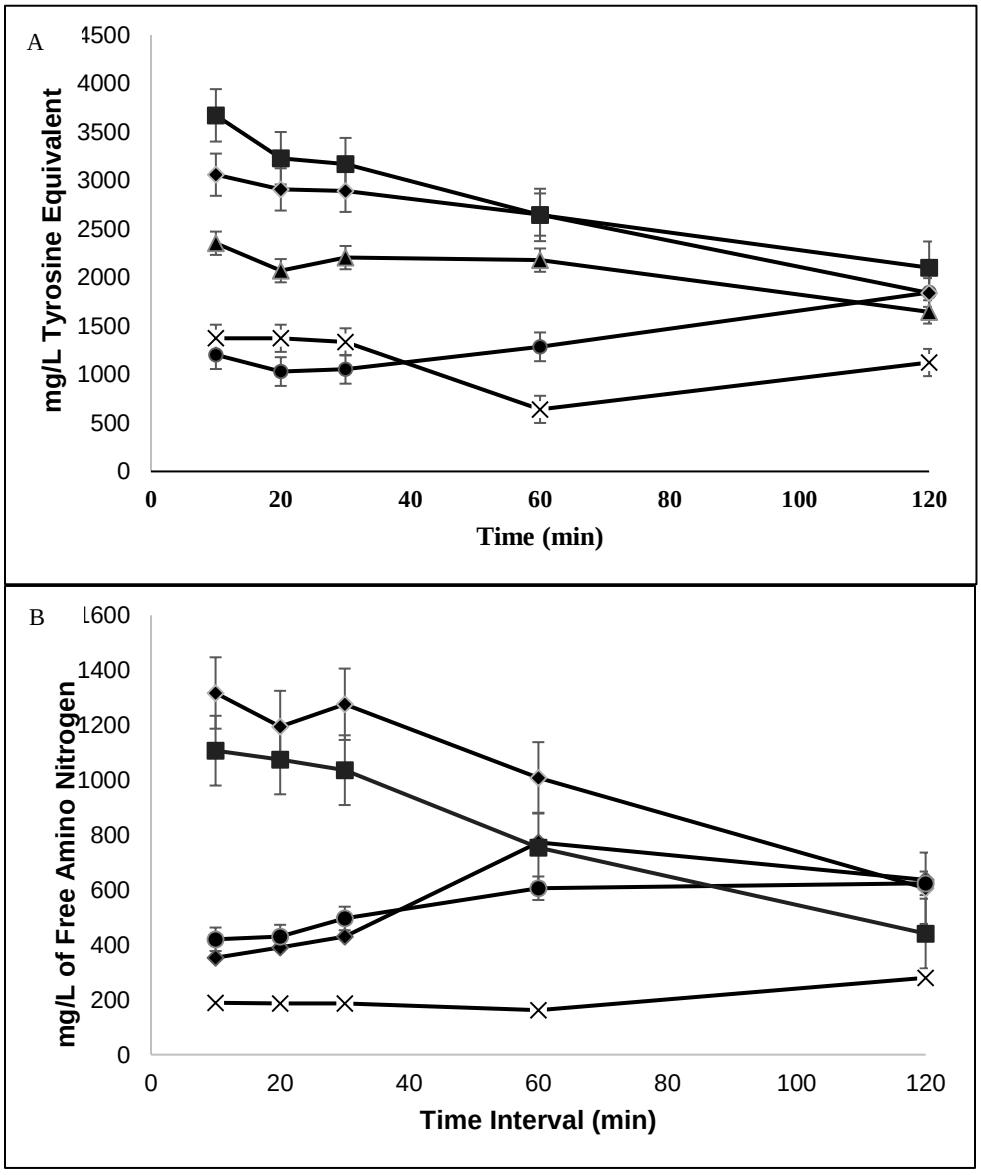

Figure 6.7. Digestion products generated for solubilized casein by secreting simulated gastric juice containing Porcine Pepsin alone (x). Results are compared to secretion of Porcine Pepsin in addition to using Acid Stable Protease (●), DS Protease (♦), Fungal Protease (▲), and Peptidase (■) in DGSM: A) Tyrosine Equivalent; B) Primary Amino Nitrogen.

Table 6.3. Supplementary Protease Performance Quantified by Product Formation of under DGSM.

Method of Analysis	Porcine Pepsin	DS Protease +porcine pepsin	Fungal Protease +porcine pepsin	Peptidase +porcine pepsin	Acid Stable Protease +porcine pepsin
Tyrosine Equivalent	1200± 200^{c}	3000 ±500^{a}	2100 ±200 ^{b}	2600 ±300^{ab}	1100 ±100^{c}
Primary Amino Nitrogen	200 ±30^{c}	920 ±180^{a}	440 ±60^{b}	1090 ±210^{a}	470 ±110^{b}

All concentrations are expressed in mg/L of Tyrosine Equivalent and mg/L of Primary Amino Nitrogen. Means that do not share a common superscript within the same row are significantly different ($P<0.05$).

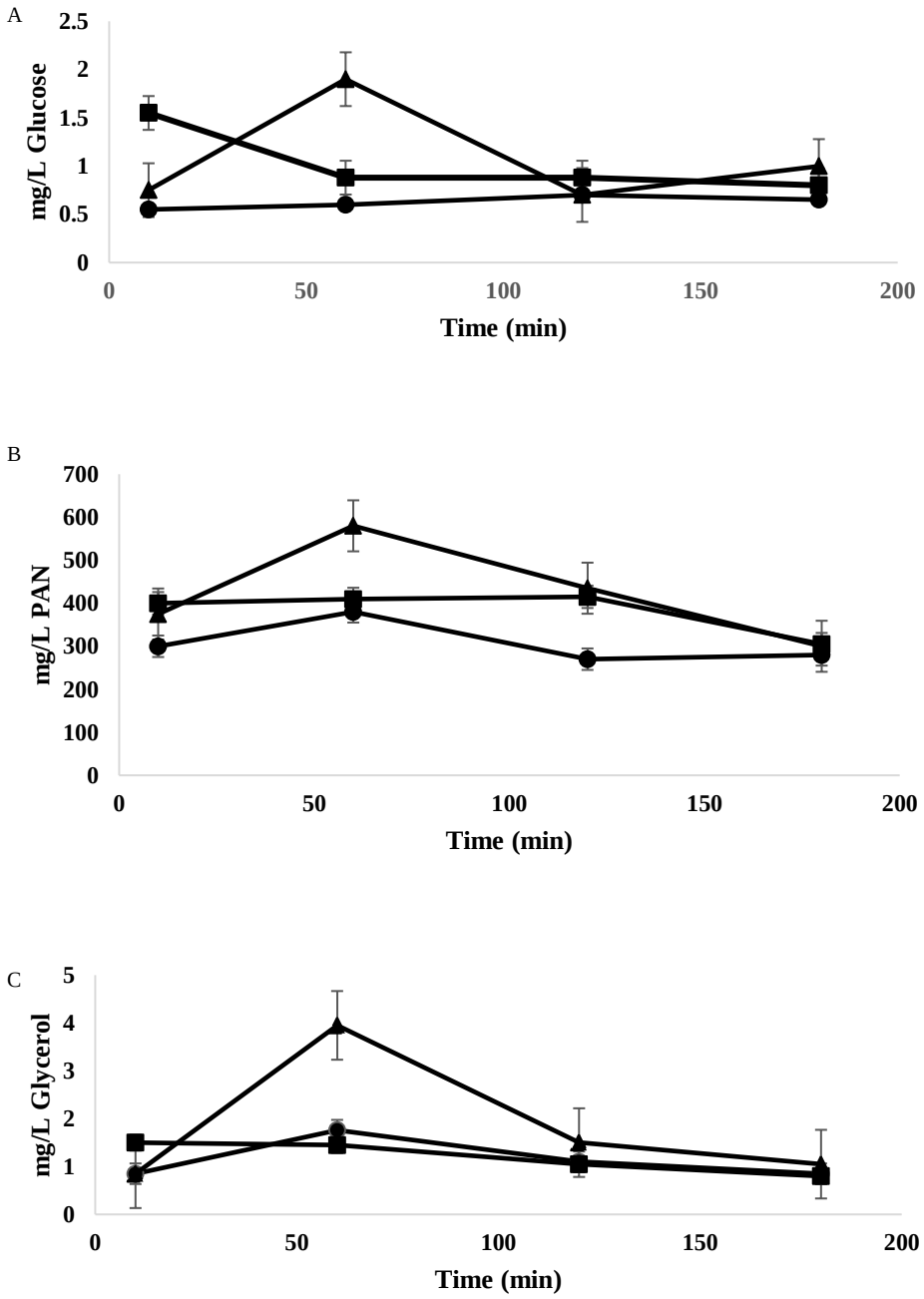

Figure 6.8. Digestion products for a complex food matrix by CREON (—●—), Low Enzyme Blend (—■—), and High Enzyme blend (—▲—) using the DGSM: A) Glucose concentrations to indicate carbohydrate hydrolysis; B) PAN concentration to indicate protein hydrolysis; C) Glycerol concentration to indicate fats hydrolysis.

CHAPTER 7

SUMMARY AND RECOMMENDATIONS

6.1. Summary

The Dynamic Gastric Simulation Model (DGSM) is an effective tool used to study food digestion in the complex gastric environment. The versatility of the model allows for controlling the rate of simulated secretion, peristaltic contractions, and gastric emptying. This model can be utilized to study several different factors that regulate the overall rates of gastric digestion.

Under gastric simulated conditions, physical properties of food affect the rates of gastric digestion by influencing the rates of disintegration and emptying kinetics. More specifically, the particle size and texture of food was shown to affect the rate of food digestion under dynamic gastric environment. Results from the first study (Chapter 2) show that carrot particles in the medium range were digested the fastest due to the gastric contractions that effectively disintegrated the food through grinding and mixing. The disintegration of medium size carrot particles was affected by gastric distension in which the morphological changes in the stomach help to regulate of amount and size of solids emptied from the stomach. Gastric disintegration of food is strongly affected by their compositions and overall structure. Food texture and the initial bulk hardness in the gastric contents are well related with the bulk hardness reduction rate and solid emptying rate during simulated gastric digestion. Several mathematical relationships were developed that can help predict the level of disintegration and emptying rates by using the initial bulk hardness.

The second study investigated the influence of viscosity on the gastric digestion. Results from the study (Chapter 3) show that increase in viscosity of gastric digesta resulted in reduced gastric disintegration in carrot, peanut, and tofu. In the same study, a mathematical model based on Particle Emptying Concentration (PEC) with modifications was effectively used to show the influences of viscosity on the rate of solids being emptied of amberlite beads and carrots. The equation indicated that the increase in viscosity decreased the settling speed and allowed greater dispersion of particles. Increasing the dispersion permitted greater amount of solids to be emptied at low viscosity. Although higher viscosities improved the dispersion of particle, the increased resistance of gastric fluid to flow reduced the overall emptying rate of the digesta and eventually diminished the emptying rates of solids. Ultimately, changing the viscosity of the digesta and the physical properties of the food (density, particle size) has great potential in regulating the overall gastric disintegration and gastric emptying rates.

Another form of regulating gastric digestion is shown in the behavior of various cheese under gastric environment. Although generally consisting of the similar components, cheeses have various structures that affect their gastric digestion. Results (Chapter 4) indicate that the protein in various cheeses resisted gastric digestion by showing increased hardness at the highly acidic gastric condition. The gastric acid with pepsin permitted Mozzarella and Cheddar cheese to develop hard outer layers further resisting the chemical degradation from gastric acids and enzymes. Digestion trials in DGSM demonstrated the ability of cheeses to resist gastric digestion, including decreasing hardness reduction and protein hydrolysis under gastric environment. Mozzarella has shown the most resistance among the three cheeses to the gastric digestion. The obtained knowledge in cheese digestion will allow researchers to develop foods with similar

structure and components that are able to regulate the gastric disintegration and the release of bioaccessible components.

Protease enzymes are critical in accomplishing gastric digestion of food. Various supplemental digestive proteases were developed to improve the hydrolysis of protein in human body. The efficacy of these supplemental digestive enzyme is commonly tested with *in vitro* static digestion model, and the results are often problematic due to over-simplified simulation in static model that cannot reflect realistic gastric conditions. The results from this study (Chapter 5) proved that testing of enzyme supplements using dynamic gastric model can provide more accurate and comprehensive information about the enzyme efficacy. Our study also demonstrated that the majority of the supplemental proteases improved the hydrolysis of protein. In addition, supplemental digestive enzyme blends showed improvement to the hydrolysis of macronutrient by generating greater amount of bioaccessible glucose, amino acids, and glycerol when added into foods. Ultimately, supplemental digestive enzymes have great potential in improving the gastric digestion of patients suffering from gastric digestive diseases.

6.2. Recommendations

Dynamic GI models may be used in the study of food digestion to examine nutrient release, nutrient absorbed, and the change of microbiota affected by food composition and structure. Combined with static models, these Dynamic GI models will provide more accurate and comprehensive information in food digestion kinetics and the health implications of bioactive compounds. Advance in technology will allow more innovative GI models to be developed. With each model improving the simulation, it is imperative that the fundamental parameters of simulation must not be omitted. When permitted, incorporating results from *in vivo* studies will help validate the *in vitro* results. The results in this study provide several solutions to help regulate

the gastric digestion of food. Further investigation of intestinal digestion will improve the knowledge in nutrient release and absorption.

For patients suffering from poor digestion due to pancreatic diseases, supplemental digestive enzymes showed great potential in releasing higher amount of bioaccessible components. Beyond supplying the body with bioaccessible components, these supplemental digestive proteases have additional benefits that need to be further investigated. One benefit includes the usage of supplemental digestive enzymes to reduce allergens. Our preliminary results (data not included in the dissertation) showed that supplemental digestive enzymes have great potential in reducing the allergens from peanut, shrimps, and gluten. Another benefit includes the usage of supplemental digestive enzymes in producing bioactive peptides. Researchers have shown that bioactive peptides have the capability to reduce pathogens and decrease hypertension in human. Using supplemental proteases to produce more bioactive peptides will have great potential in benefiting the human health.